UNIVERSITÀ DEGLI STUDI DI PADOVA

SCUOLA DI INGEGNERIA

DIPARTIMENTO DI INGEGNERIA INDUSTRIALE

CORSO DI LAUREA MAGISTRALE IN IGNEGNERIA MECCANICA

VIBRATION ENERGY HARVESTING FROM RAINDROPS

Relatore:

Prof Ing. ALBERTO DORIA

Studente:

GINO FILIPI

1132128

Anno Accademico 2018/2019

“Wissenschaft und Kunst gehören der Welt. Vor ihnen verschwinden die Schranken der Nationalität „

Johann Wolfgang von Goethe

“Il est bien plus beau de savoir quelque chose de tout que de savoir tout d'une chose„

Blaise Pascal

Index

INTRODUCTION

The global trend of renewable energies is in steady growth: nowadays it is possible to obtain a very large amount of energy from hydroelectric, wind and solar power facilities. Nevertheless, according to climate researchers, this trend may still be not sufficient to diminish the alarming increase of global temperatures.
For this reason, it is necessary to both improve our current renewable energy technologies as well as to develop new ideas and new energy sources. Specifically, the field of energy harvesting is deeply entwined with that of renewable energies: indeed it could be said that the great majority of renewable energies is exploited via some processes of "harvesting the energy" from a natural and environmental source.

For example, solar energy and wind energy, two of the most important form of renewable energy, may be considered as "environmental sources" that can be extracted and employed after a process of harvesting.
However, it was not until recent that the great potential of further form of energy harvesting began to be fully recognized.

Furthermore, at the present time, it is not exaggerate to say that the research in the field of nanotechnologies is thriving, and so is the research in the field of micro-generation. Once again, when dealing with microgenerators, one of the main subject becomes energy harvesting: in fact, it is now possible to succeed in extracting energy from environmental energy sources such as electromagnetic waves, wasted heat, mechanical vibrations et similia, avoiding the use of batteries and accumulators.

As previously mentioned hereabove, it is now very easy and ordinary to produce energy from sun light and wind: however, in some very rainy regions of the world, it seems it could be also promising to develop a technology that permits to harvest energy during rainstorms. In fact, in these regions of the world, it is not possible to rely only to solar plants, especially during the rainy seasons.

More humbly, the main purpose of this Thesis, is that of evaluate the performance of a raindrop energy harvester, studying and analysing it in order to better understand its behaviour. As a deep and complete study of raindrop energy harvesting would require a far larger amount of time than that it had been possible to employ, this Thesis will deal only with the mechanical aspects. However, it must be strongly underlined that in order to achieve an efficient and successful energy conversion, the electrical part is at least as fundamental as the mechanic one.
At first, this work required a previous bibliographic research, In order to comprehend the current state of the art for raindrop energy harvesters.

This study was then followed by experimental tests, aimed at the comprehension of the behaviour of the harvester. For such a purpose, it was at first necessary to construct a particular experimental apparatus. Due to the general simplicity of the devices, that was overall a simple task.

The scope of this apparatus was that of recreating the conditions under which a real performing device would be subjected.

After performing the tests, aimed at the reproduction of the operative conditions of the system, a data analysis of the data acquired from the software **LabView SignalExpress™** was then executed. This analysis was pursued mainly with the software **Mathworks MATLAB™.**

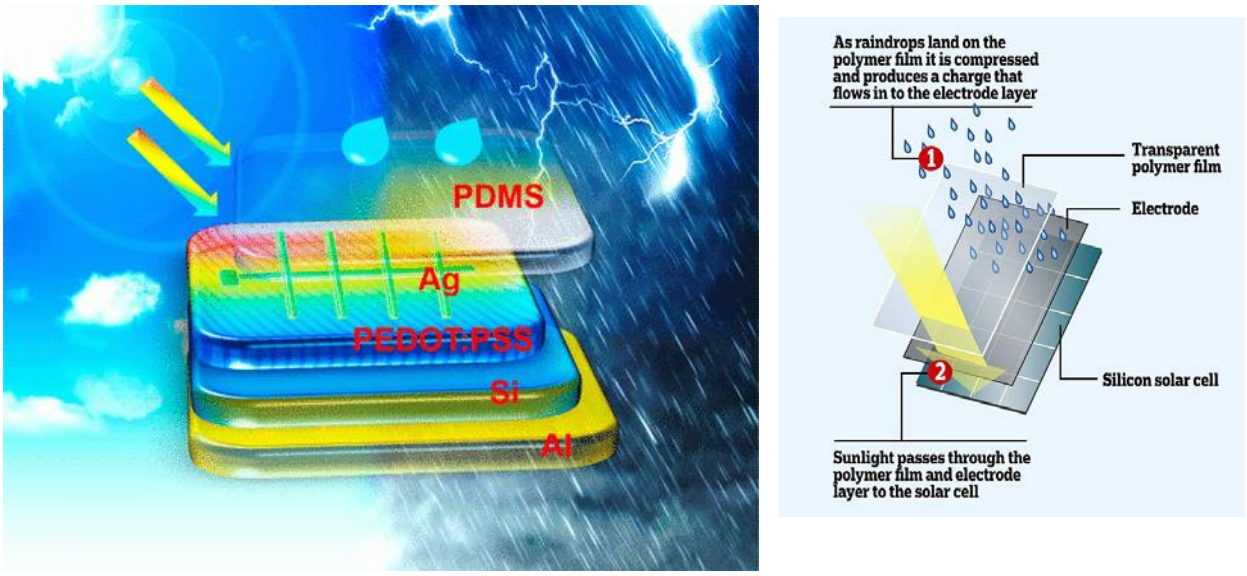

Figure 1: An hypothetical solar panel that can extract energy from both sunlight and raindrops

Chapter 1: Energy harvesting basis

It can be stated that one of the main global challenges of our current era is that of addressing the ever growing problems caused by energy production. We are indeed starting to experience the nefarious effect of global warming but we are also extremely concerned with keeping our current world economic growth rate, which requires increasing amount of energy.

For this reason, it can be easily stated that the development of cheap and sustainable energies is one of the most urgent necessity of humanity. Because of all this, there is a growing interest about a somewhat recent research field, that of "*energy harvesting*".

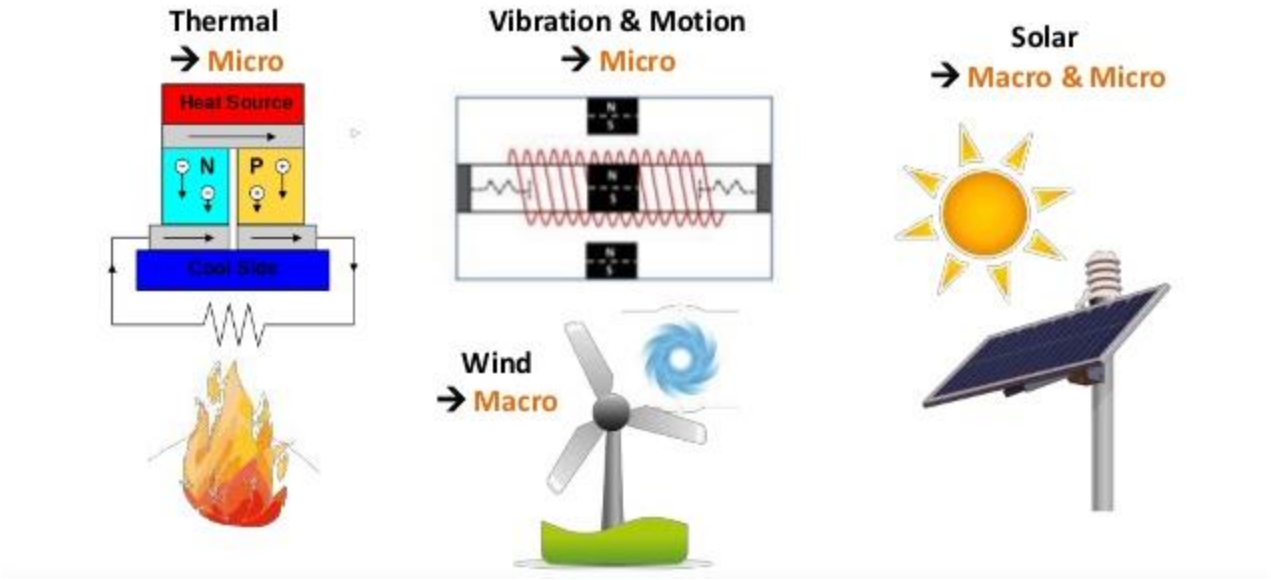

Figure 2: Examples of energy harvesting, [11]

In detail, the technology of "*energy harvesting*" aims at the extraction and storage of energy form various and usually rather weak environmental sources: they can be, for example, heat, light and other electromagnetic, waves, mechanical vibrations etc. It is easy to understand the reason why these source are interesting: in fact, outside the contest of energy harvesting, some of them would probably be defined with derogatory terms such as "disturbances" or "wasted energy".

Thus the main objective of energy harvesting is the use of this sort of "*environmental energy sources*", which can be rightly considered as "*renewable*". However, it could be legitimate to ask: "*what could be the purpose of the employment of such weak and rather unpredictable energy sources*?"
Of course it is not even slightly possible to imagine them as a substitute of ordinary energy systems (energy power plant producing energy from ordinary sources).

However, with the increasing development of **MEMS** (*micro electrical mechanical system*), which are one of the boundaries of our current technologies, it is easy to imagine that energy harvesting could become a very interesting technique to address the energy requirements of such devices. In fact, due to their size and their function, their energy consumption is also extremely low and would require an expensive, heavy and complicate system to properly feed them (at least with ordinary solutions as batteries).

The reader may find this latter sentence not totally convincing: it is not immediate to think to a field where ordinary electrical supply is expensive, complicate and invasive.

For instance, one of the most thriving fields for energy harvesting is that of biomedical devices. With the current development of miniaturization and medical technique it is now possible to create a huge amount of micro-medical devices, for very different purposes: these may range from the avoidance of invasive surgery to the continuous measurement of biological parameters through micro-sensors. It is easy to understand that for these devices ordinary supply technologies are extremely limiting and invasive.

For example, the need of feeding a cardiac device with batteries is extremely undesirable for a patient and could potentially pose a threat to their own life, in case of malfunction or exhaustion. If it were possible to feed such devices with body energy, most of the problems would disappear and the quality of life of the patient would dramatically improve. For this reason, the development of energy harvesting has a great chance of deeply transform medical technology. The figure below offers an example of all this, showing a prototype of a cardiac mechanical energy harvester.

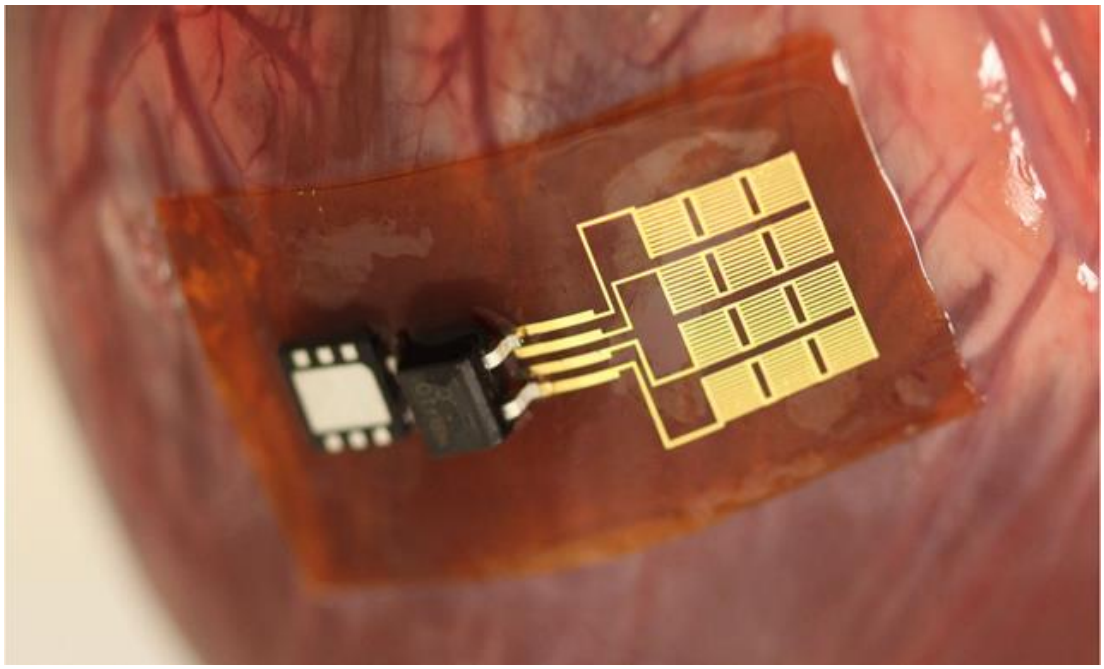

Figure 3: An energy harvester for the extraction of mechanical energy applied on a cow heart

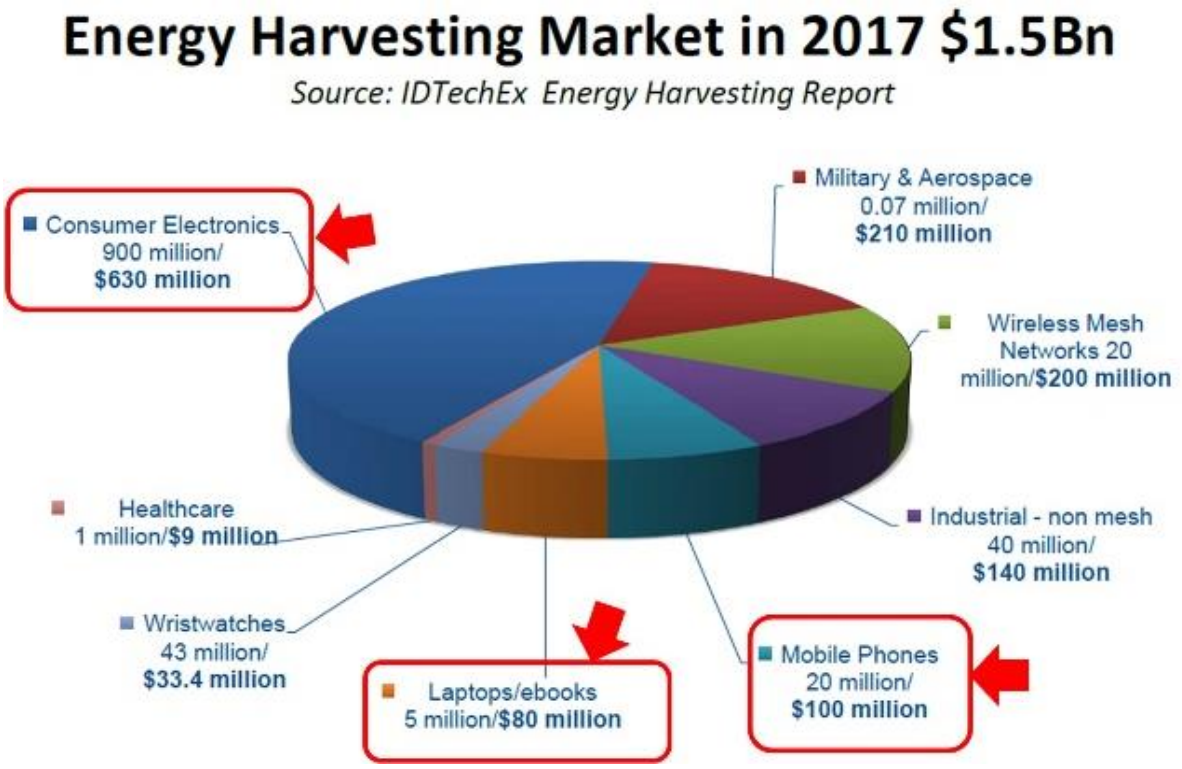

Figure 4: This chart shows the recent development of energy harvesting technologies and the fields where they are at most currently employed

Figure 5: This image shows possible new sensors in future automobiles: these sensors could be easily fed with a wise use of energy harvesters

One of the most important aspects of energy harvesting is the **complex electronics** that it requires for a proper functioning: in fact ambient energy sources are usually affected by some disturbances that prevent from obtaining a steady and regular energy output (that it is usually required by electronic devices), see [5]. One of the biggest challenges of this technology is therefore the development of flexible and simple energy conversion and energy storage systems that can yet satisfy the requirements for an efficient energy production.

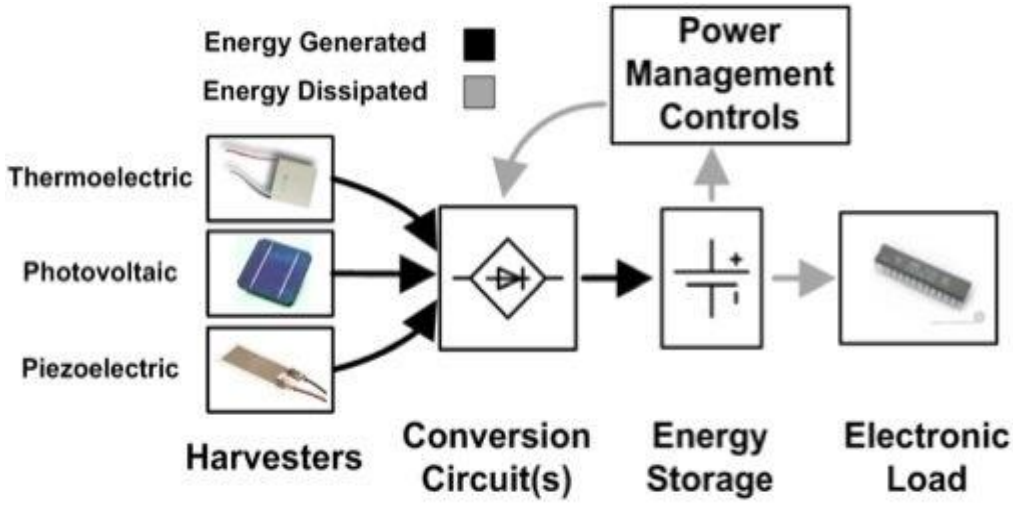

Figure 6: Basic components of an energy harvesting system. Image courtesy of harvesting-energy.com.

More in detail, ambient energy sources are of course "less reliable" and less steady than ordinary energies sources: therefore the component will need to be designed to work under transient condition. It is than task of the conversion circuit that of converting a transient amount of energy into a steady electric power output.

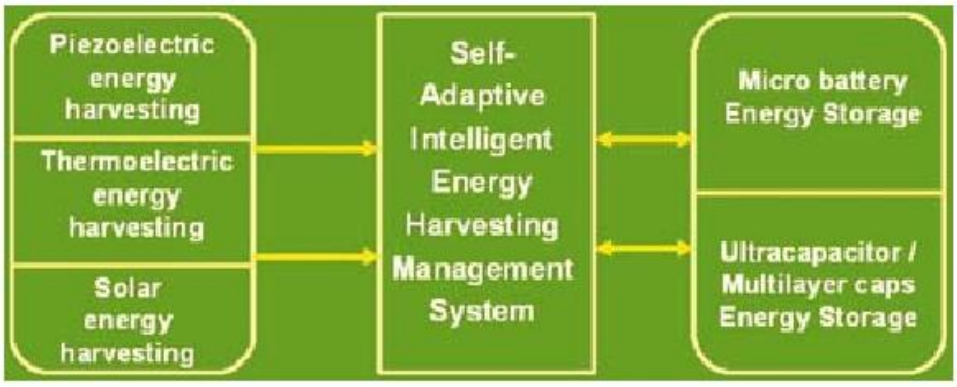

Figure 7: Schematic of the architecture required for self-powered wireless sensor network to achieve desired reliability for long period of time [1]

1.1 Examples of energy harvesting

The energy harvesting techniques can be applied with a wide range of ambient energy sources: the next figures will provide some examples.

Thermoelectric energy harvesting

The thermoelectric energy harvesting is the production of electrical energy from an environmental thermal source. In fact, thanks to the Seebeck effect, it is possible to obtain an electrical tension in presence of a temperature gradient. This is the same effect used to measure temperatures through thermocouples.

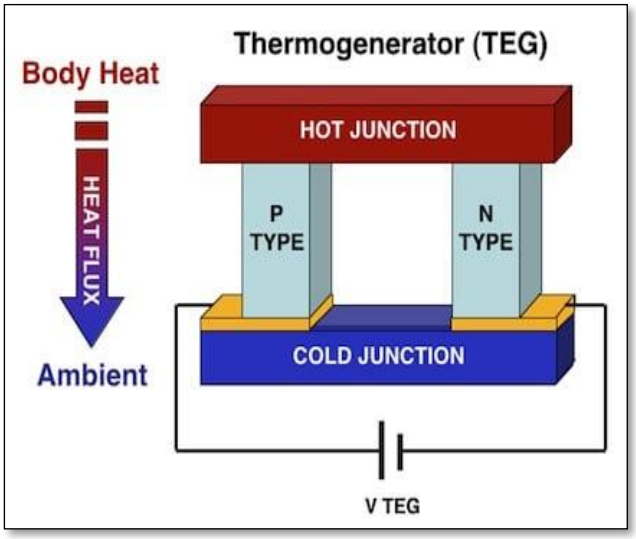

Photovoltaic energy harvesting

The photovoltaic energy harvesting is surely the most successful energy harvesting technique. It is possible to convert light in electrical energy thanks to the so called "photovoltaic effect": in an adequate constructed PN junction it is possible for free charges to absorb photons from incident light. Then, these excited free charges manifest themselves macroscopically as an electric current moving in the circuit connected to the PN junction.

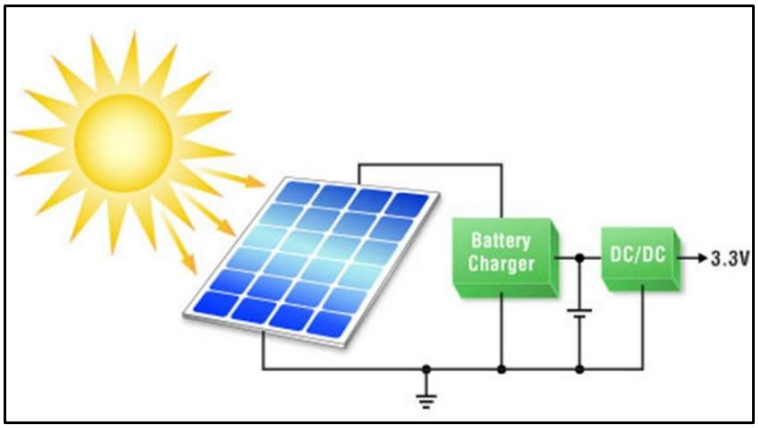

Radio frequencies energy harvesting

RF energy harvester are able to extract energy from electromagnetic waves: they are substantially antennas whose purpose is not that of picking a radio signal to decode information, but rather to use that signal as an energy source. It is evident that the energies involved in these devices are extreme low, indeed the lowest even among the other energy harvesters, as shown in figure 9.

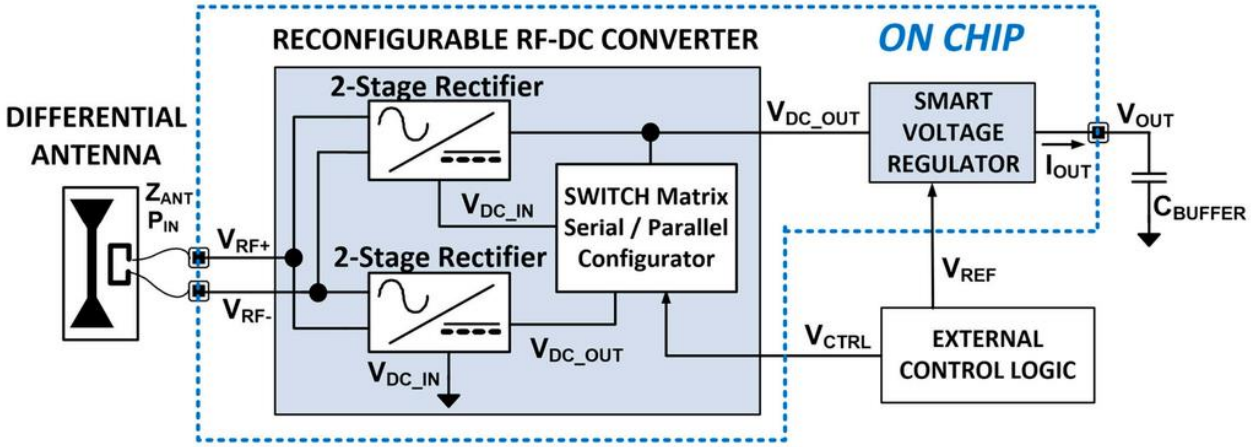

Figure 8: A scheme of a reconfigurable RF energy harvester, from [14]

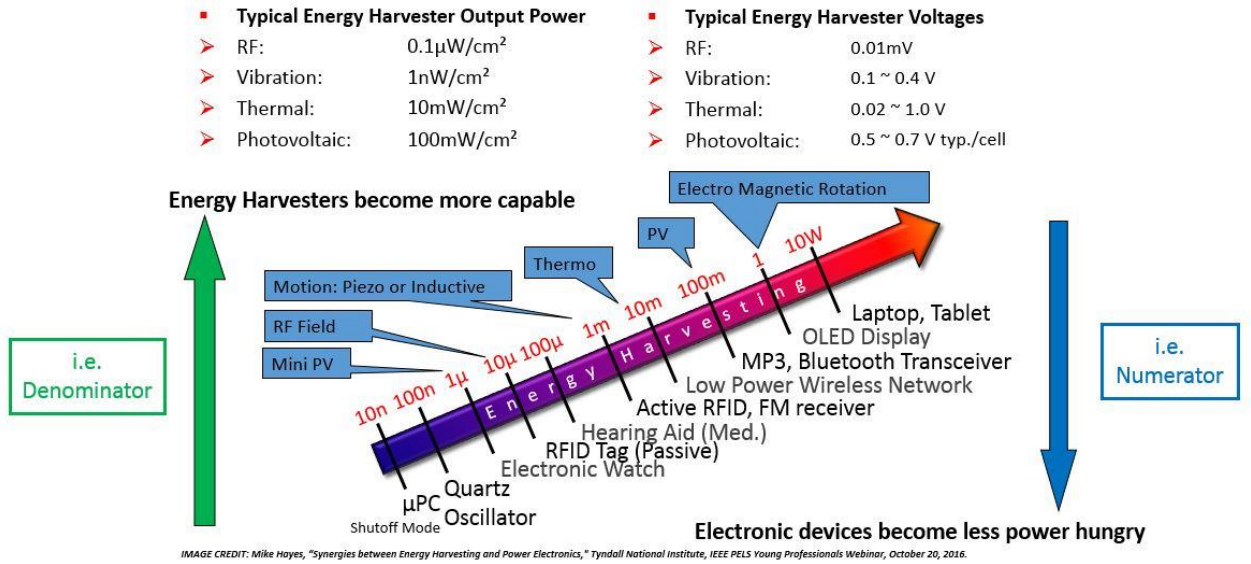

Figure 9: This figure compares the power produced by different energy harvesters to the power requirements of various electronic devices

1.2 Vibration energy harvesting

One of the most interesting sources for energy harvesting is for sure **vibrational energy**. This is indeed one of the most common form of "*environmental energy*": vibration are usually one of the most undesired and yet unavoidable results of mechanical motion in machines.

It is possible in some cases to harvest part of the wasted energy of the vibration, and then to use it to feed sensors or other MEMS, removing the need of batteries or electrical connections, as well as reducing maintenance costs.

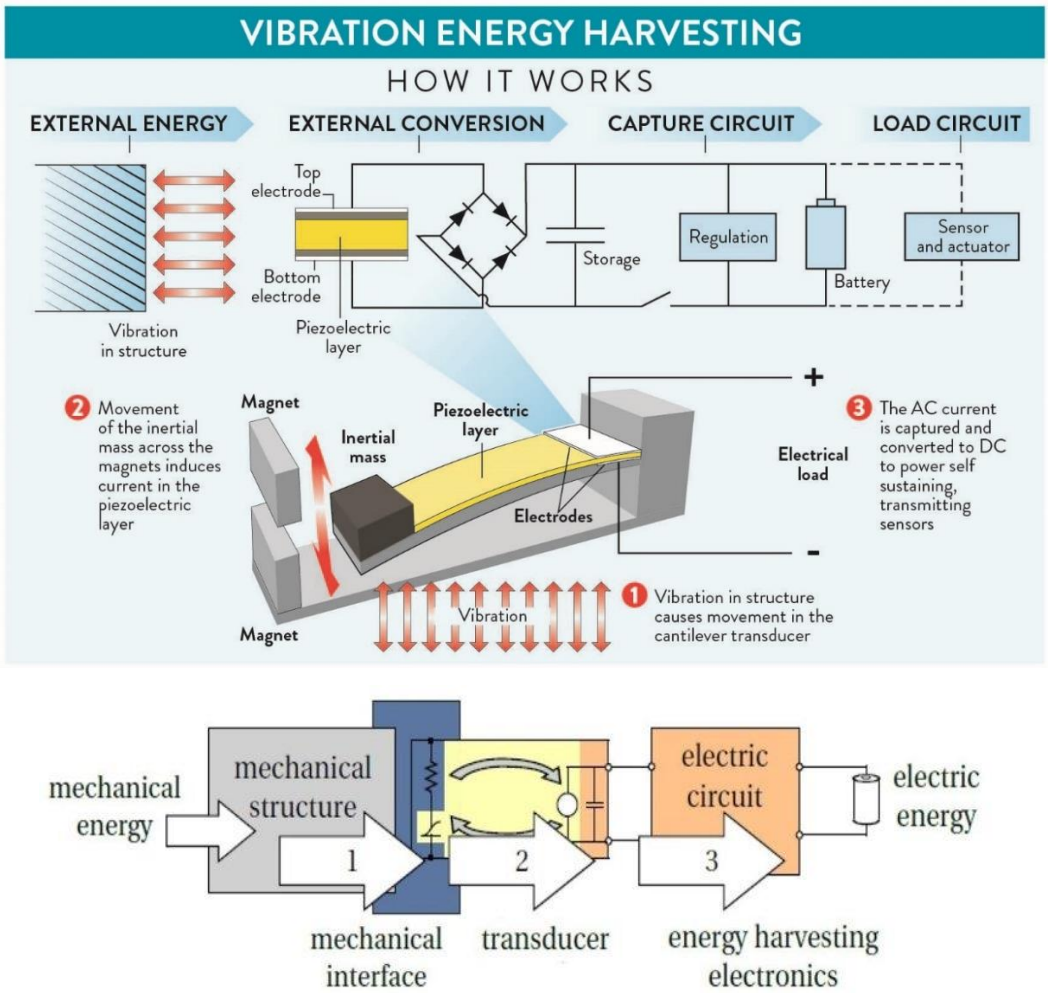

Figure 10: Scheme of vibration energy harvesting, [12]

Vibrational harvesters are usually made with mass-spring systems: the kinetic energy is beforehand mechanically converted and stored, and then transduced into electrical energy. There are three types of kinetic-electrical transduction, as shown in the next figure:

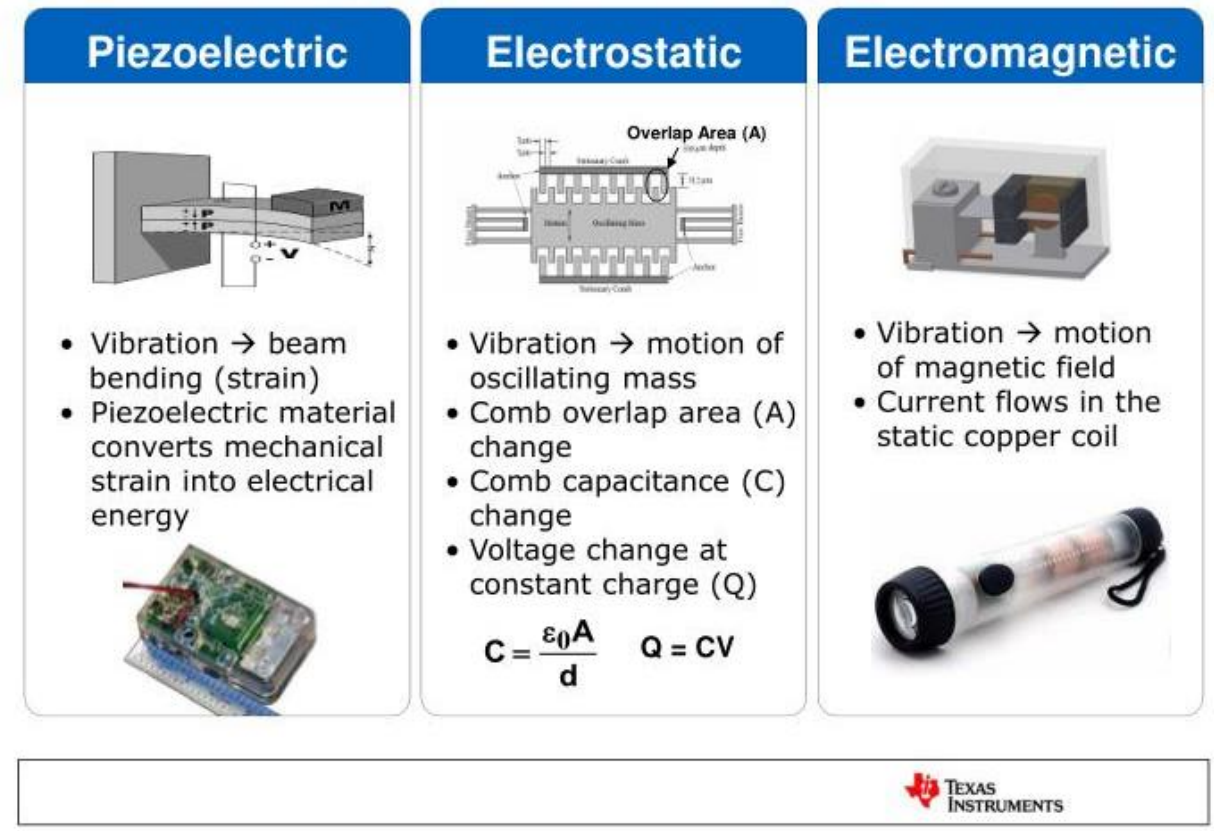

Figure 11: Different types of vibrational harvesting

In **electromagnetic transducers** the motion of a permanent magnet induces in the coils around it a tension, according to Faraday's induction law. That is, the tension is in proportion with the rate of variation of the flux of the magnetic field through the coils.

Electrostatic transducers use variable capacitors to transform the differential motion of the plate into electrostatic energy, varying the overall capacity of the capacitor. However, in order to function, these convertors require to possess and maintain an initial electrical charge.

Piezoelectric transducer use the piezoelectric effect to convert kinetic energy in deformation energy and then in electrostatic energy. These are the transducer adopted for raindrop energy harvesters: their characteristics will be explored further in detail in the following section.

This next table shows the advantages and the drawbacks for each type of mechanical energy harvester.

Type	Advantages	Disadvantages
Electromagnetic	• No external voltage source • No mechanical constraints needed • High output current	• Difficult to integrate with MEMS fabrication process • Poor performance in micro-scale • Low output voltage
Piezoelectric	• Simple structure • No external voltage source • Compatible with MEMS • High output voltage • No mechanical constraints needed	• Thin films have poor coupling • Poor mechanical properties • High output impedance • Charge leakage • Low output current
Electrostatic	• Easy to integrate with MEMS fabrication process • High output voltage	• Mechanical constraints needed • External voltage source or pre-charged electret needed • High output impedance • Low output current
Magnetostrictive	• Ultra-high coupling coefficient • High flexibility	• Non-linear effect • May need bias magnets • Difficult to integrate with MEMS fabrication process

Table 1: Comparison of different transduction mechanism of kinetic energy harvester and their advantages and disadvantages, [3]

1.3 Piezoelectric harvesters

Piezoelectric harvesters are mainly constructed with cantilever beam with one or two layers of piezoelectric material added to the surfaces normal to the motion. As shown in figure 12, the vertical displacement induces flexion stresses in the beam that, thanks to the piezoelectric effect, generate displacement of the net electrical charge: by the application of an external electric field, this results then in an electrical current. As the upper surface is extended and the lower contracted, opposite electrical charges appears on them. So, with the connection of these surfaces to an electrical circuit, it is possible to feed a load with an electric current.

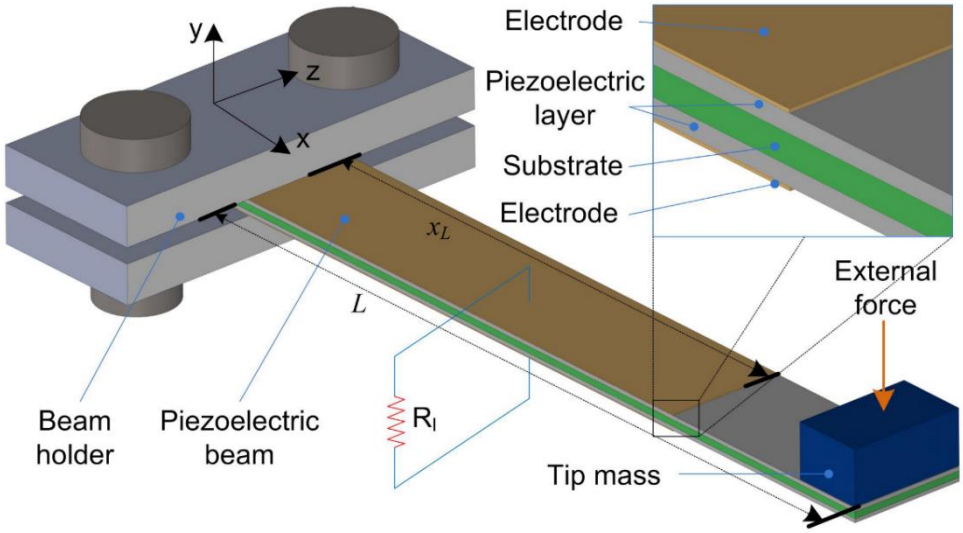

Figure 12: Example of piezoelectric cantilever beam [9]

One of the main disadvantages of piezoelectric harvesters is that they need to work under design condition, otherwise they are not able to convert properly mechanical energy. In fact, they ideal work condition is when they oscillate at their lowest **resonance frequency**. In figure 13 it is possible to understand the reason of this: in a system subjected to forced vibrations, the energy absorbed by the equivalent mass and spring is the highest when the system vibrates at its resonance frequency.

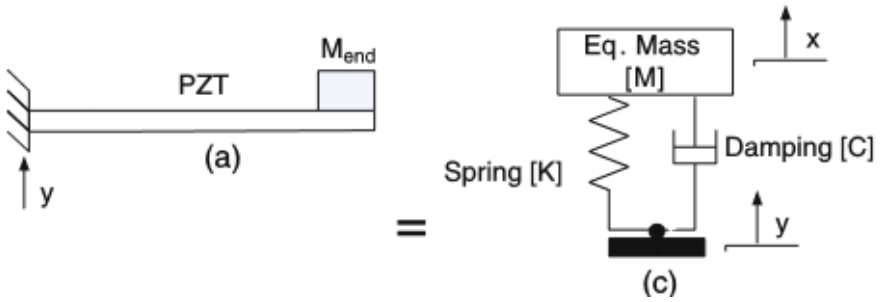

Figure 13: Mechanical scheme of a cantilever piezoelectric harvester (a), and its lumped parameters equivalent (c), from [1]

1.3.1 Piezoelectricity

The purpose of this section is to briefly explain how the harvester converts mechanical energy in electrical energy. For this reason, it is necessary at first to describe the piezoelectric effect. The piezoelectric effect is that particular phaenomenon that happens when an **electrical charge** appears as a result of a **mechanical deformation** of a solid material.

The piezoelectric effect is reversible: when the mechanical strain is removed, the net electrical charge disappears. It is also possible to invert this effect, that is, in a piezoelectric material an **electric field** (that can be induced by simply applying an electrical tension between two surfaces of the material) results in a **mechanical deformation**.

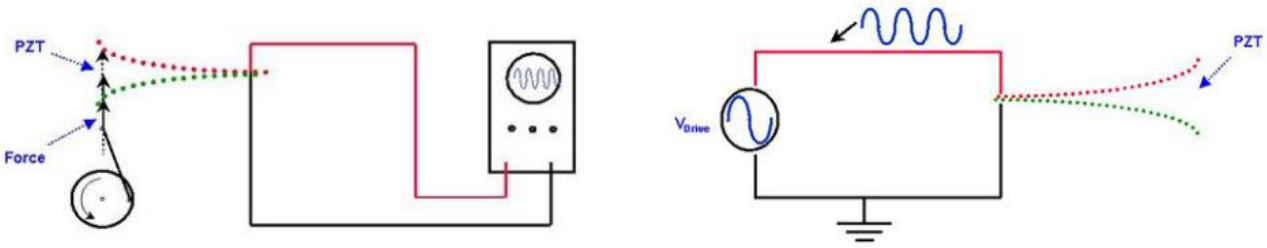

Figure 14: Scheme of the piezoelectric effect. In the left, direct piezoelectric effect (a mechanical strain generates an electrical tension). In the right, inverse piezoelectric effect (a sinusoidal tension results in a mechanical vibration)

However the reader is legitimate to ask themselves, why are some material able to manifest the piezoelectric effect? The reason lies in the crystal structure of such materials: as they basically do not possess a symmetrical crystal structure, both a mechanical deformation or an external electric field result in the alteration of the balance of the atomic disposition resulting in the piezoelectric effect, as presented in the figure 15 below.

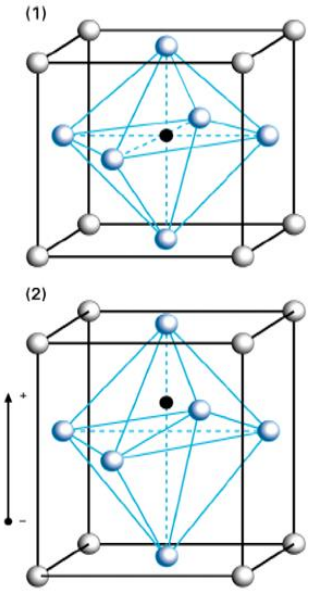

Figure 15: Piezoelectric materials possess usually the perovskite structure. This figure shows the structure of a perovskite lattice. The displacement of the central black atom alters the symmetry of the lattice, creating a net electric dipole. This can be also inverted: an external electrical field alters the position of the central black atom, resulting in a displacement and thus in a deformation.

1.3.2 Mathematical description of piezoelectricity

There are various mathematical models to express the piezoelectric effect. The one adopted in all analytical analyses is descended directly from [1] and [3].

Nomenclature

- σ_{ij}: *components of the stress tensor*
- D_j: *components of the electrical displacement vector*
- k_{ijkl}: *components of the stiffnes matrix*
- ε_{kl}: *components of the strain tensor*
- $\tilde{p}_{mij}$: *components of the piezoelectric tensor*
- E_m: *components of the electrical field vector*
- $e_{ij}^{\varepsilon=con.}$: *components of the dielectrical tensor at constant strain*

$$\sigma_{ij} = k_{ijkl}\varepsilon_{kl} - \tilde{p}_{mij}^{T} E_m$$
$$D_j = \tilde{p}_{ijk}\varepsilon_{jk} - e_{ij}^{\varepsilon=cost} E_j \tag{1.1}$$

That written as matrixes become:

$$\bar{\sigma} = [k]\bar{\varepsilon} - [\tilde{p}]^T \bar{E}$$
$$\bar{D} = [\tilde{p}]\bar{\varepsilon} - [e]\bar{E}$$
$$\begin{Bmatrix} \sigma \\ D \end{Bmatrix} = \begin{bmatrix} k & \tilde{p} \\ d & e^{\varepsilon=cost} \end{bmatrix} \cdot \begin{Bmatrix} \varepsilon \\ E \end{Bmatrix} \tag{1.2}$$

$$\begin{Bmatrix} \sigma_{11} \\ \sigma_{22} \\ \sigma_{33} \\ \sigma_{23} \\ \sigma_{13} \\ \sigma_{12} \\ D_1 \\ D_2 \\ D_3 \end{Bmatrix} = \begin{bmatrix} k_{11} & k_{12} & k_{13} & 0 & 0 & 0 & 0 & 0 & \tilde{p}_{31} \\ k_{21} & k_{22} & k_{23} & 0 & 0 & 0 & 0 & 0 & \tilde{p}_{31} \\ k_{31} & k_{32} & k_{33} & 0 & 0 & 0 & 0 & 0 & \tilde{p}_{33} \\ 0 & 0 & 0 & k_{44} & 0 & 0 & 0 & \tilde{p}_{15} & 0 \\ 0 & 0 & 0 & 0 & k_{44} & 0 & \tilde{p}_{15} & 0 & 0 \\ 0 & 0 & 0 & 0 & 0 & \frac{k_{11}-k_{12}}{2} & 0 & 0 & 0 \\ 0 & 0 & 0 & 0 & \tilde{p}_{15} & 0 & e_{11}^{\varepsilon} & 0 & 0 \\ 0 & 0 & 0 & \tilde{p}_{15} & 0 & 0 & 0 & e_{11}^{\varepsilon} & 0 \\ \tilde{p}_{31} & \tilde{p}_{31} & \tilde{p}_{33} & 0 & 0 & 0 & 0 & 0 & e_{33}^{\varepsilon} \end{bmatrix} \cdot \begin{Bmatrix} \varepsilon_{11} \\ \varepsilon_{22} \\ \varepsilon_{33} \\ 2\varepsilon_{23} \\ 2\varepsilon_{13} \\ 2\varepsilon_{12} \\ E_1 \\ E_2 \\ E_3 \end{Bmatrix}$$

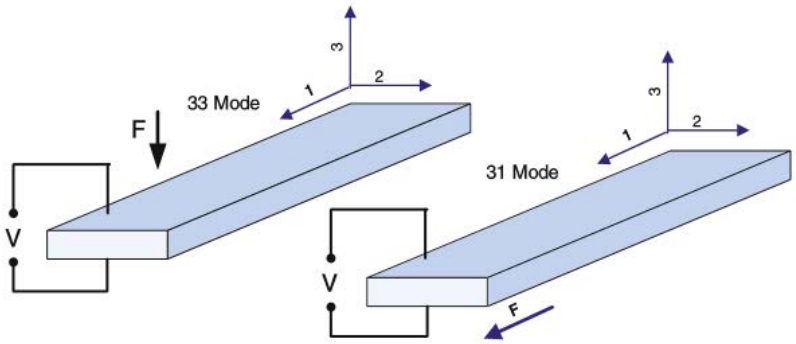

Figure 16: The piezoelectric effect can be used in two different ways to create an electrical tension in cantilever beams: with the 33 mode the stress follows the same direction of the electric field; in the 31 mode, the stress is in the longitudinal direction, while the electric field is now orthogonal to it.

1.3.3 Electro-mechanic model of a piezoelectric cantilever beam

Piezoelectric cantilever beams can assume three configurations: the one adopted in calculations is the simplest one, the "*unimorph*".

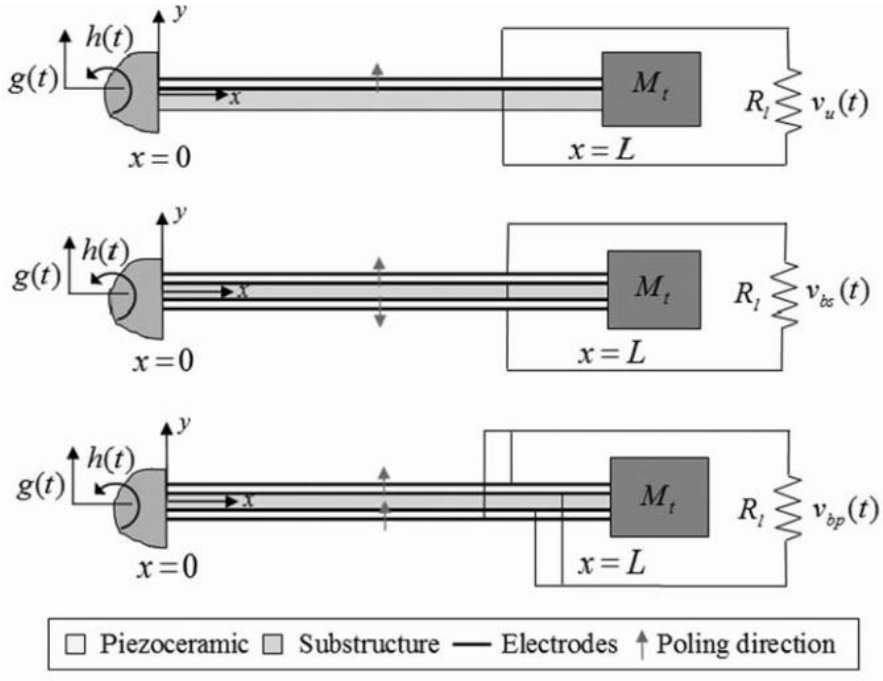

Figure 17: Cantilevered piezoelectric energy harvester configurations under base excitation; (a) unimorph configuration, (b) bimorph configuration (series connection), and (c) bimorph configuration (parallel connection)

This section follows describing briefly the model of lump parameters for unimorph cantilevers and their closed form solution for an harmonic base excitation For further information and the complete demonstration, see [1]. The cantilever is studied with Euler-Bernoulli beam theory with external and internal damping. The equation of motion for vibrations is:

$$EI\frac{\partial^4 w(x,t)}{\partial x^4} + c_s I\frac{\partial^5 w(x,t)}{\partial x^4 \partial t} + c_a\frac{\partial w(x,t)}{\partial t} + \rho\frac{\partial^2 w(x,t)}{\partial t^2} = 0 \tag{1.3}$$

With **E** is **Young's modulus**, **I** the **second moment of the section**, $\boldsymbol{c_s}$**I** the **internal strain rate**, **w** the **displacement in the transverse direction** and **ρ** the **linear mass density of the beam.** For what concerns the displacement it is then possible to divide it into the **displacement of the basis** and the **displacement of the beam** with respect of the basis:

$$w(x,t) = w_b(x,t) + w_{rel}(x,t) \tag{1.4}$$

This differential equation can be solved with the **separation of variables**. This results in:

$$w^s_{rel}(x,t) = \sum_{k=1}^{\infty} W_k(x)\cdot T^s_k(t) \tag{1.5}$$

Where $\boldsymbol{W_k(x)}$ is the **modal shape of the k mode** and $\boldsymbol{T^s_k(t)}$ **the modal coordinate k**. After normalising the modal coordinates by the application of orthogonal conditions (1.5) can be finally written as:

$$\frac{d^2 T^s_k(t)}{dt^2} + 2\zeta_k\omega_k\frac{dT^s_k(t)}{dt} + \omega_k^2 T^s_k(t) - \chi^s_k\cdot v^s(t) = f_k(t) \tag{1.6}$$

This is the equation of motion in **modal coordinates**: $\boldsymbol{v^s}$ is **the tension across the load** connected to the harvester, $\boldsymbol{\chi^s_k}$ is **the "backward" modal electro-mechanic coupling term** (it is the modal constant that brings the tension into the mechanical equation) and $\boldsymbol{f_k}$ the **modal force**. The apex "*s*" indicates the unimorph connection.

In order to complete the description, it is necessary to study the electrical circuit of the harvester: each piezoelectric layer can be described as a current generator connected in parallel with a capacitator.

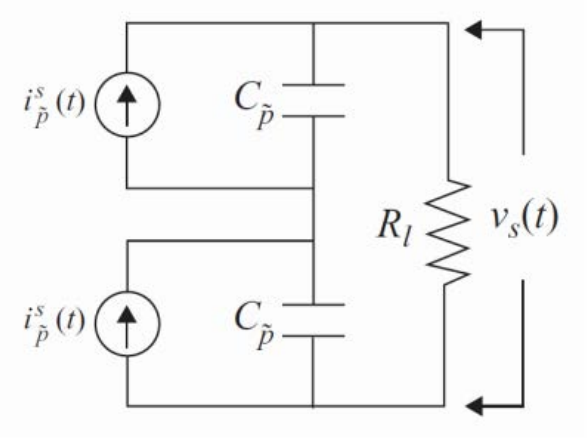

Figure 18: Electrical circuit model of the piezoelectric layers. Each layer is represented with a generator and a capacitor, connected with an resistive load

The application of Kirchhoff's laws then yields to:

$$\frac{C_{\tilde{p}}}{2} \cdot \frac{dv^s(t)}{dt} + \frac{v^s(t)}{R_l} - i_{\tilde{p}}^{s}(t) = 0 \tag{1.7}$$

Finally the piezoelectric cantilever beam can be described by the **state variables** $[\boldsymbol{v^s(t)}, \boldsymbol{T_k^s(t)}]$ in the following **system of differential equations:**

$$\begin{cases} \dfrac{d^2T_k^s(t)}{dt^2} + 2\zeta_k\omega_k \dfrac{dT_k^s(t)}{dt} + \omega_k^2 T_k^s(t) - \chi_k^s \cdot v^s(t) = f_k(t) \\ \dfrac{C_{\tilde{p}}}{2} \cdot \dfrac{dv^s(t)}{dt} + \dfrac{v^s(t)}{R_l} - i_{\tilde{p}}^{s}(t) = 0 \end{cases} \tag{1.8}$$

It is also possible to express the circuit characteristic as function of the properties of the piezoelectric layers:

$$C_{\tilde{p}} = \frac{\varepsilon_{33}^{S} bL}{h_{pu}} \quad , \qquad i_{\tilde{p}}^{S} = \sum_{k=1}^{\infty} \varphi_k^S \frac{dT_k^S}{dt} \tag{1.9}$$

Where **L is the length** of the beam, **b its width**, $\boldsymbol{h_{pu}}$ **the distance between the neutral axis of the beam and the centre of the piezoelectric layer**, and $\boldsymbol{\varphi_k^S}$ is the **"foreward" modal electro-mechanic coupling term** (it is the modal constant that brings the modal velocity in the electrical equation).

Chapter 2: Raindrop energy harvesting

The interest about energy harvesting from raindrops has been steadily growing in recent years: however it can be said that the full potential of this technology is yet to be understood and developed. The easiest method utilised to harvest raindrop energy is that of extracting mechanical energy via a piezoelectric device.

Obviously, the energy output using such a method will be extremely low in comparison to ordinary renewable sources. However, it is still possible that even this low energy output could be used in very **low power application**, where the use of batteries or the connection to an external supply grid would not be a feasible solution [2]. In fact, while it is true that mechanical harvesters require as well to develop a supply circuit, on the other hand it is clear that harvesters have a longer lifespan, do not require the same rare materials of batteries and usually are not as big in size and mass.

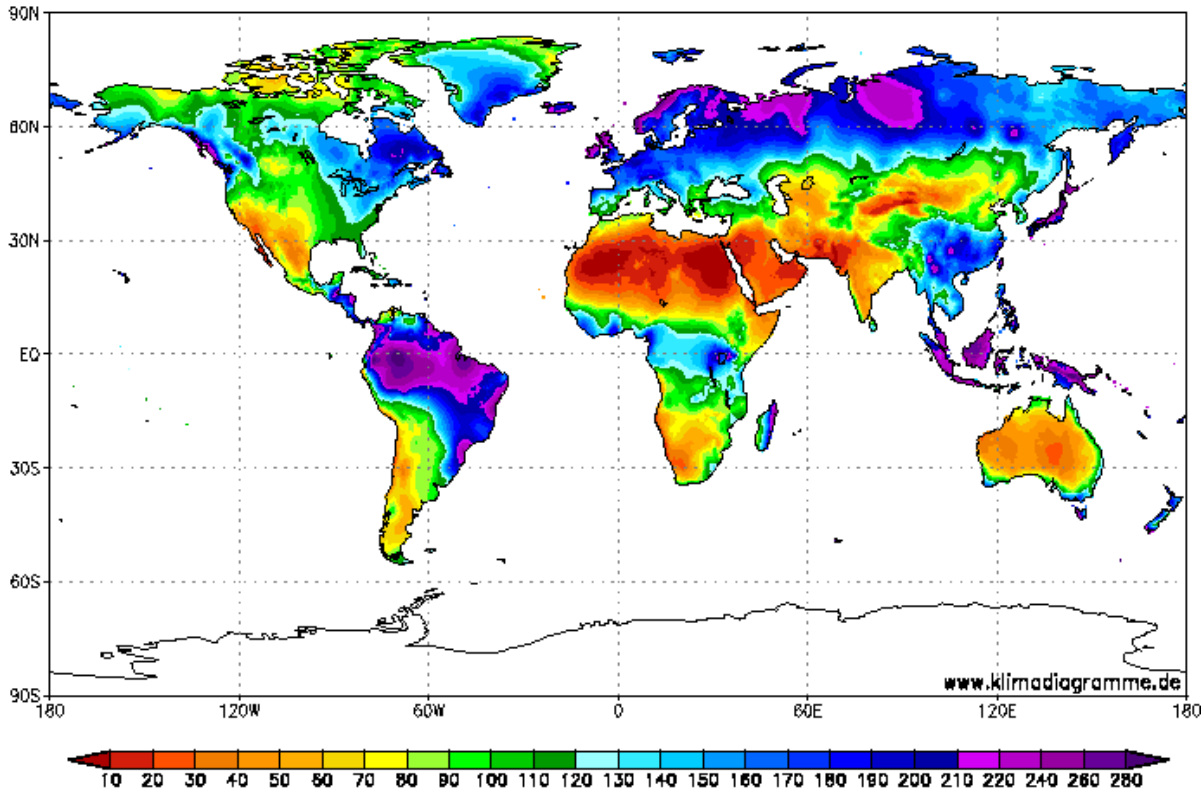

Figure 19: Average number of rainy days per year, from 1961 to 1990

As shown in the previous figure 19, there are some places in the world that experience a very **rainy climate** (the tropical zone around the Equator): in these places, the development of rain drop energy harvesting could become comparable to one of the ordinary energy sources as solar energy. These countries are also rapidly developing countries (Brazil, Indonesia, Malaysia) and possess a rather advanced technology in the fields of electronic (that is why many of the biggest investors in raindrop energy harvesting usually are from these countries).

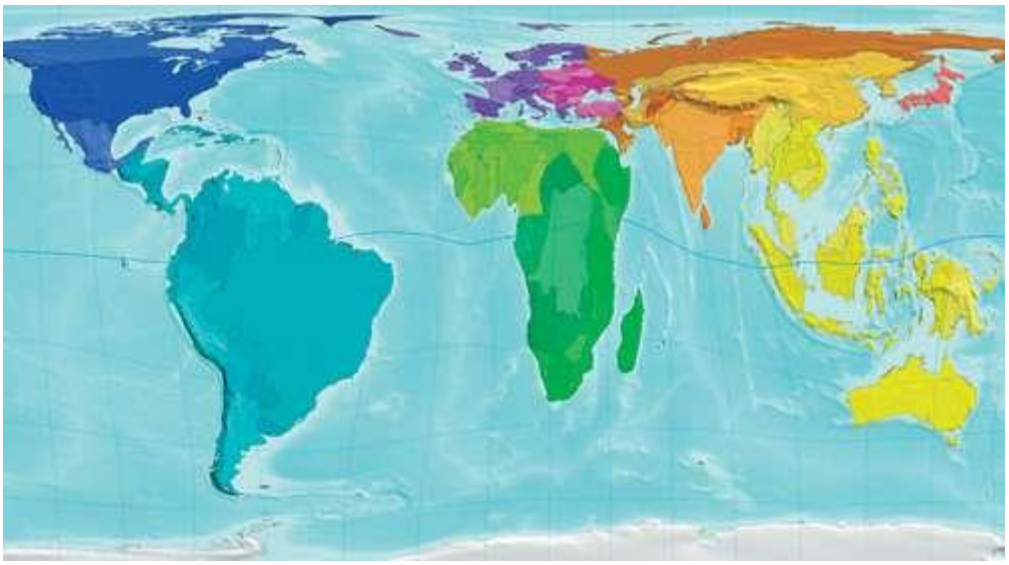

Figure 20: Volume of rainfall. The more the region is deformed, the more is the volume of rainfall, [13]

Moreover, the rainfall in these countries is not only frequent, it is also very intense due to the low latitude: in fact both the radius and the velocity of raindrops are relatively higher when compared to the values typical of temperate zones (see further Tab. 2). As this obviously implies a much higher kinetic energy, consequently it is in these places that raindrop energy harvesting has the greatest and most promising potential.

2.1 Behaviour of raindrops

The key factors that influence the output of a rain energy harvester are all related to the **energy of the waterdrops**. Thus they are the radius and the shape, the mass and the velocity at the instant of impact.
The force that causes the freefall is obviously the **gravity force**, that is:

$$F_g = \frac{4}{3}\pi r^3 \rho_w g \qquad (2.1)$$

Where r is the radius of the droplet, ρ_w the density of water and g the acceleration of gravity.

Each droplet is subjected also to the **drag force** generated by the air that can be expressed as:

$$F_{air} = \frac{1}{2}\rho_a A C_d v^2 \qquad (2.2)$$

Where A is the **projected surface** of the droplet in the direction of motion, ρ_a is the **density** of air, C_d the **drag coefficient** and v the **velocity** of the droplet. During its freefall from the upper troposphere, the droplet travels long enough to reach its **terminal velocity**:

$$v_t = \sqrt{\frac{\pi d^3 \rho_w g}{6\rho_a A C}} \qquad (2.3)$$

For the sake of simplicity, it was assumed that each droplet maintains a **spherical shape** during its fall. In reality, the shape is influenced by air resistance and wind: however, as the experiments were performed indoor, it could safely assumed that the droplets possess a spherical shape [2].

The impact behaviour of the water can be extremely different, depending on the conditions of the surface it hits.

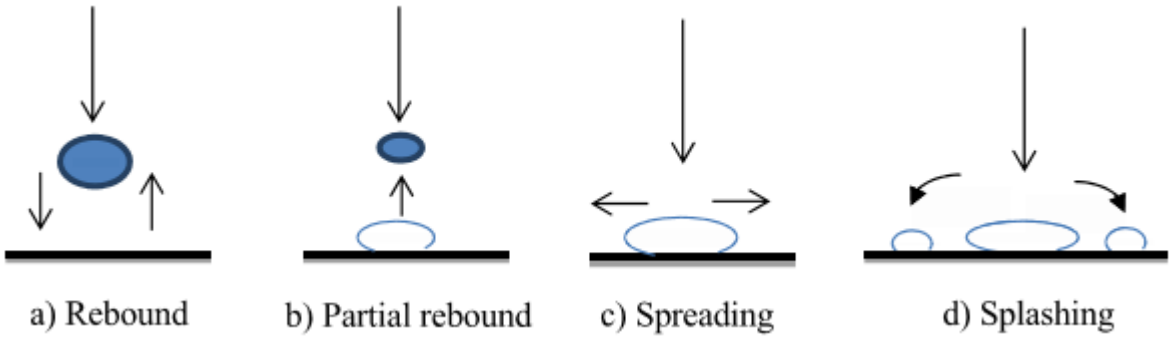

Figure 21: Types of impact of a droplet with a solid surface, [2]

It has been discovered that the diameter of the droplet and their terminal speed are not independent factors, but they are instead related to the intensity of the rain.

Rain type	Drop size (mm)	Terminal velocity (m/s)
Light stratiform rain		
Small	0.5	2.06
Large	2.0	6.49
Moderate stratiform rain		
Small	1.0	4.03
Large	2.6	7.57
Heavy thundershower		
Small	1.2	4.64
Large	4.0	8.83
Largest	5.0	9.09

Table 2: Rain types and their influence on drop diameter and terminal velocity, see [4]

The equation of motion for a falling droplet can be written from 2.1 and 2.2:

$$F_g - F_d = m\dot{v}$$

$$\frac{4}{3}\pi r^3 \rho_w g - \frac{1}{2}\rho_a \pi r^2 C_d v^2 = \frac{4}{3}\pi r^3 \rho_w \dot{v} \tag{2.4}$$

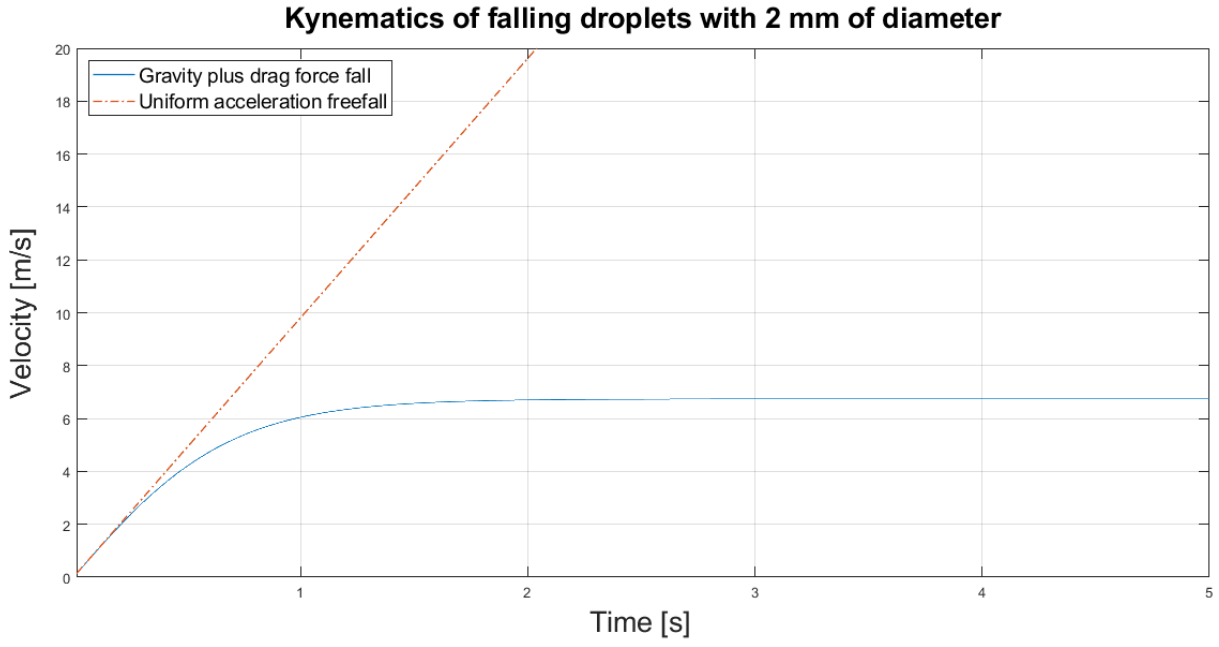

Figure 22: Velocity of a falling droplet with 2 mm of diameter, solved with Matlab. Its terminal velocity (6.74 m/s) is comparable to the value of Table 2

In order to solve the non-linear differential equation, the software **Matlab** was used. The equation was solved with the **finite difference method**. Figure 23 and 24 show the results of the calculation.

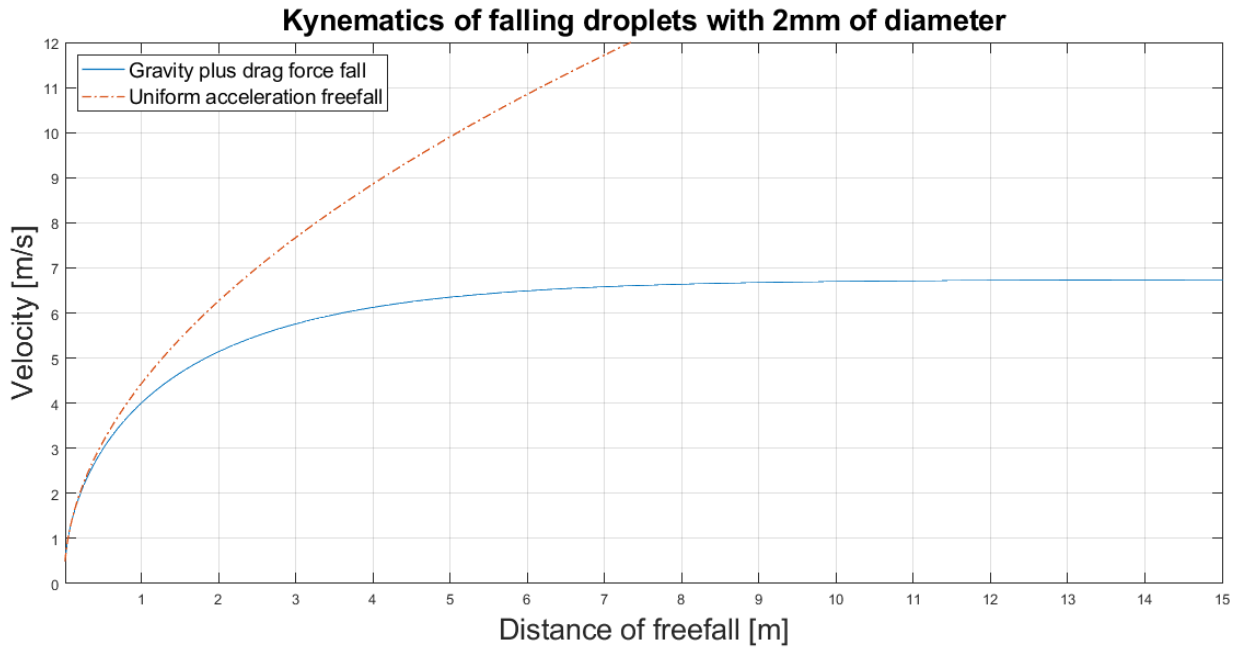

Figure 23: This figure shows the velocity of the droplet with respect to the distance of freefall

As the figure 24 shows, a water droplet with a diameter of 2 mm reaches its terminal velocity after circa 10 meters in freefall. It is also worth to note that after a fall of **2 m**, the droplet reaches **76% of its terminal velocity**.

During the indoor simulations, the more is the height of the fall, the more is difficult to hit the harvester with the drop. Thus, for the sake of simplicity, the experiments were performed mostly at an height of **1 m**. In this case, the velocity of the droplet is circa **60% of its terminal velocity**.

2.2 Behaviour of raindrop energy harvesters

A first analysis of the behaviour of a raindrop energy harvester can be found in [2]. This paper, describes the output of an Harvester when hit with waterdrop from small heights (h ≤ 50 cm). The main difference with the tests performed during this work is the absence of a spoon that acts as a tip mass and collects the water.

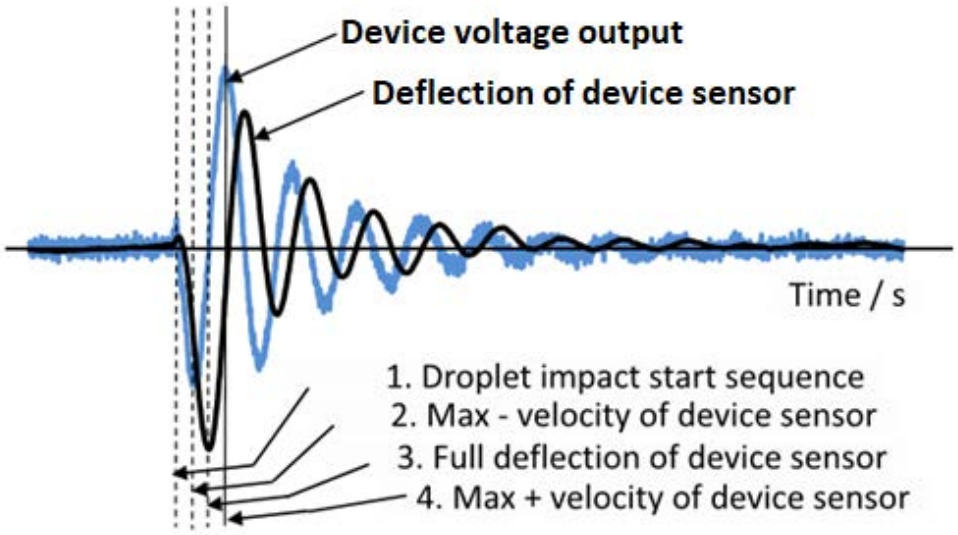

Figure 24: Voltage output and deflection in the impact point of the harvester, from [2]

As it can be seen in the figure 24 above, the impulse created by a droplet generates a signal of tension that can be said to be similar to an exponential-sinusoidal function. This behaviour is rather predictable: this harvester acts more or less like an *underdamped* **mass-spring-damper system**, with an exponential decay of the oscillations. The only difference happens at the first peaks: in fact, it is possible to see that the maximum value of the voltage is not that of the first (negative) peak, but rather that of the second (positive) peak. For this reason, the voltage experiences a growth in its amplitude during the first oscillation, before the ensuing exponential decay.

According to [2], the voltage output reaches the 0 for the first time after the impact when the device experiences the full deflection (figure 24 again). In such condition, the exchange of energy between the drop and the piezoelectric beam is completed.. For this reason, the maximal velocity is reached at the second (positive) peak and that also yields the maximal tension. As it can be seen, in the same

instant the deflection is 0: thus, according to this model, tension and deflexion are in quadrature to each other.

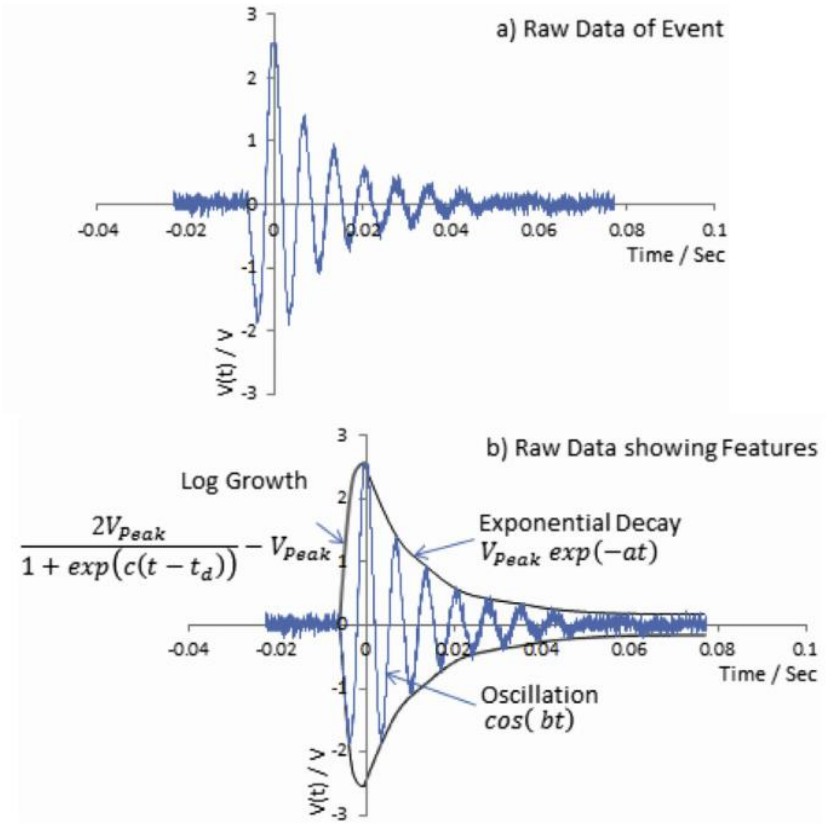

Figure 25: *This figure shows the signal of the tension after the impact with a waterdrop. In particular, in b) it is possible to show the mathematical functions that fit the evolution of the amplitude in the time (see [2]).*

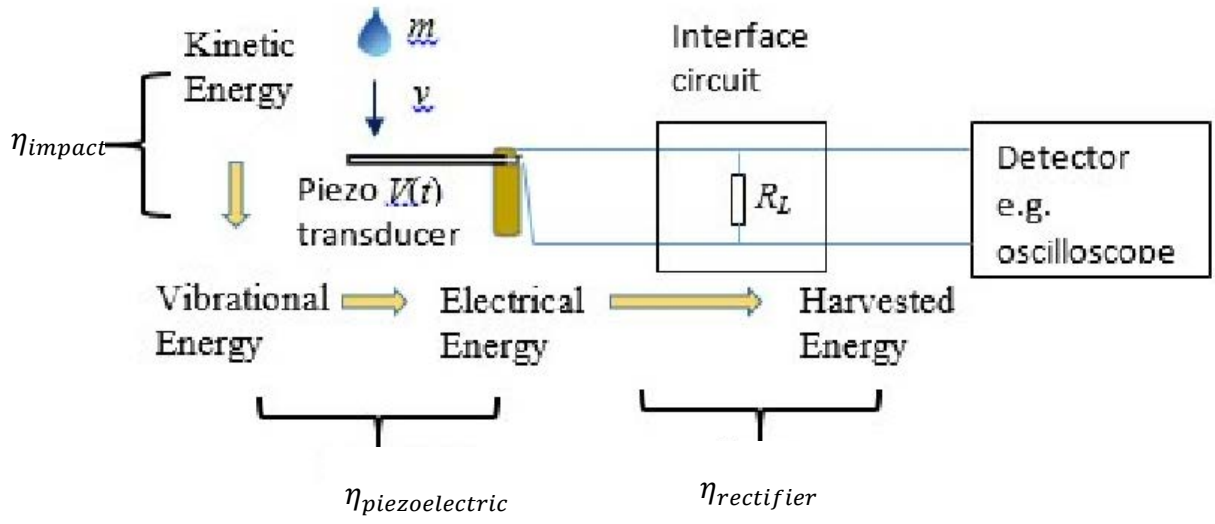

Figure 26: *Scheme of measuring system for a raindrop energy harvester*

One of the main issues with this kind of energy harvester is their **low efficiency of overall energy conversion**. This can be easily seen as well in tab. 3. However, unlike what stated in [2], in all the tests performed for this work it appeared clear that the presence of water, while enhancing the overall damping factor, increases both maximal amplitude in tension and the electrical output power, thus resulting among the highest efficiencies in this table. In fact, not only the presence of a water layer acts as an extra tip mass, (which actually has been proved to be a negative effect in the considered harvester) but it allows also to absorb more energy during the impact with an otherwise hydrophobic surface.

Authors	**Type of harvester structures**	**Water drop *D* or *m* *v* or *h***	**Harvested energy /Kinetic energy, E/E_k**	**Energy Conversion Efficiency $\eta_E = E/E_k \times 100$ %)**
R. Guigon, *et al.* [16]	Bridge (PVDF)	$D = 3$ mm, $v = 4.5$ ms^{-1}	147 nJ / 0.143 mJ	0.1 %
		$D = 1.6$ mm $v = 3.2$ ms^{-1}	16 nJ / 0.011 mJ	0.146 %
V. K. Wong, *et al.* [21, 22] (2014)	Cantilever (bimorph PZT)	LSR	*6.5 µJ/1.96 mJ	0.33 %
		MSR	*12.625 µJ/3.92 mJ	0.32 %
		HT $m = 47.7$ mg $v = 3.7$ ms^{-1}	*23 µJ/5.88 mJ	0.39 %
M. Al Ahmad [23]	Cantilever (5 layer PZT)	$m = 0.23$ g $v = 3.43$ ms^{-1}	0.08 µJ / 1.353 mJ (75 drop /s)	0.006 %
			1.739 µJ/1.353 mJ (at 200 drop/s intensity)	0.128 %
S. Gart, *et al.* [28]	leaf cantilever (PVDF)	$D = 2 \times 1.73$ mm	23 nJ / 62 µJ	0.037 %
Ilyas, *et al.* [25]	Cantilever (PVDF)	$D = 4$ mm, $v = 2.13$ ms^{-1} $E = 0.5 \times (0.0335) \times v^2$ $= 27.4$ µJ – 76 µJ	85 nJ / 76 µJ	0.11 %

Table 3: Energy collected from raindrop harvesters and overall efficiency, see [6]

Chapter 3: Experimental setup and planning

3.1 Description of objectives and method

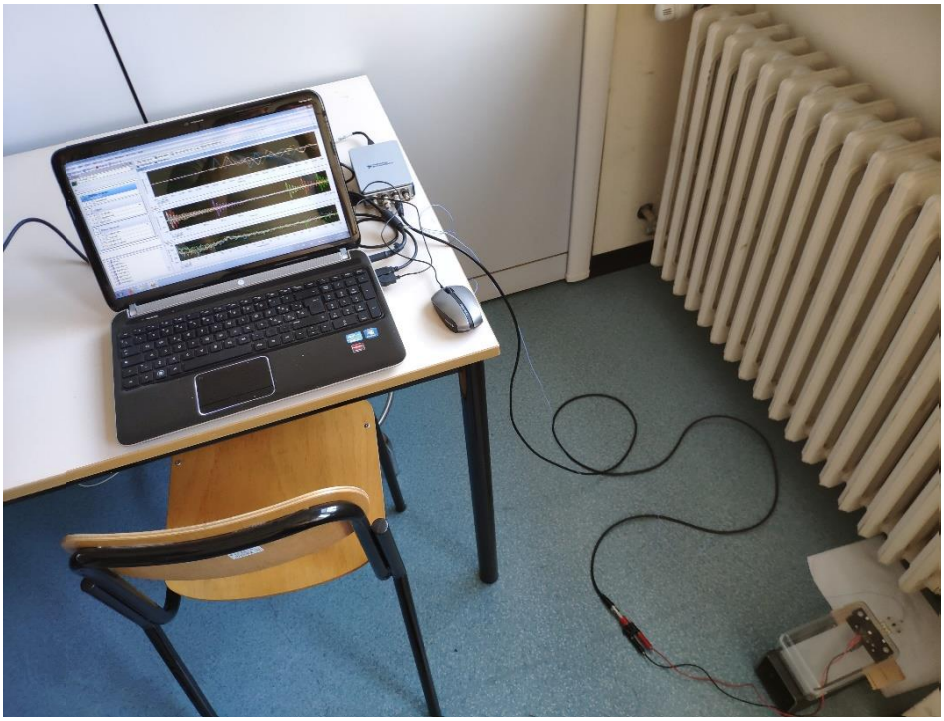

Figure 27: Photo of the work station, with the harvester below in the right

The experimental tests were performed mainly in the **modal analysis laboratory**, inside the industrial engineering department in Padua (DII): the instrument required were already part of the equipment of the laboratory.

These are the instruments adopted for the various analyses:

1. **Piezoelectric raindrop energy harvester** (from a PPA 1001 harvester)
2. ***PCB accelerometer***
3. ***USB data acquisition system (DAQ)*** *"NI 9171"*
4. ***PCB hammer***
5. ***Personal computer*** *for data processing, equipped with the software* ***Labview SignalExpress*** *and* ***Mathworks Matlab***
6. ***Arduino breadboard,*** *to create the required load resistance*
7. ***A syringe****, in order to create artificial waterdrops*

The first experimental test was performed by hitting the Harvester tip with syringe-made waterdrop falling from **various height**.
This main experimental analysis aimed at measuring the **response of the Harvester** considering **different velocities** of the drop as well as **different conditions** on the tip mass of the harvester: the

response was indeed shown to be very different when the spoon at the end of the harvester was respectively **full of water** or totally **empty**.

So, by connecting the harvester to the DAQ and the PC, it was possible to measure the tension generated via the piezoelectric effect by the impact of the drop with the surface of the spoon. Subsequently, in order to study the effect of the **impact**, it was decided to perform a further test, using an **accelerometer** to measure the acceleration of the spoon during the impact.
Eventually, to further comprehend the behaviour of the system, it was then decided to evaluate also **frequency response functions**, obtained by hitting the harvester with the PCB hammer and then measuring the response of the tip acceleration as well as the tension generated by the harvester.

3.2 Description of the components

The aim of this section is that of briefly describing and introducing the components and the instruments used during the various tests

Waterdrop piezoelectric Harvester

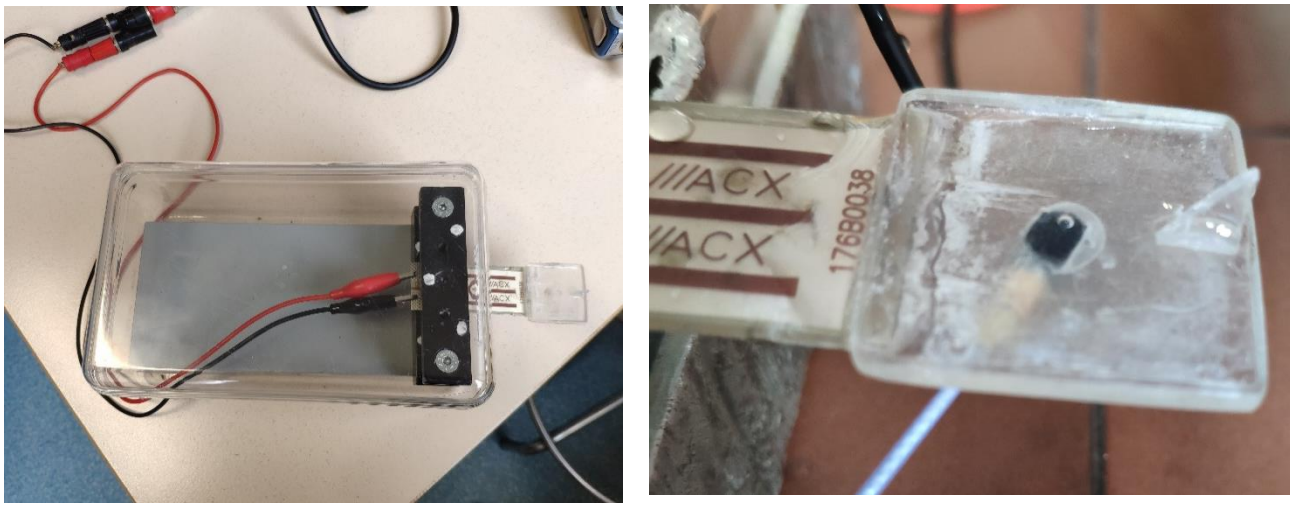

Figure 28: The waterdrop harvester and a detail of the spoon, with the accelerometer beneath it

The waterdrop piezoelectric harvester is the main component in all studies and experiments. It is made with a **PPA 1001 harvester** [3], that creates the body of the beam; a clamp that creates the cantilever constraint; a box to protect the electrical terminals form accidental contacts with water and a polystyrene rectangular spoon, whose purpose is that of act as a tip mass and to absorb the impact with the waterdrops. The spoon is able to accommodate a thin water film above it

PCB accelerometer

Figure 29: The accelerometer PCB

The instrument used to measure the vertical acceleration of the spoon is a **piezoelectric monoaxial accelerometer** (PCB). The accelerometer was connected to the lower surface of the spoon (to protect it from accidental contacts with water) using wax. This was the **smallest accelerometer (0,2 g)** that could be provided for these experiments: nonetheless, the pre-tension induced by the connecting cable, as well as the masses of the accelerometer and the cable itself, were shown to **disturb** the measurements. In fact, as a droplet hit the spoon of the harvester starting its vibration, the cable act as a dynamic vibration absorber, absorbing part of the vibration and both reducing the amplitude of the signal and enhancing its damping.

DAQ NI9171

The NI9171 is the data acquisition module used for the analyses. It possesses **4 analogic input channels** and **a digital USB output** (thus it converts the analogical input signals into digital output signals). It can sustain a maximal amplitude in voltage of **±5 V**: thus if the signal were to be too intense, the DAQ module would saturate it, resulting in its distortion.

Figure 30: The DAQ module NI9171

PCB hammer

Figure 31: PCB hammer with red point sensor

The impulse force hammer was used to determine the FRF of the harvester. It possesses a force sensor in its tip with which it is possible to measure the impulsive force that appear during the interaction between the hammer and the hit object. The hammer was used only in the last tests to calculate the **FRF.**

PC for data processing

The **DAQ module** was connected to a lap top equipped with the software **LabView SignalExpress**. This data logging software allows to control of the data acquisition process and their presentation: it allows functions such as the insertions of triggers or the simultaneous comparison of signal from different channels in **both time and frequency domain**. **Triggers** are necessary to properly acquire the signal: they permit to start the test only after a certain threshold condition is met (for example, when the tension or the acceleration reach an appropriate value), thus eliminating the influence of external noise and disturbances. The results can be furtherly processed in a time domain analysis: the software can calculate the **power spectrum** of the signal or the **magnitude/phase frequency response function** of a couple of input-output signals.

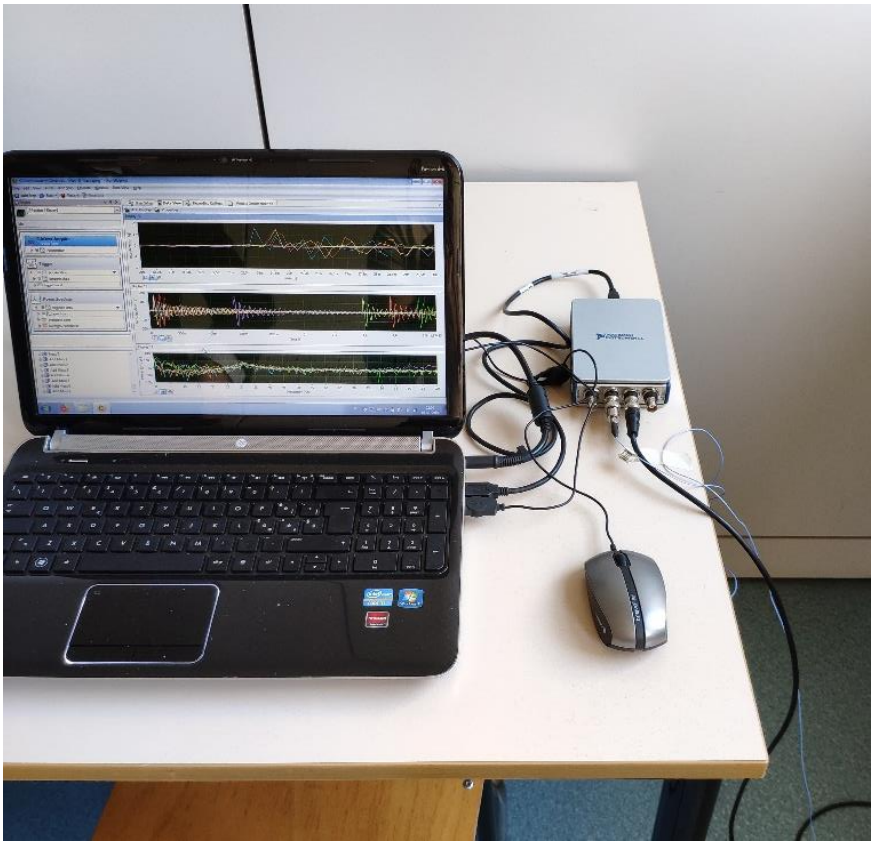

Figure 32: The PC running an analysis with SignalExpress

Figure 33: Logo of the software LabView SignalExpress

Arduino breadboard

The Arduino breadboard was used to explore the response of the harvester when connected to a **resistive load**. The resistors used were also those included in the Arduino kit. This was solution was used uniquely to manage the load circuit and to obtain the ideal resistance at which the **Harvester absorb the highest power** (that depends from the first vibrational mode frequency, see [3]).

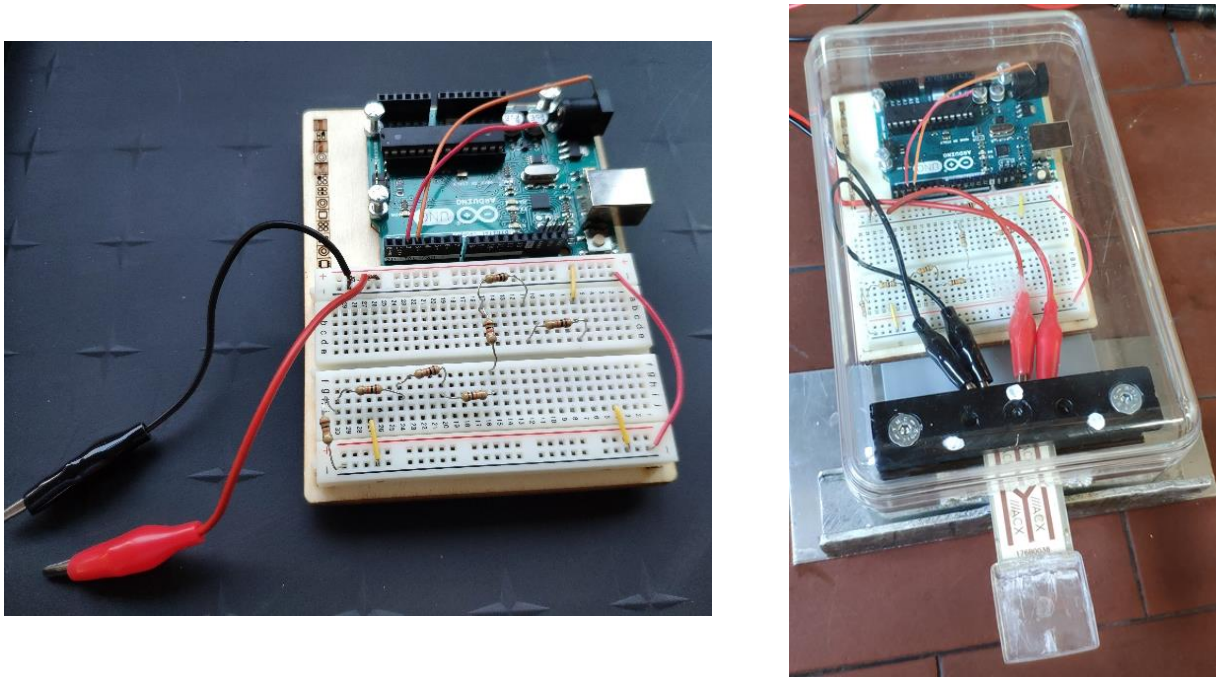

Figure 34: The Arduino breadboard and its connection with the harvester

Syringe and its installation

Figure 35: On the left, the harvester positioned underneath the fixed location of the syringe. Above on the right, the syringe, after having been inserted and fixed in its position. As it is possible to see, the distance between the centre of the harvester and the surface of the piston is circa 98 cm. Below in the right, a detail of the needle with a droplet of 2 mm attached to it.

The syringe was adopted in order to create waterdrops with **controllable velocity**: this latter can be obviously controlled by simply raising the syringe's height, changing thus the distance of freefall. The instrument used came from a common medical syringe set albeit with a very **thin needle**. To perform the tests, it was previously confronted the diameter of the drops created by the syringe with that of raindrops during normal rainfall (in Padua). Then, as it was possible to asses that the dimension of the drops were similar, it was considered possible to use the syringe as a source of droplets, instead of natural rainfall.

After having fixed the syringe in its designed position, droplets were created by simply pushing the piston while at the same time launching the analysis with SignalExpress. Nonetheless, it was proved rather difficult to obtain accurate results: in fact the **pressure applied to the piston** needed to be very precise, in order not to alter the results. In detail, the **droplet** had to be created **beforehand on the tip on the needle** (sustained to it only thanks to cohesive forces). By applying a very small hit to the piston, it was possible to detach it and to start its freefall towards the Harvester. The most common problems were the separation one the single droplet into two smaller ones (with two different instants of impact) and the deviation from the vertical trajectory, something that would have often led the droplet to totally miss the harvester. After a couple of months, probably because of the wear and the dust, the syringe became unable to create proper droplet and thus had to be replaced with another identical model.

Figure 36: Detail of the syringe

3.3 Droplet examination

Before the execution of the experiments, it had been necessary to compare the droplet of the syringe with those from a mild natural rainfall. In order to do that, a plane surface was exposed to rainfall. Then the same surface was exposed to an “artificial rainfall” created with the syringe.

As can be seen in the figure below, the rainfall produced by the syringe is comparable to natural rainfall. They both shows a mean diameter of circa 2 mm(see also chapter 2, table 2) .

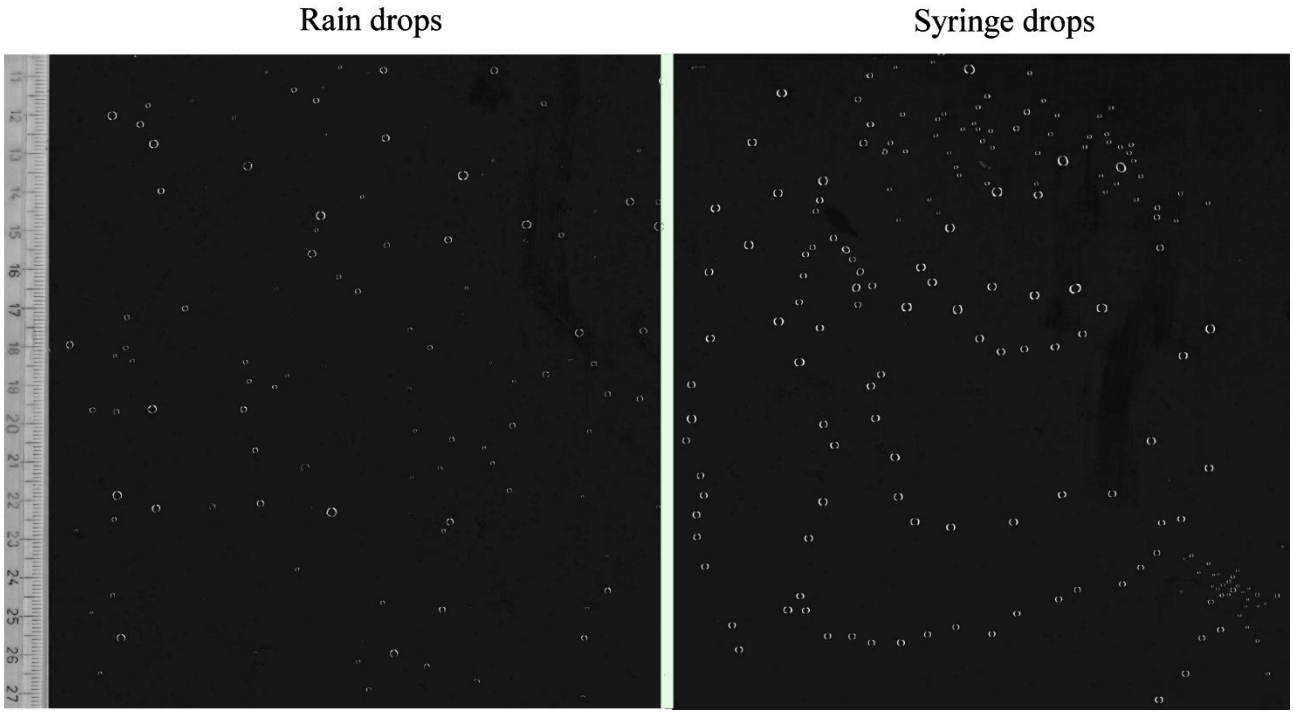

Figure 37: Comparison between natural and artificial rainfall

For a better description of the droplets, it was then decided to weigh them with a precision scale. The procedure followed was rather simple: it was at first set the zero in the scale, then a drop created with the syringe was deposited on the measuring plate.

The results obtained in this fashion were then furtherly processed: assuming again that the droplets maintain a **perfect spherical shape**, it is possible to calculate the radius of a single droplet. The results are shown in the following table:

Weighing of syringe water droplets: results

Measure	*Mass [g]*	*r [mm]*	*d [mm]*
#1	*0.0056*	*1.101623*	*2.203247*
#2	*0.0064*	*1.151765*	*2.30353*
#3	*0.0052*	*1.074744*	*2.149487*
#4	*0.0051*	*1.06781*	*2.135619*
Mean	**0.0056**	*1.098985*	**2.197971**

Table 4: Measured mass of droplets with a precision balance and consequent radius

Both these two experiences and table 2 in chapter 2.1, confirm that the syringe adopted creates waterdrop that are **comparable** with those of natural rainfall.

3.4 Data acquisition

The data were acquired with the software **LabView**, which acts as an oscilloscope measuring the electrical output signal as a function of time. In order to analyse the signal properly, it is necessary beforehand to set a **Trigger** on, at least, one of the input channel. In this way it is the acquisition system starts its acquisition only after the overcoming of a trigger threshold. As a result of this, all the signals start almost when, for example, the voltage reaches the threshold value, not only making the entire acquisition process easier (it is possible to drop another droplet after the previous has missed the target without interrupting and then re-starting the acquisition) but also obtaining very similar signals, with the same sampling time and a very comparable evolution in time.

The software allows also to perform an analysis in the frequency domain: this feature was used to compare power spectra of various signals and to evaluate the FRF of the tension to the force applied at the tip. An example of the analysis result and postprocessing can be seen in the next figure 38.

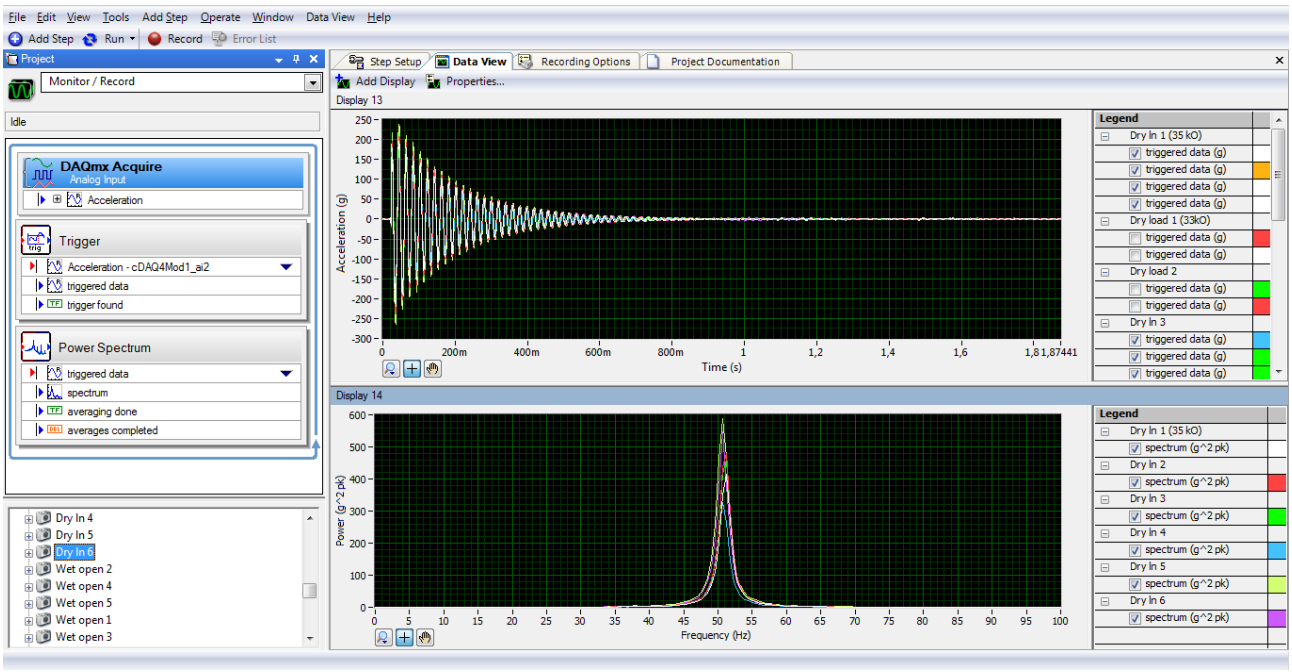

Figure 38: Screenshot of the PC display during the data collection and analysis. In the left of the screen, the operations performed by the software: acquisition, trigger and power spectrum of the signal. Note that the output, while labelled as acceleration, is in fact a tension (the software measures the output voltage and multiply it by a sensibility constant of 1 g/mV)

The software permits to overlap the real time acquired signal to previously saved signals, therefore permitting an immediate comparison and an eventual elimination in case of not consistent results as shown in the next images. The most common errors were:

- ***Droplet totally missing or not effectively hitting the spoon****: this results in a very low voltage output and in an enhanced presence of superior modes such as torsional modes when the droplet hits the lateral extremity with respect to the central beam axis.*
- ***Separation of a droplet into two smaller ones or hit of two consecutive droplets:*** *in this case the main interference can be seen in the frequency domain, with a very disturbed signal. As the aim of the tests was usually that of examining the behaviour to a single hit, signal resulting from multiple hits were, when possible, discarded.*
- ***Signal interference:*** *in some cases the signal obtained were afflicted by disturbs, usually producing beats. The presence of the accelerometer and its connecting cable was one of the possible sources of interference: the hit of a droplet resulted not only in the excitation of the harvester, but also of the cable itself.*

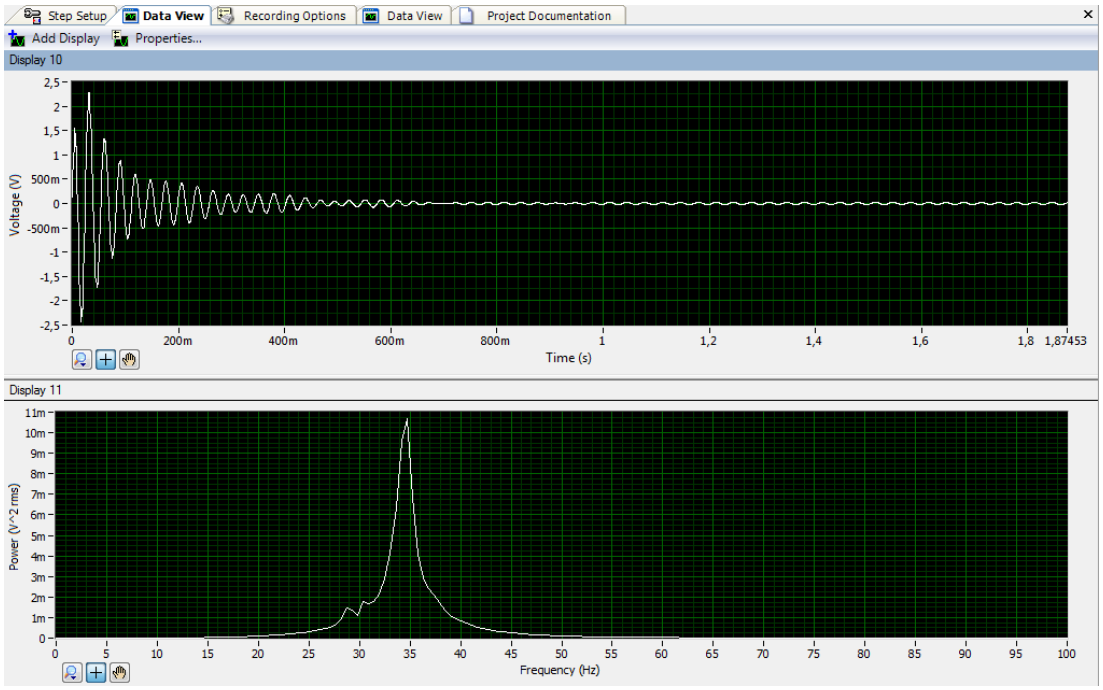

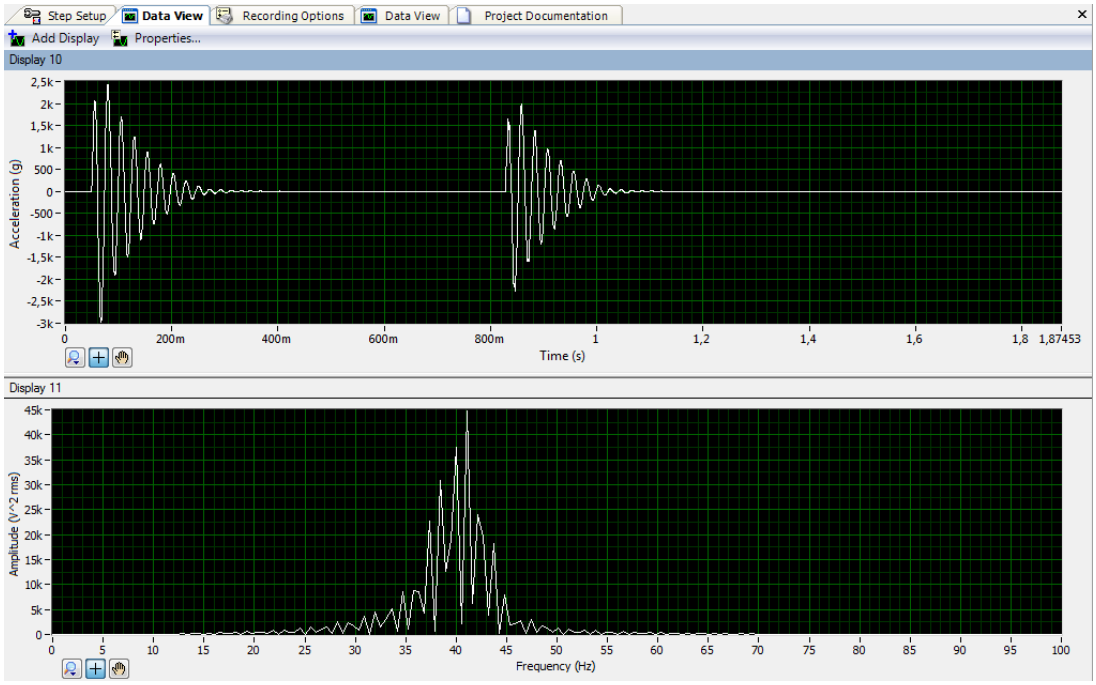

Figure 39: Example of disturbed signals: the first shows the presence of a small beat, the second is the result of two droplet hitting the spoon instead of one

3.5 Test planning

This paragraph will describe more in detail the logic behind each experiment , whose tests aimed at generally widening and deepening the comprehension of the behaviour of the raindrop energy harvester. However, such tests were not immediately scheduled all together: in fact, the later tests were decided after the elaboration, the study and the interpretation of the previous ones. More in detail, this was briefly the scheme followed by the tests:

- ***Study of the effect of the height on harvester with a film of water on the spoon***
  The initial tests were conducted with the spoon totally filled with water: indeed, this can be considered the "stationary condition" of the harvester (imagining that the harvester collects raindrops until its spoon becomes full during a rainfall)
  In the scientific literature of raindrop energy harvesters, it appears clearly that the ***peak to peak voltage*** *is a quantity that can be correlated with the energy harvested from the impact with the droplet (see Ilyas et al. [2], for example). Thus, the scope of the first tests was that of understanding the relation between the* ***height of fall*** *(and thus the impact velocity) and the* ***peak to peak voltage****. The height range exanimated was from 1 to 3 meters (it becomes more difficult to perform the experiments as the height increases; furthermore, it was not possible to examine bigger heights in the laboratory)*
  The results showed an increase in the value of the peak to peak tension as the height of fall increased as well: however there was not a linear correlation. In fact, the growth in voltage decreases as the height increases, eventually becoming zero (when the height of fall does not influence the maximal speed of the droplet anymore, i.e. the droplet reaches its ***terminal velocity****). See also 2.2, figure 23.*
  One of the most evident results was the rather unpredictable shape of the signal, that was different from that of an impulse excited harvester: more in detail, the ***first positive peak appeared not to be the highest.***

- ***Study of the effect of a totally empty spoon***
  In order to explain the unusual signal form in the previous cases, it was then decided to perform also tests in which raindrops were supposed to impact with a totally empty spoon. The tests were performed as well at different heights. The result of these tests showed an ***ordinary signal shape****, that is comparable to that of an impulse excited cantilever beam but a* ***significantly lower peak to peak voltage compared to the previous test****. This was in sharp contrast with the scientific literature, were it was clearly advised (although providing no demonstration for such assertion) to use empty harvesters to obtain the bests results (compare [2]).*

- ***Study of the effect of an empty spoon with added masses***
  *To comprehend whether the **higher peak to peak voltage** that appeared with full spoon was a **consequence of the added mass** of the water or not, it was then decided to perform other experiments with the **empty spoon** and **an additional mass on it.** The first value was that of the mass of water needed to fill the spoon (circa 2.4 g): it was obtained by sticking some lead spheres. As the use of glue could alter the surface of the spoon, the next tests were executed by simply adding some different washers on the tip of the spoon after having weighed them. The signal shape delivered by this experiments was somewhat in between of that with the full spoon and that with the empty spoon. However, it appeared also clear that **the more the mass was increased, the less resulted the peak to peak value**, thus implying that **the added mass was a negative effect.***

- ***Study of the effect of the impact in the spoon acceleration***
  As the added mass experiments showed that the signal shape and the peak to peak voltage obtained for the full of water configuration were not related to the added mass, it was then decided to investigate the behaviour of the impact. The mechanical vibration laboratory does not possess instruments properly intended for such a purpose: for this reason, it was decided to study the effect of the impact by simply analysing the acceleration that a droplet could impress to the spoon. This was easily done by adding an accelerometer under the spoon. However, it must be underlined that while this solution is very easy, it possesses also the drawback of disturbing the system: not only the accelerometer adds its mass to the spoon, but the connection cable absorbs also a non-negligible part of the kinetic energy of the initial droplet.

- ***Study of the effect of an external electric load***
  This study was decided to properly examine the performance of the harvester when connected to a resistive load. In order to obtain the best performance, the tests were conducted applying the ideal resistance (that is, the resistance that allows the generation of the maximal electric power). These results were then used to compute the overall electric power and efficiency of the device: these results were comparable to those reported in scientific literature

Chapter 4: Experimental results

4.1 Elaboration of experimental data

The aim of this section is the presentation of the data elaboration praxis that was followed throughout this entire work. The data were elaborated mostly with **Matlab**: they were at first pre-viewed and saved in the SignalExpress environment (discarding non-valid results), then imported to Matlab. In order to perform the analysis of the voltage signal in the time domain, a **Matlab script** was created. The script has been published in the appendix. For each performed test, it was created a variable with the voltage data (for example, after obtaining 7 valid results with a drop height of 1 m on full spoon, 7 variables for each voltage signal were created).

Although the main object of the tests was surely the peak to peak voltage, obtained with a mathematical analysis of relative minima and maxima, the results of this preliminary analysis were used to obtain also some further information. The next passages show how the other quantities were obtained.

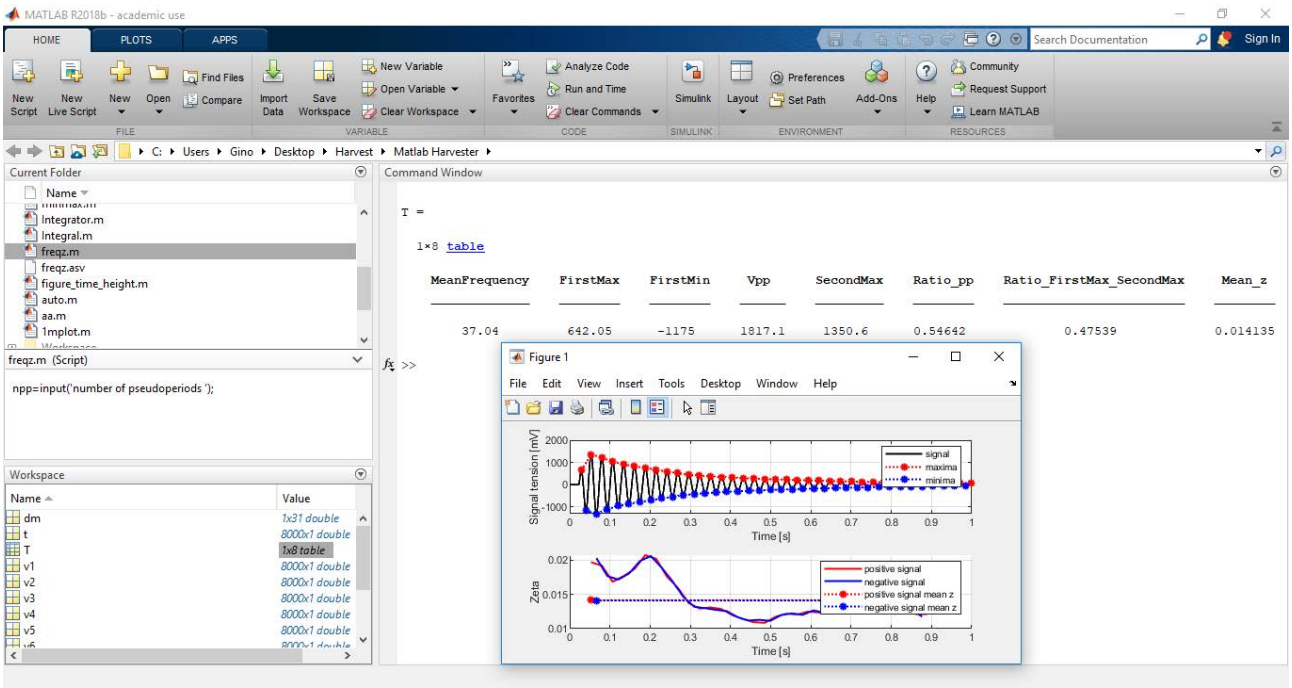

Figure 40: Screenshot of Matlab during the data analysis, after the execution of the script that analyses the signals

The script was created in order to calculate:

- *The envelope curve of the signal*
- *An average pseudo-frequency of the signal, by calculating the width between each relative maxima and relative minima. The scripts calculates then a mean of all intervals*
- *First maximum, first minimum and second maximum.*
- ***Peak to peak voltage**, obtained as first maximum minus first minimum*
- *The ratio between these quantities*

- *A mean damping ratio (ζ) of the signal. The damping ratio is the term that regulate the decay of the signal. In case of linear harmonic vibration the signal is described by:*

$$x(t) = Xe_n^{-\zeta\omega_n t} cos(\sqrt{1-\zeta^2}\,\omega_n t - \Phi) \tag{4.1}$$

In detail, the average frequency $f_{mean} = 1/T_{mean}$ was calculated as:

$$T_{mean} = \frac{1}{M}\sum_{i=1}^{M} t(X_{i+1}^{MAX}) - t(X_i^{MAX}) \tag{4.2}$$

The mean damping ratio (ζ) was calculated with the logarithmic decrement method. This method estimates ζ by considering the ratio between the amplitude of the signal after an certain number of periods n. More in detail, **δ** is the "**logarithmic decrement**", defined as follows:

$$\delta = \frac{1}{n}\ln\left(\frac{X(t)}{X(t+nT)}\right) \tag{4.3}$$

Then the damping ratio can be expressed as :

$$\zeta = \delta/\sqrt{4\pi^2+\delta^2} \tag{4.4}$$

The next figures present the result of the analysis of the damping ratio, in order to explain the procedure adopted in the analysis of the damping of signals. The test results will be presented more in detail in the next section.

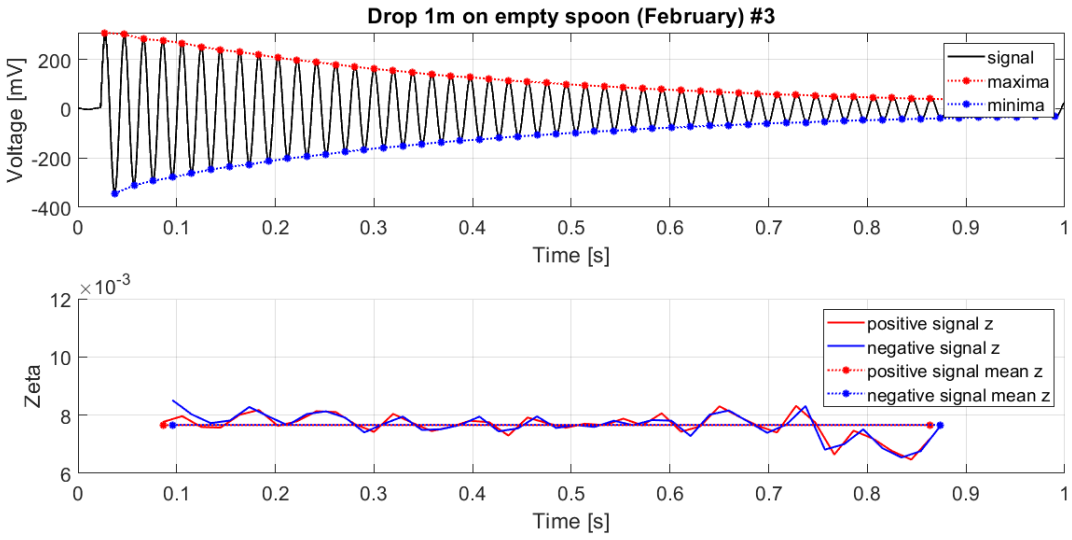

Figure 41: Results obtained for the signal #3 of the test "drop from 1m on empty spoon of February" (see next paragraph). The damping ratio was calculated between 6 periods: the value does not change much in the various instant.

The results for the damping ratio are very different with the presence of water, as shown in the next figures:

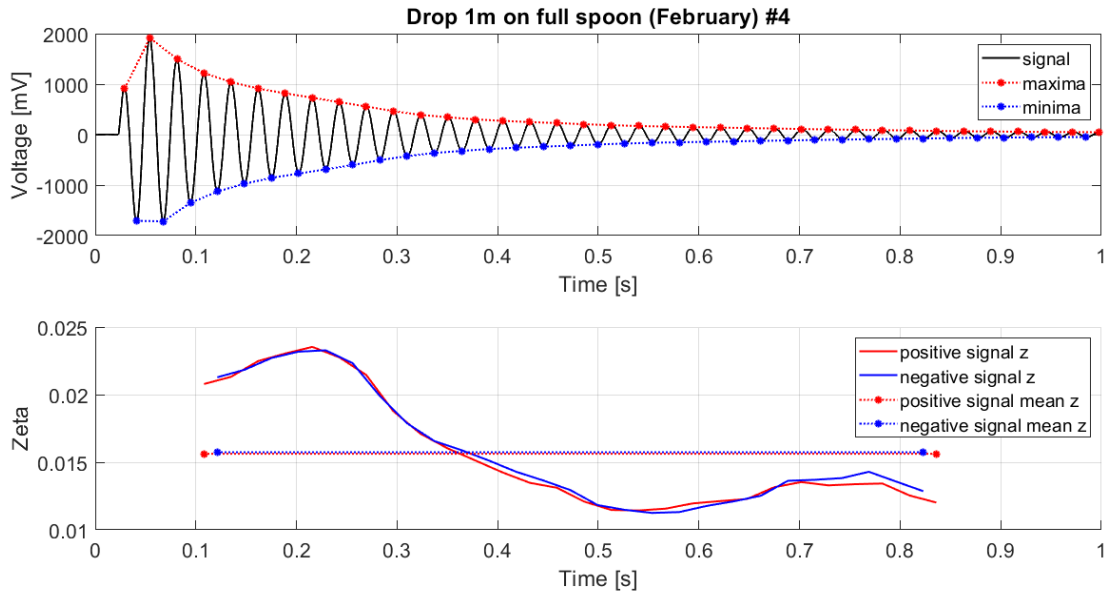

Figure 42: Results obtained for the signal #4 of the test "drop from 1m on full spoon of February" (see next paragraph.

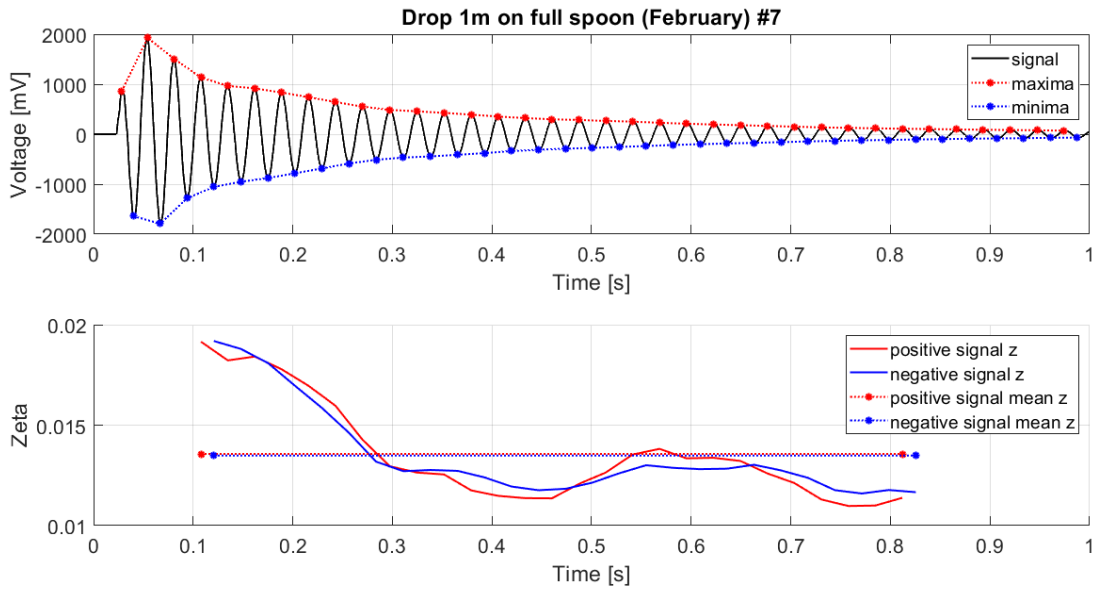

Figure 43: Results obtained for the signal #7 of the test "drop from 1m on full spoon of February" (see next paragraph).

It is possible to see that in these cases, **the damping ratio is not constant** (thus the damping **not linear** as well).

At the contrary, the behaviour of the damping ratio is totally different in the tests with added mass, as shown in the next page.

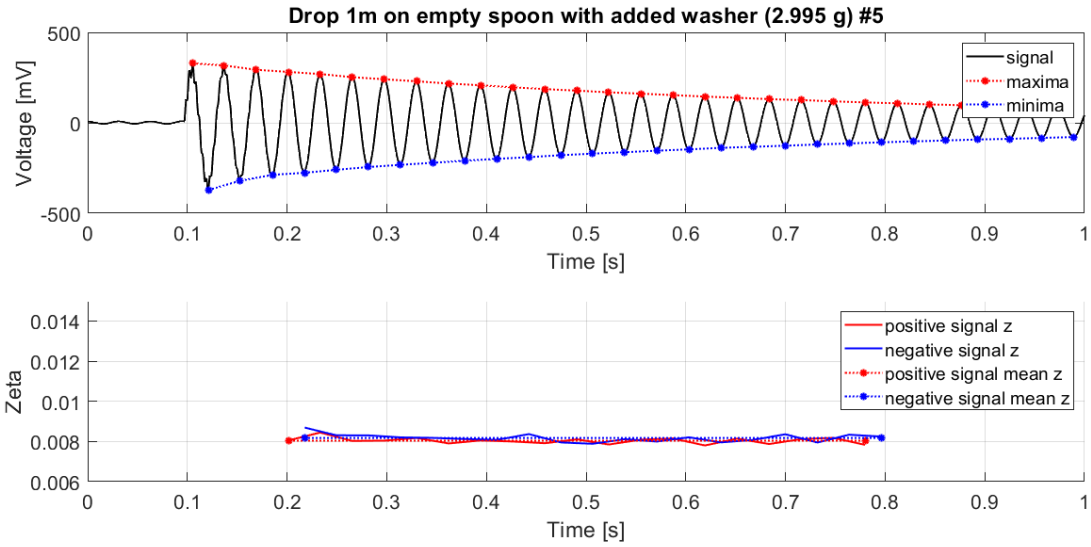

Figure 44: Results obtained for the signal #5 of the test "drop from 1m on empty spoon added washer (1.913g)" (see next paragraph).

This trend is equally manifested in all the samples of the various tests. To summarize the results, it appears that:

- ***The presence of water enhances the mean damping ratio and creates a high non linearity in the damping behaviour.***

- ***The damping ratio in absence of water on the spoon surface is 0.008.***

This damping ratio is result of both mechanical and electrical damping: while the first is surely negative (the mechanical damping reduces the overall kinetic energy of the beam and thus the energy that can be converted), the second appears as a result of the conversion of mechanical energy into electric energy. Most of the tests were performed with no electrical load: in these cases the effect of the electric load on the damping ratio is negligible. However, when considering the load tests, it appears an evident increase of the overall damping ratio, because of the energy successively converted.

4.2 Effect of height on performance

Test: drop from 1m on full spoon (October)

Test sample	Mean frequency [Hz]	$V_{MAX}\#1$ [mV]	$V_{MIN}\#1$ [mV]	V peak to peak	$V_{MAX}\#2$ [mV]	$\frac{V_{MAX}\#1}{\lvert V_{MIN}\rvert\#1}$	$\frac{V_{MAX}\#1}{V_{MAX}\#2}$	Mean ζ
#1	32.88	648	-820	1468	910	0.789	0.712	0.018
#2	32.67	1008	-1413	2421	1331	0.713	0.757	0.020
#3	33.39	1788	-3028	4816	2932	0.590	0.610	0.029
#4	33.55	1832	-3084	4916	2688	0.594	0.682	0.029
#5	34.25	1588	-2563	4152	2231	0.620	0.712	0.020
#6	34.61	2076	-3395	5470	2895	0.612	0.717	0.030
Mean	**33.56**	**1490**	**-2384**	**3874**	**2164**	**0.653**	**0.698**	**0.024**
SD	0.76	548	1034	1581	857	0.081	0.050	0.006

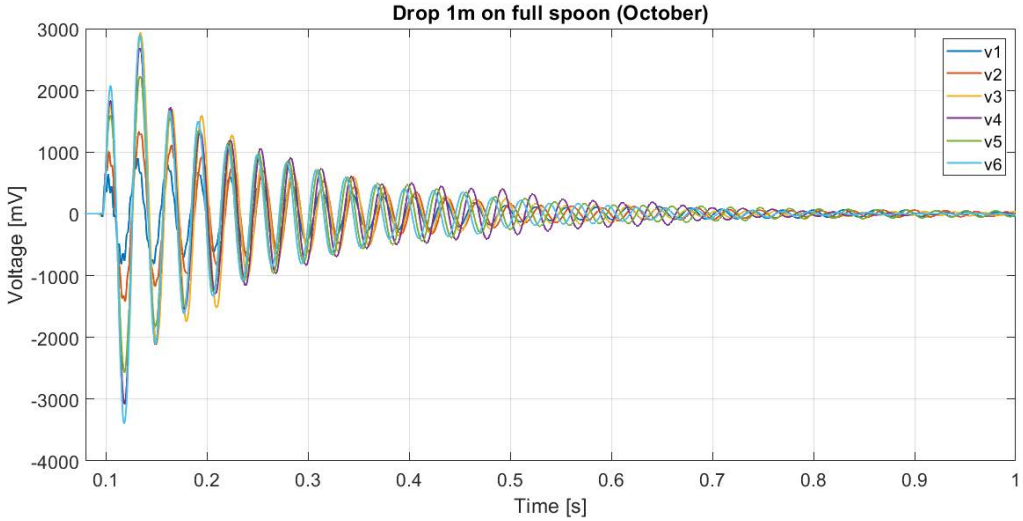

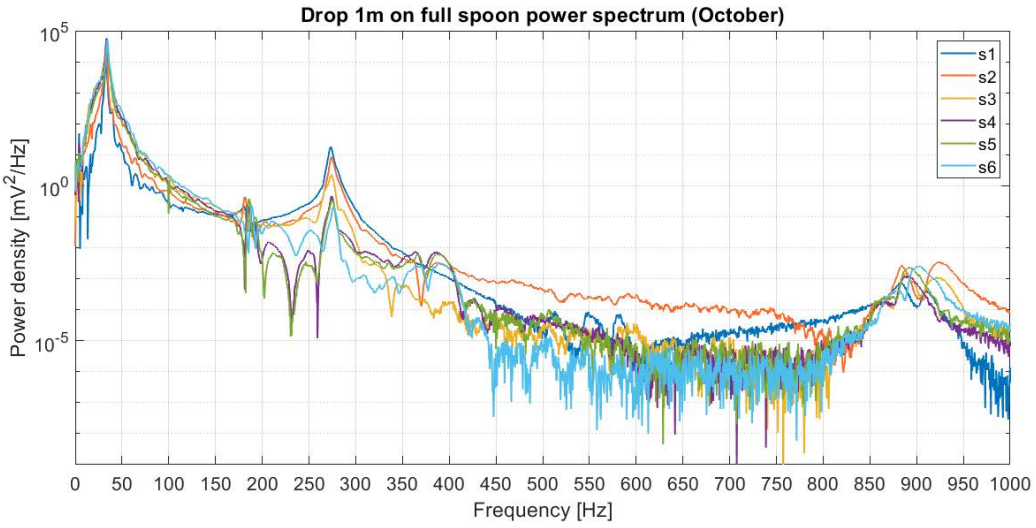

Test: drop from 1m on full spoon (February)

Test sample	Mean frequency [Hz]	$V_{MAX}\#1$ [mV]	$V_{MIN}\#1$ [mV]	V peak to peak	$V_{MAX}\#2$ [mV]	$\frac{V_{MAX}\#1}{\lvert V_{MIN}\rvert\#1}$	$\frac{V_{MAX}\#1}{V_{MAX}\#2}$	Mean ζ
#1	37.04	642	-1175	1817	1351	0.546	0.475	0.014
#2	37.03	953	-1769	2722	1936	0.539	0.492	0.019
#3	36.98	986	-1829	2815	2034	0.539	0.485	0.014
#4	37.07	913	-1709	2622	1916	0.534	0.477	0.016
#5	37.05	813	-1521	2334	1699	0.535	0.479	0.015
#6	36.99	1226	-1075	2301	981	1.140	1.250	0.013
#7	36.91	863	-1641	2504	1927	0.526	0.448	0.014
Mean	37.01	914	-1531	2445	1692	0.623	0.586	0.015
SD	0.06	178	295	336	388	0.228	0.293	0.002

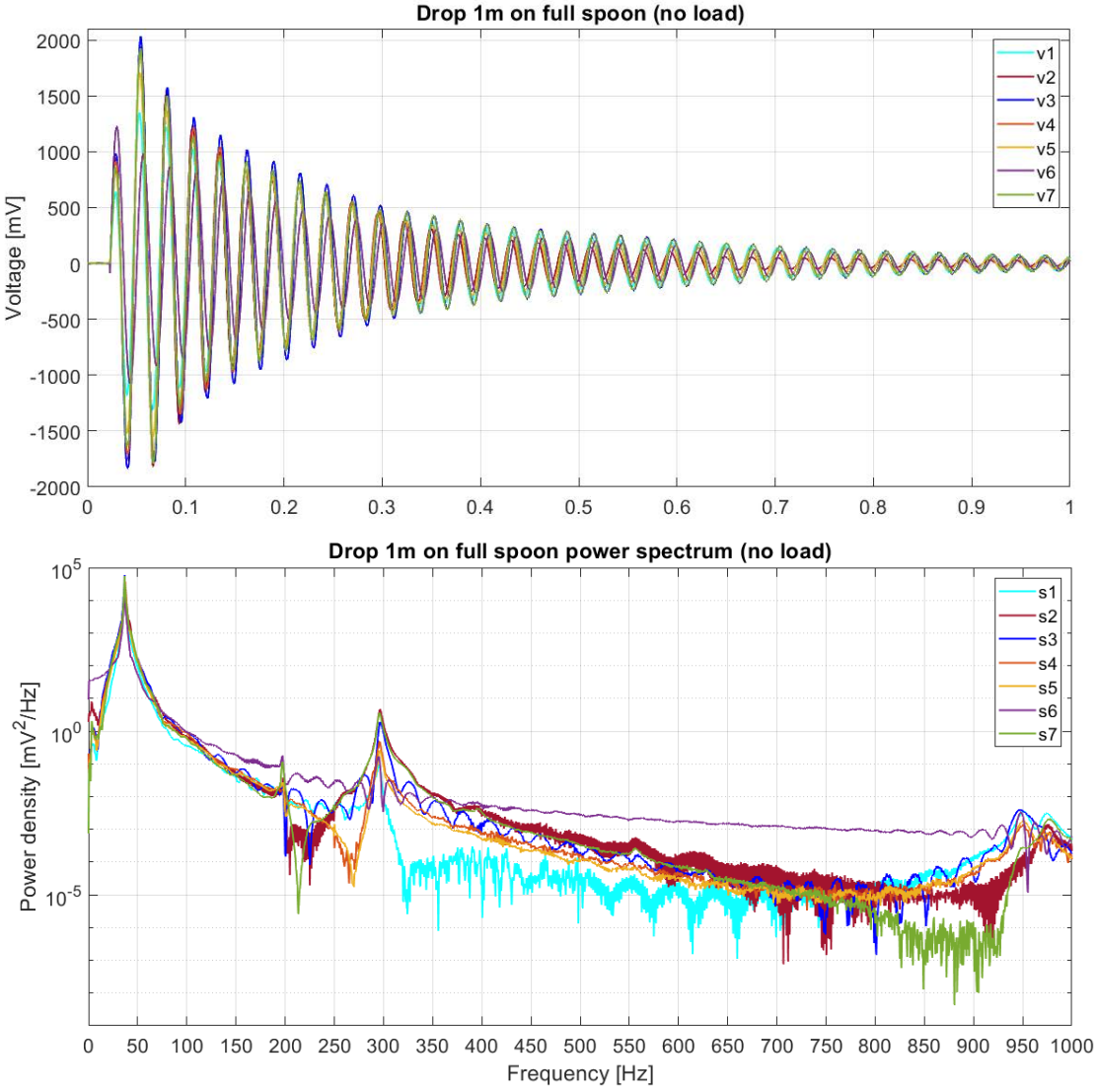

Test: drop from 1m on full spoon (March)

Test sample	Mean frequency [Hz]	$V_{MAX}\#1$ [mV]	$V_{MIN}\#1$ [mV]	V peak to peak	$V_{MAX}\#2$ [mV]	$\frac{V_{MAX}\#1}{\lvert V_{MIN}\rvert\#1}$	$\frac{V_{MAX}\#1}{V_{MAX}\#2}$	Mean ζ
#1	31.29	1046	-1870	2917	1878	0.560	0.557	0.020
#2	30.38	2360	-1779	4139	1353	1.327	1.745	0.020
#3	30.63	1180	-2242	3422	2400	0.526	0.492	0.018
#4	30.11	1195	-2318	3513	2412	0.515	0.495	0.021
#5	30.14	1201	-2313	3514	2445	0.519	0.491	0.020
#6	30.43	1221	-2349	3571	2468	0.520	0.495	0.019
Mean	30.50	1367	-2145	3513	2159	0.661	0.712	0.020
SD	0.43	490	253	390	453	0.326	0.506	0.001

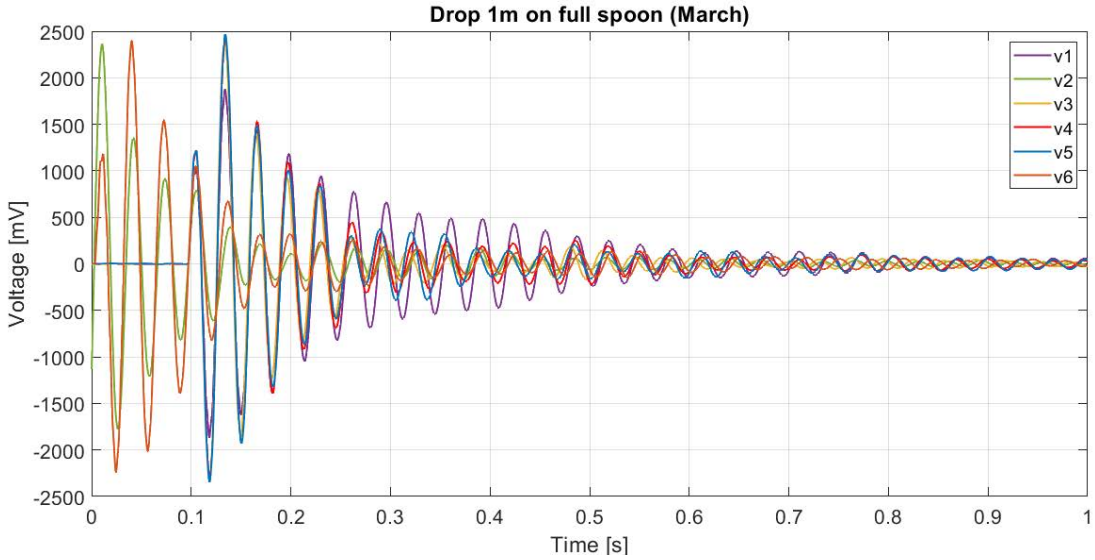

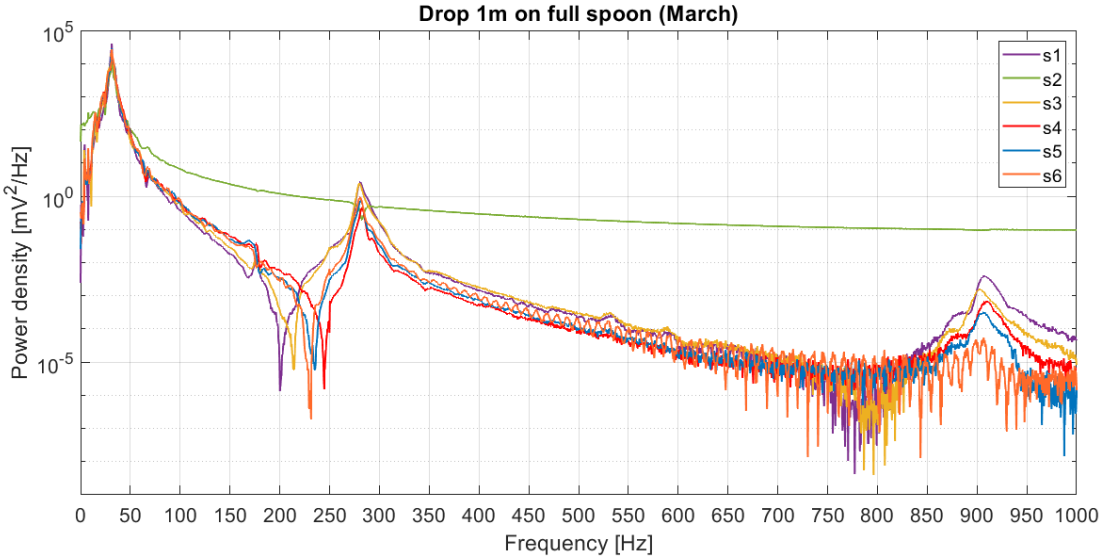

Test: drop from 1.5m on full spoon

Test sample	Mean frequency [Hz]	$V_{MAX}\#1$ [mV]	$V_{MIN}\#1$ [mV]	V peak to peak	$V_{MAX}\#2$ [mV]	$\frac{V_{MAX}\#1}{\lvert V_{MIN}\rvert\#1}$	$\frac{V_{MAX}\#1}{V_{MAX}\#2}$	Mean ζ
#1	36.01	2628	-3819	6448	2951	0.688	0.891	0.016
#2	36.10	1338	-1688	3026	1396	0.792	0.959	0.024
#3	37.33	3359	-5047	8405	3196	0.666	1.051	0.015
#4	37.61	2182	-3123	5305	2455	0.699	0.888	0.014
#5	41.55	3618	-5116	8734	3746	0.707	0.966	0.011
#6	34.38	3383	-5116	8499	3256	0.661	1.039	0.020
Mean	**37.16**	**2751**	**-3985**	**6736**	**2833**	**0.702**	**0.966**	**0.017**
SD	2.43	878	1395	2271	821	0.048	0.070	0.005

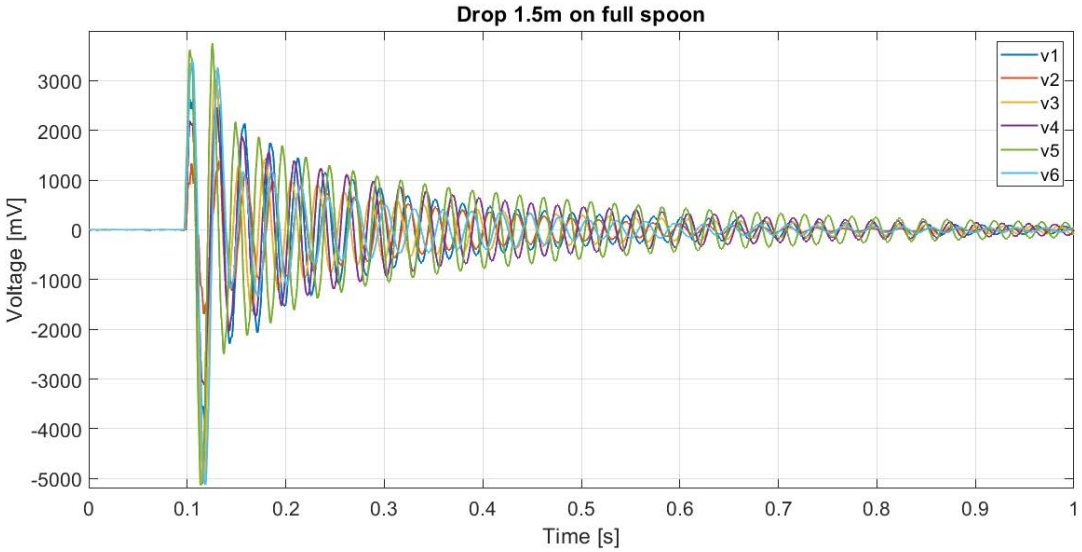

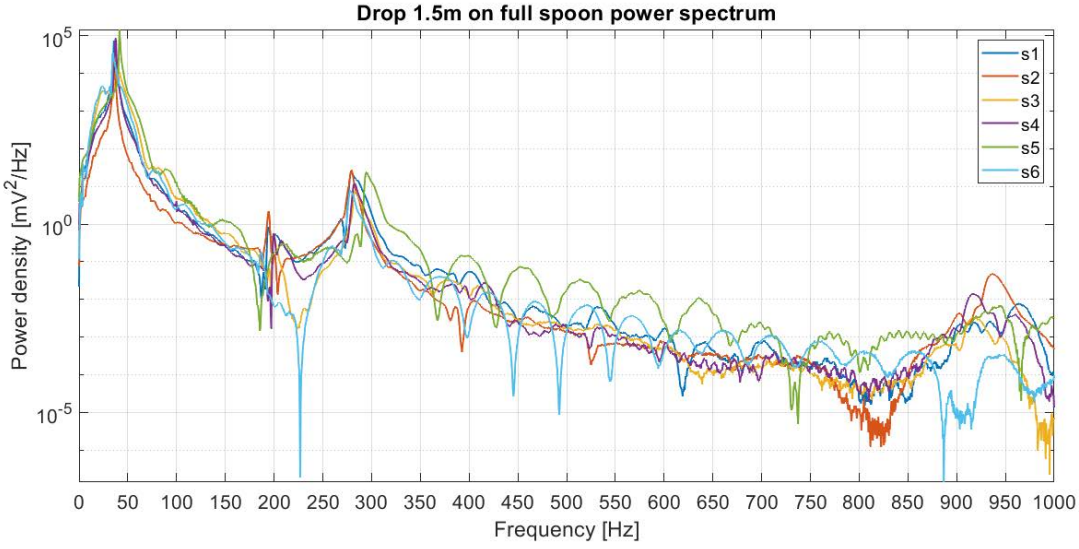

Test: drop from 2m on full spoon

Test sample	Mean frequency [Hz]	$V_{MAX}\#1$ [mV]	$V_{MIN}\#1$ [mV]	V peak to peak	$V_{MAX}\#2$ [mV]	$\frac{V_{MAX}\#1}{\lvert V_{MIN}\rvert\#1}$	$\frac{V_{MAX}\#1}{V_{MAX}\#2}$	Mean ζ
#1	35.02	3373	-5116	8490	3004	0.659	1.123	0.019
#2	34.58	2424	-3406	5830	2540	0.712	0.954	0.016
#3	35.66	3011	-4664	7675	3236	0.645	0.930	0.017
#4	35.70	2550	-3522	6072	2519	0.724	1.013	0.016
#5	35.94	3794	-5116	8910	3297	0.741	1.150	0.015
Mean	35.38	3030	-4365	7395	2919	0.696	1.034	0.017
SD	0.56	570	844	1394	372	0.042	0.099	0.002

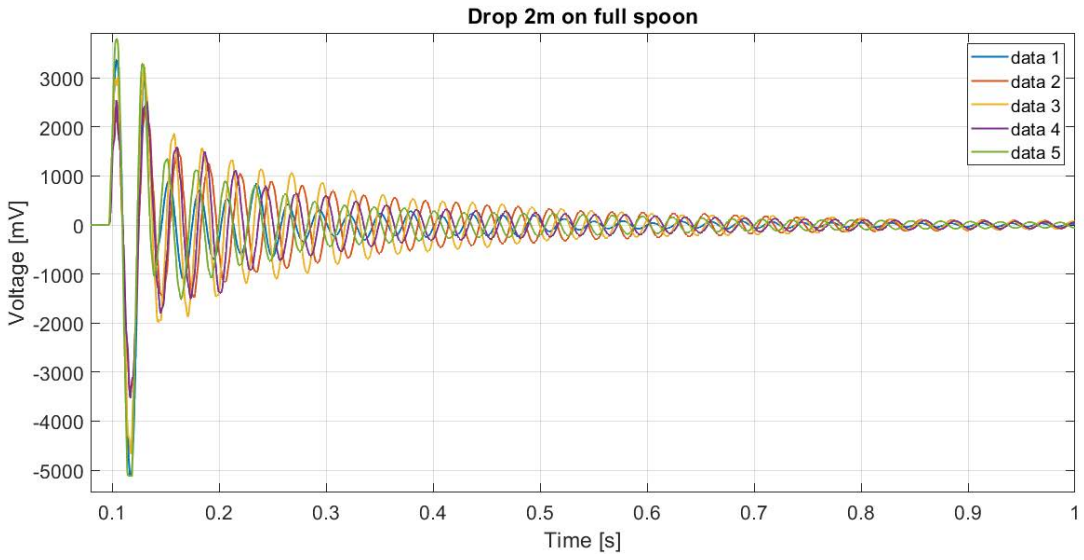

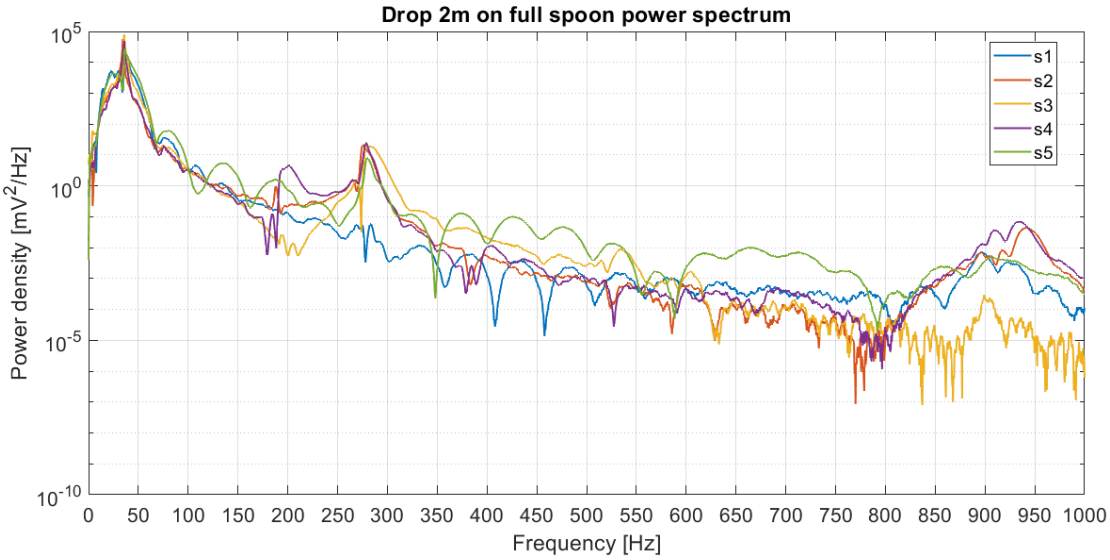

Test: drop from 3m on full spoon

Test sample	Mean frequency [Hz]	$V_{MAX}\#1$ [mV]	$V_{MIN}\#1$ [mV]	V peak to peak	$V_{MAX}\#2$ [mV]	$\frac{V_{MAX}\#1}{\lvert V_{MIN}\rvert\#1}$	$\frac{V_{MAX}\#1}{V_{MAX}\#2}$	Mean ζ
#1	35.85	2433	-3029	5462	2180	0.803	1.116	0.015
#2	36.07	3022	-4158	7180	3077	0.727	0.982	0.015
#3	37.09	2869	-3964	6833	3125	0.724	0.918	0.019
#4	37.37	3959	-5090	9049	3880	0.778	1.020	0.015
Mean	36.60	3071	-4060	7131	3066	0.758	1.009	0.016
SD	0.75	643	845	1478	696	0.039	0.083	0.002

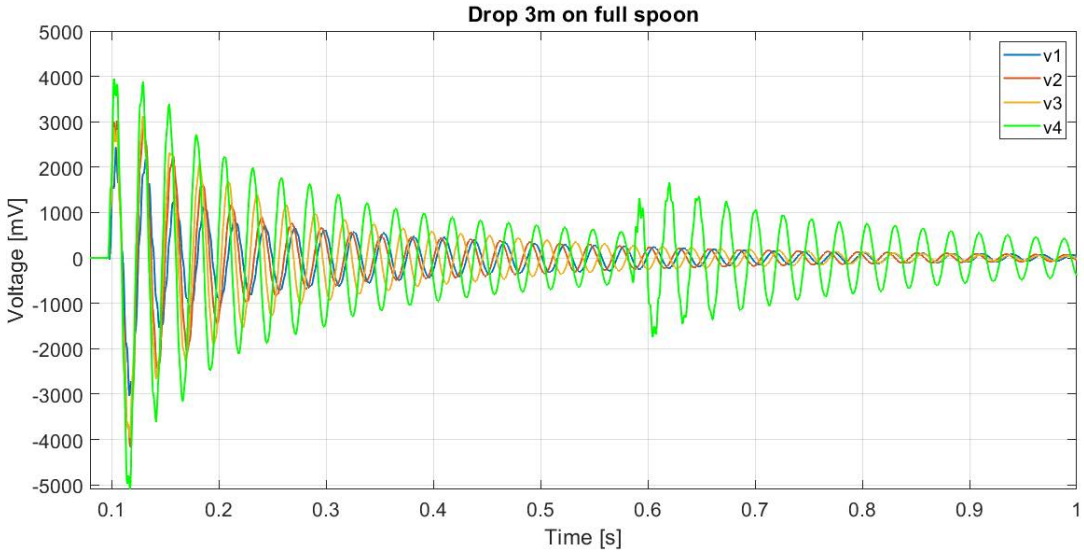

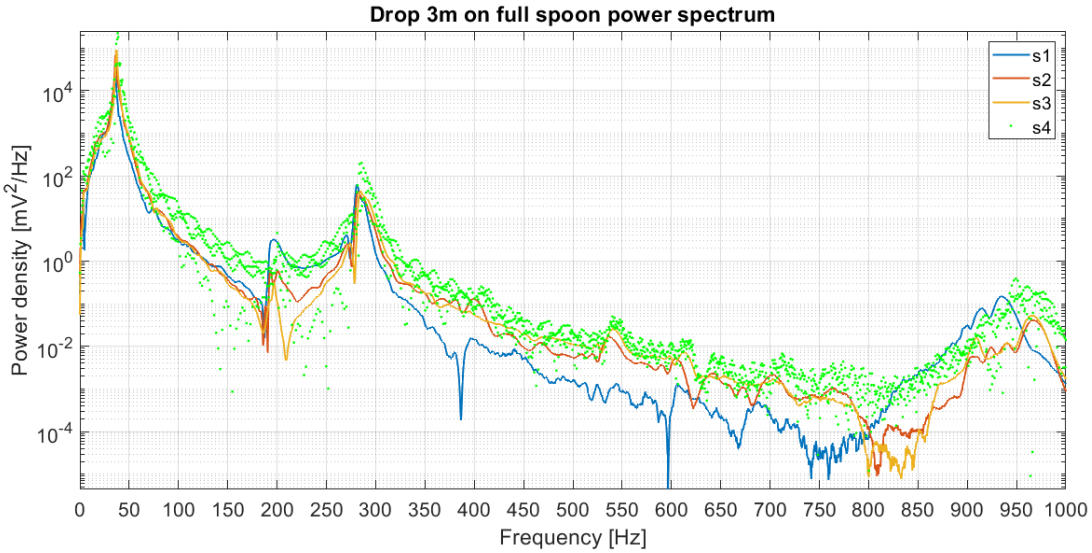

4.2.1 Summary of the results

Mean values for: full spoon condition								
Test results	**Mean frequency [Hz]**	$V_{MAX}\#1$ **[mV]**	$V_{MIN}\#1$ **[mV]**	**Peak to peak V**	$V_{MAX}\ \#2$ **[mV]**	$\frac{V_{MAX}\#1}{\lvert V_{MIN}\rvert\#1}$	$\frac{V_{MAX}\ \#1}{V_{MAX}\ \#2}$	**Mean ζ**
Drop 1m Oct*	33.56	1490	-2384	3874	2164	0.653	0.698	0.024
Drop 1m Feb	37.01	914	-1531	2445	1692	0.623	0.586	0.015
Drop 1m Mar	30.5	1367	-2145	3513	2159	0.661	0.712	0.020
Drop 1.5m	37.16	2751	-3985	6736	2833	0.702	0.966	0.017
Drop 2m	35.38	3030	-4365	7395	2919	0.696	1.034	0.017
Drop 3m	36.6	3071	-4060	7131	3066	0.758	1.009	0.016

**these results are not consistent with the others and might be afflicted by some errors*

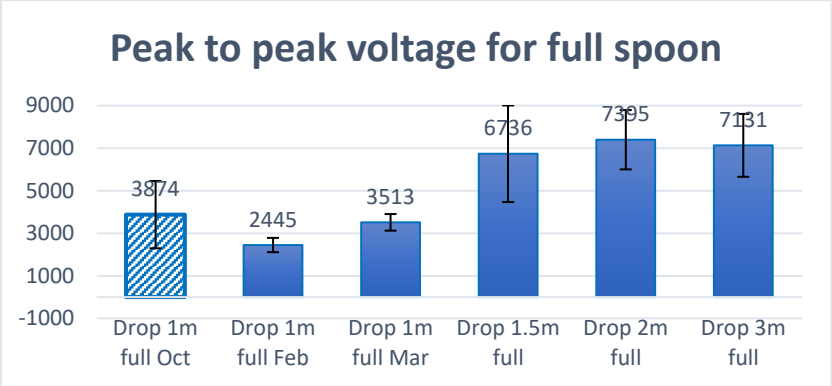

The results of the test show clearly an **increase of the peak to peak voltage with the height of fall**, with a significant exception however: the results for 3m appear to be worse than those for 2. This might be simply explained by the fact that at such a height it is almost impossible to hit the centre of the spoon and thus to reproduce the same condition of the other tests. Moreover, the natural frequency appears to be circa 36 Hz in mean (different values may happen during the tests because it is not possible to constantly keep the same quantity of water on the surface of the spoon).

As it is possible to see from the above table and the example in the right, the signals obtained during the tests show a peculiar feature: **the first peak of tension was almost never higher than the second.**

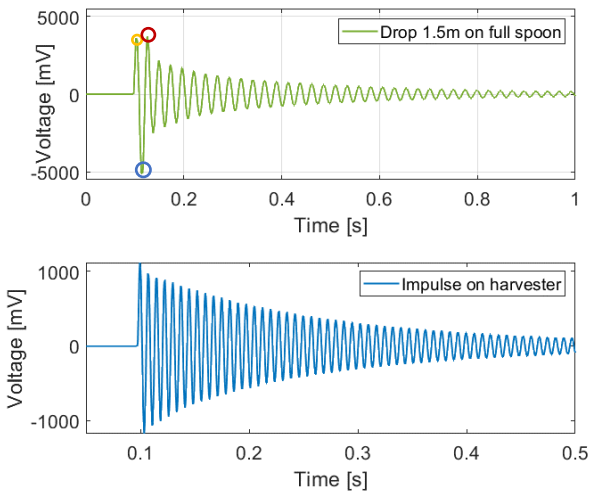

Figure 45: Comparison of a signal sample from one test and the expected signal from an impulsive excitation

4.3 Effect of empty spoon

Test: drop from 1m on empty spoon (November)*

Test sample	Mean frequency [Hz]	V_{MAX}#1 [mV]	V_{MIN}#1 [mV]	V peak to peak	V_{MAX} #2 [mV]	$\frac{V_{MAX}}{\lvert V_{MIN}\rvert}$	$\frac{V_{MAX}\ \#1}{V_{MAX}\ \#2}$	Mean ζ
#1	53.53	1343	-1488	2832	1232	0.903	1.091	0.012
#2	53.60	1047	-1212	2259	945	0.864	1.107	0.010
#3	52.81	1129	-1287	2417	1070	0.877	1.056	0.010
#4	53.57	1019	-1147	2165	946	0.888	1.077	0.011
#5	53.49	1105	-1239	2343	980	0.892	1.127	0.010
Mean	53.40	1129	-1275	2403	1035	0.885	1.091	0.011
SD	0.33	128	130	257	121	0.015	0.027	0.001

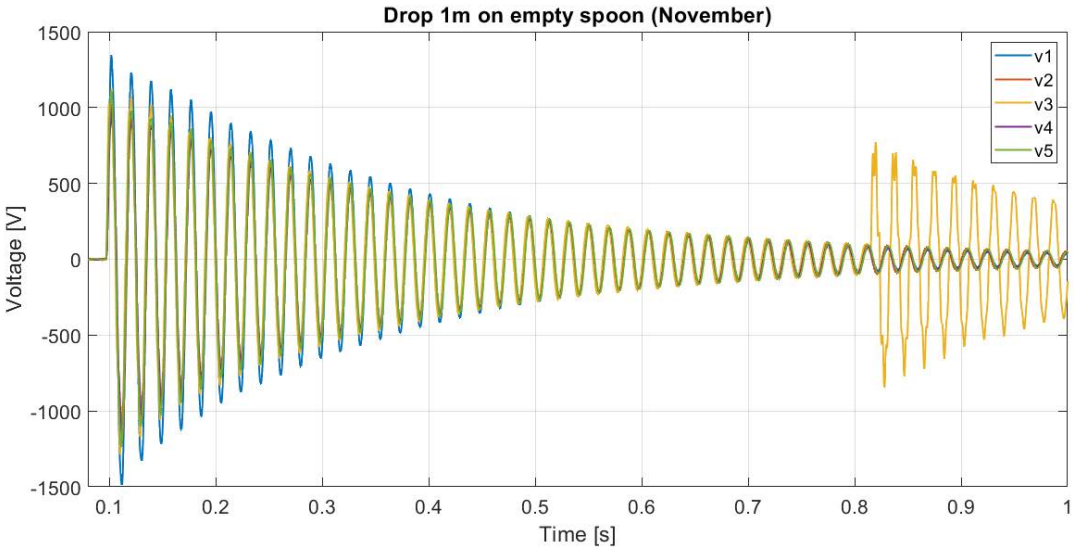

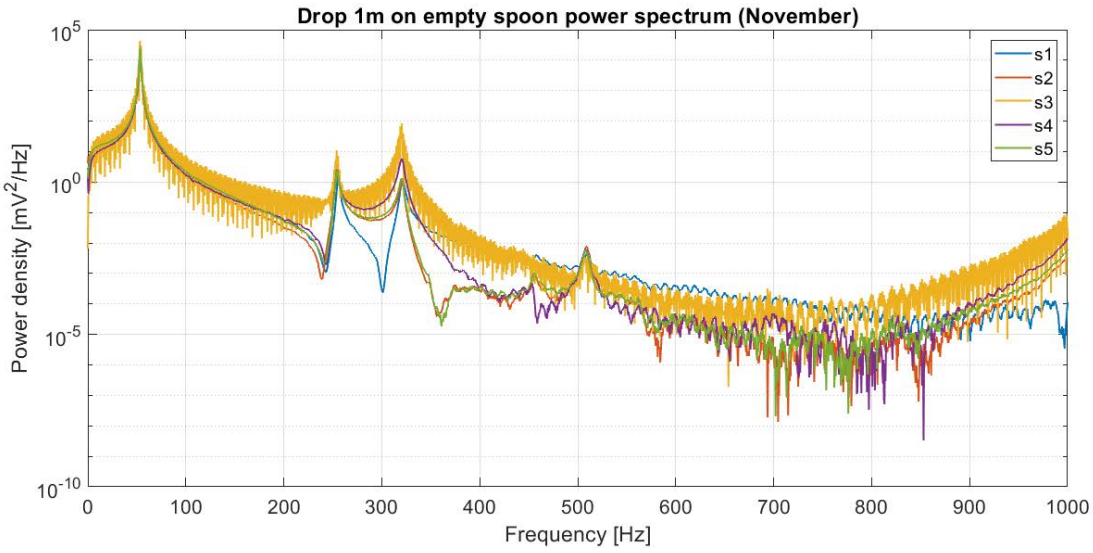

Test: drop from 1m on empty spoon (February)

Test sample	Mean frequency [Hz]	V_{MAX}#1 [mV]	V_{MIN}#1 [mV]	V peak to peak	V_{MAX} #2 [mV]	$\frac{V_{MAX}}{\lvert V_{MIN}\rvert}$	$\frac{V_{MAX}\ \#1}{V_{MAX}\ \#2}$	Mean ζ
#1	51.57	370	-394	764	332	0.938	1.113	0.009
#2	51.75	406	-453	858	371	0.896	1.093	0.009
#3	51.43	309	-344	653	302	0.897	1.023	0.008
#4	51.41	319	-328	647	300	0.974	1.065	0.008
#5	51.47	272	-278	550	256	0.979	1.064	0.008
#6	51.37	261	-296	557	247	0.885	1.059	0.008
Mean	51.50	323	-349	672	301	0.928	1.069	0.008
SD	0.14	56	65	120	47	0.042	0.031	0.000

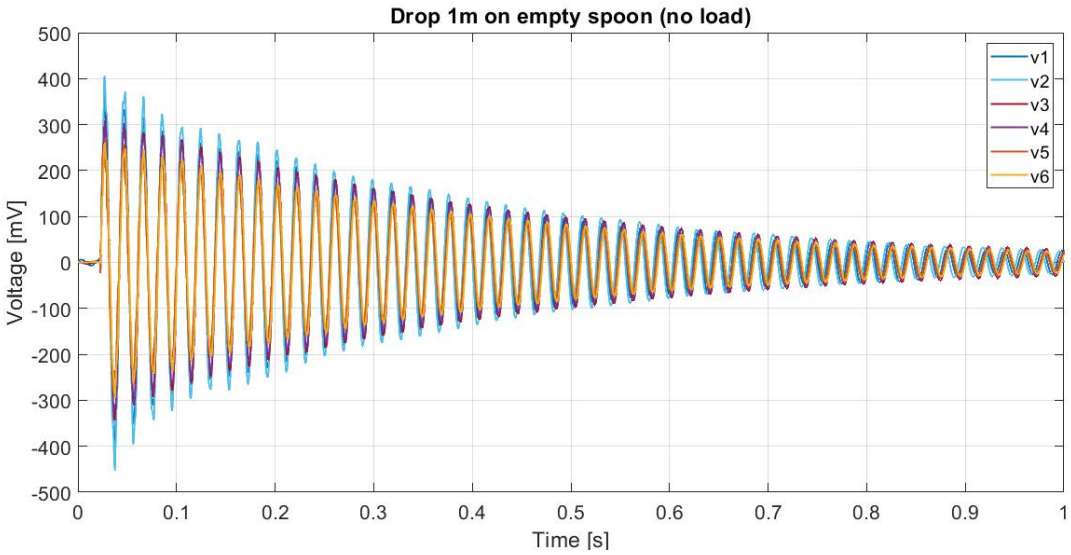

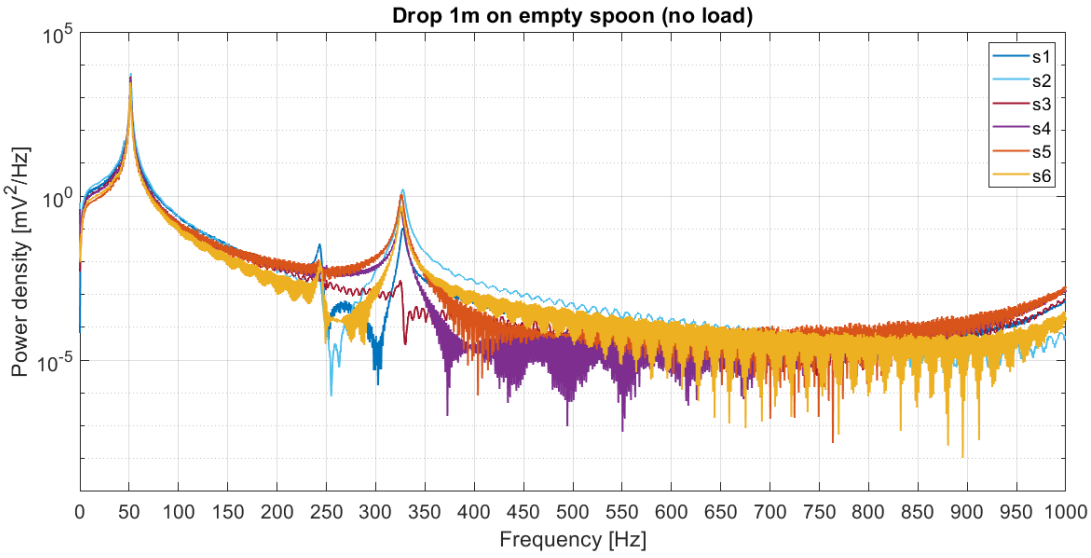

Test: drop from 1m on empty spoon (March)

Test sample	Mean frequency [Hz]	$V_{MAX}\#1$ [mV]	$V_{MIN}\#1$ [mV]	V peak to peak	$V_{MAX}\#2$ [mV]	$\frac{V_{MAX}}{\lvert V_{MIN}\rvert}$	$\frac{V_{MAX}\#1}{V_{MAX}\#2}$	Mean ζ
#1	52.47	515	-561	1076	499	0.918	1.032	0.007
#2	52.69	466	-532	998	460	0.875	1.013	0.010
#3	52.25	333	-339	672	315	0.984	1.058	0.008
#4	50.90	445	-501	946	415	0.889	1.073	0.009
#5	52.64	537	-605	1142	478	0.887	1.123	0.010
#6	52.05	514	-575	1089	456	0.894	1.127	0.011
#7	51.26	591	-640	1232	508	0.924	1.163	0.010
#8	52.45	497	-556	1053	449	0.895	1.107	0.011
Mean	52.09	487	-539	1026	448	0.908	1.087	0.010
SD	0.66	76	91	167	61	0.034	0.052	0.001

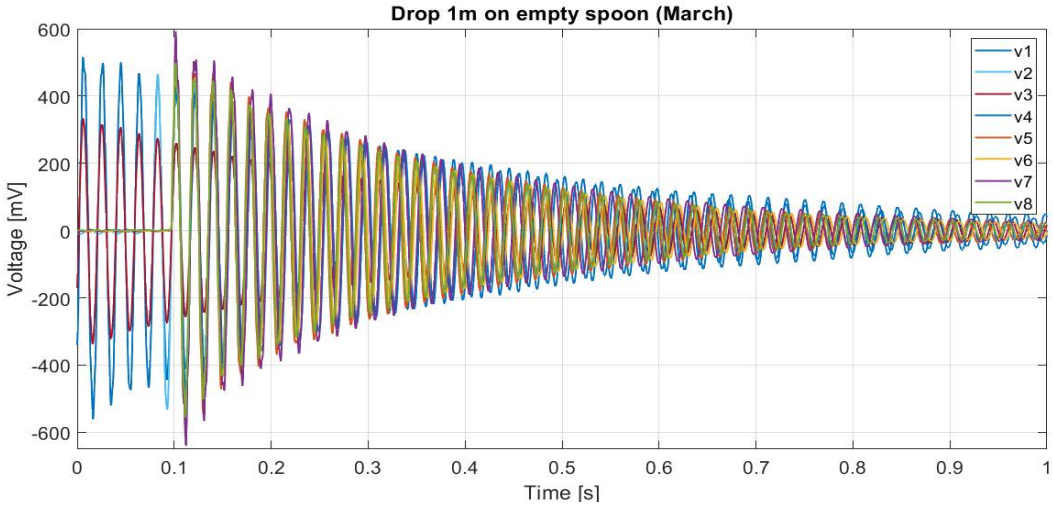

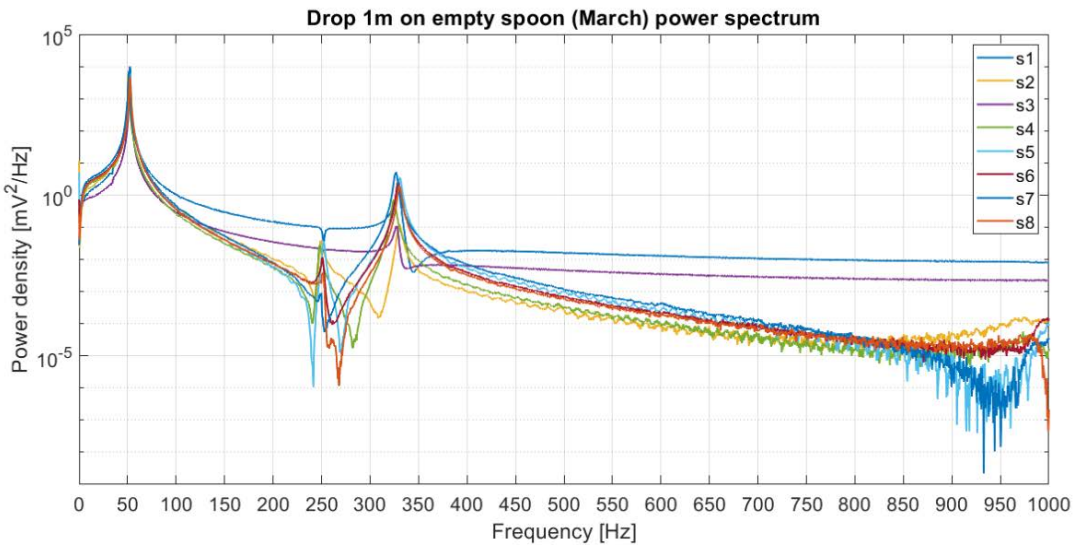

Test: drop from 2m on empty spoon

Test sample	Mean frequency [Hz]	$V_{MAX}\#1$ [mV]	$V_{MIN}\#1$ [mV]	V peak to peak	$V_{MAX}\#2$ [mV]	$\frac{V_{MAX}\#1}{\lvert V_{MIN}\rvert\#1}$	$\frac{V_{MAX}\#1}{V_{MAX}\#2}$	Mean ζ
#1	53.47	912	-1039	1950	893	0.878	1.021	0.009
#2	54.28	83	-98	181	82	0.850	1.009	0.008
#3	53.06	1019	-1113	2132	1003	0.915	1.016	0.008
#4	54.39	158	-187	345	149	0.847	1.062	0.007
#5	53.66	1955	-1821	3775	1804	1.074	1.083	0.008
Mean	**53.77**	825	-851	1677	786	**0.913**	**1.038**	**0.008**
SD	0.56	761	716	1475	706	0.094	0.033	0.001

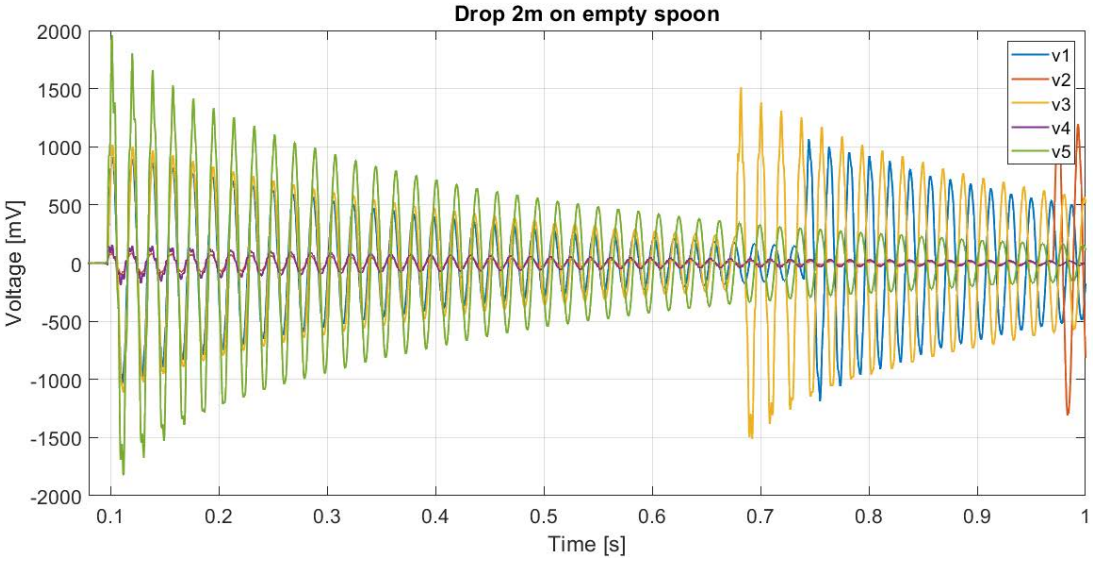

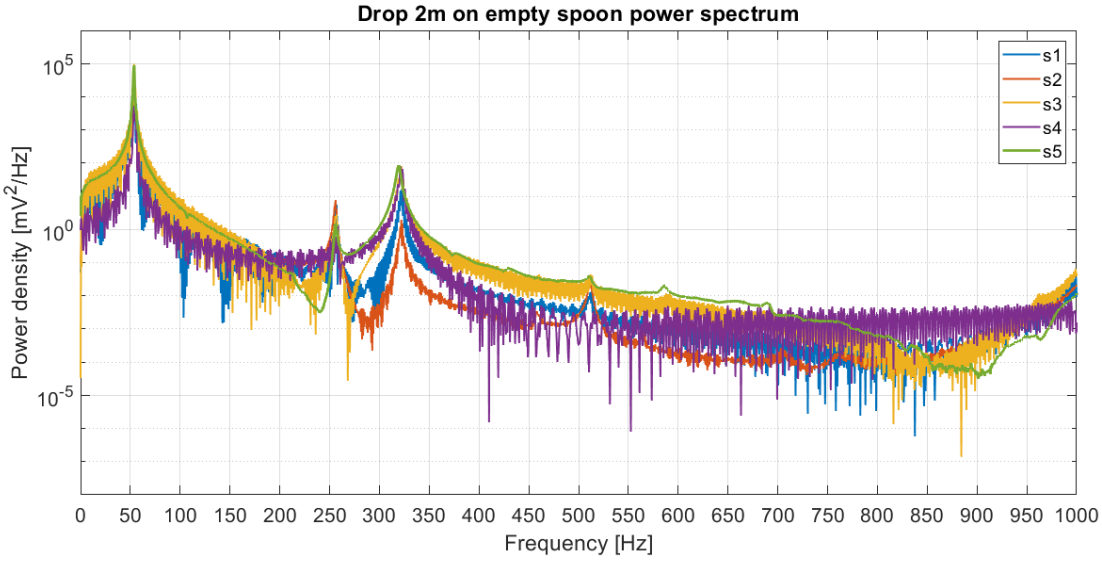

4.3.1 Summary of the results

Mean values for: empty spoon condition								
Test results	**Mean frequency [Hz]**	$V_{MAX}\#1$ **[mV]**	$V_{MIN}\#1$ **[mV]**	**Peak to peak V**	$V_{MAX}\ \#2$ **[mV]**	$\frac{V_{MAX}\#1}{\lvert V_{MIN}\rvert\#1}$	$\frac{V_{MAX}\ \#1}{V_{MAX}\ \#2}$	**Mean ζ**
Drop 1m Nov*	53.4	1129	-1275	2403	1035	0.885	1.091	0.011
Drop 1m Feb*	51.5	323	-349	672	301	0.928	1.069	0.008
Drop 1m Mar	52.09	487	-539	1026	448	0.908	1.087	0.010
Drop 2m	53.40	1295	-1324	2619	1233	0.956	1.040	0.008

**these results are not consistent with the others and might be afflicted by some errors*

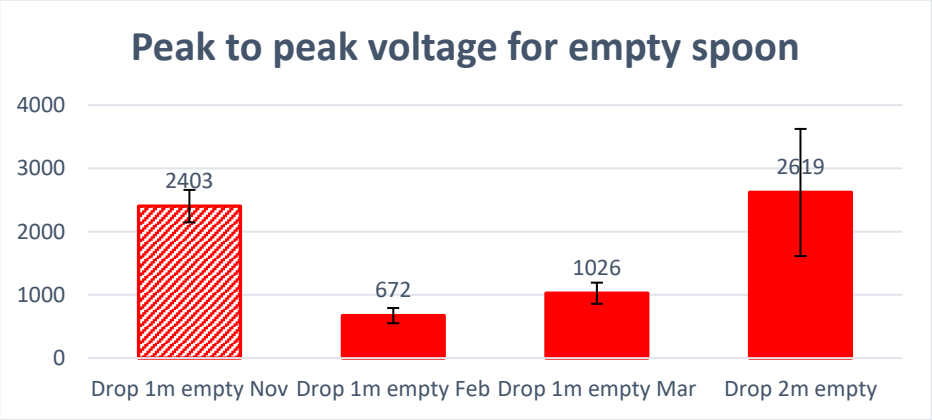

When comparing the results with these of the previous section, it appears clearly that an empty surface of the spoon hinders a proper exchange of energy**: the peak to peak voltages are conspicuously lower than when the spoon is covered with the film of water**.

Moreover it is possible to see from the above table and the figure in the right, the signals of these tests are totally "ordinary": except for the very first peak (see 2.2), they show an almost perfect exponential-sinusoidal behaviour, as it would be expected from a short impulse hit cantilever beam. The damping ratio appears to be almost constant as well (see 4.1).

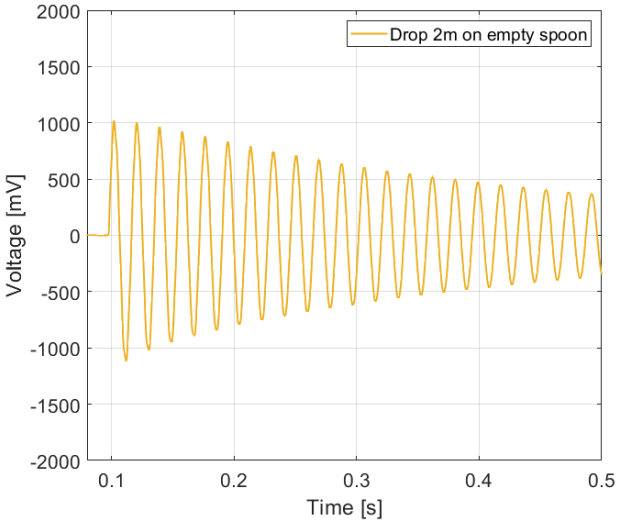

Figure 46: In the right, an example of a sample obtained in the tests

4.4 Effect of empty spoon and added mass

Test: drop from 1m on empty spoon with added mass (2.4g)*

Test sample	Mean frequency [Hz]	$V_{MAX}\#1$ [mV]	$V_{MIN}\#1$ [mV]	V peak to peak	$V_{MAX}\ \#2$ [mV]	$\frac{V_{MAX}\#1}{\lvert V_{MIN}\rvert\#1}$	$\frac{V_{MAX}\ \#1}{V_{MAX}\ \#2}$	Mean ζ
#1	27.23	780	-916	1696	809	0.851	0.964	0.014
#2	32.16	847	-1003	1851	806	0.844	1.051	0.009
#3	32.27	925	-1071	1996	897	0.864	1.032	0.008
#4	32.35	1163	-1311	2473	1104	0.887	1.053	0.008
#5	32.46	848	-964	1811	815	0.880	1.040	0.008
#6	31.32	844	-1018	1861	807	0.829	1.045	0.008
Mean	31.30	901	-1047	1948	873	0.859	1.031	0.009
SD	2.03	136	139	275	118	0.022	0.034	0.002

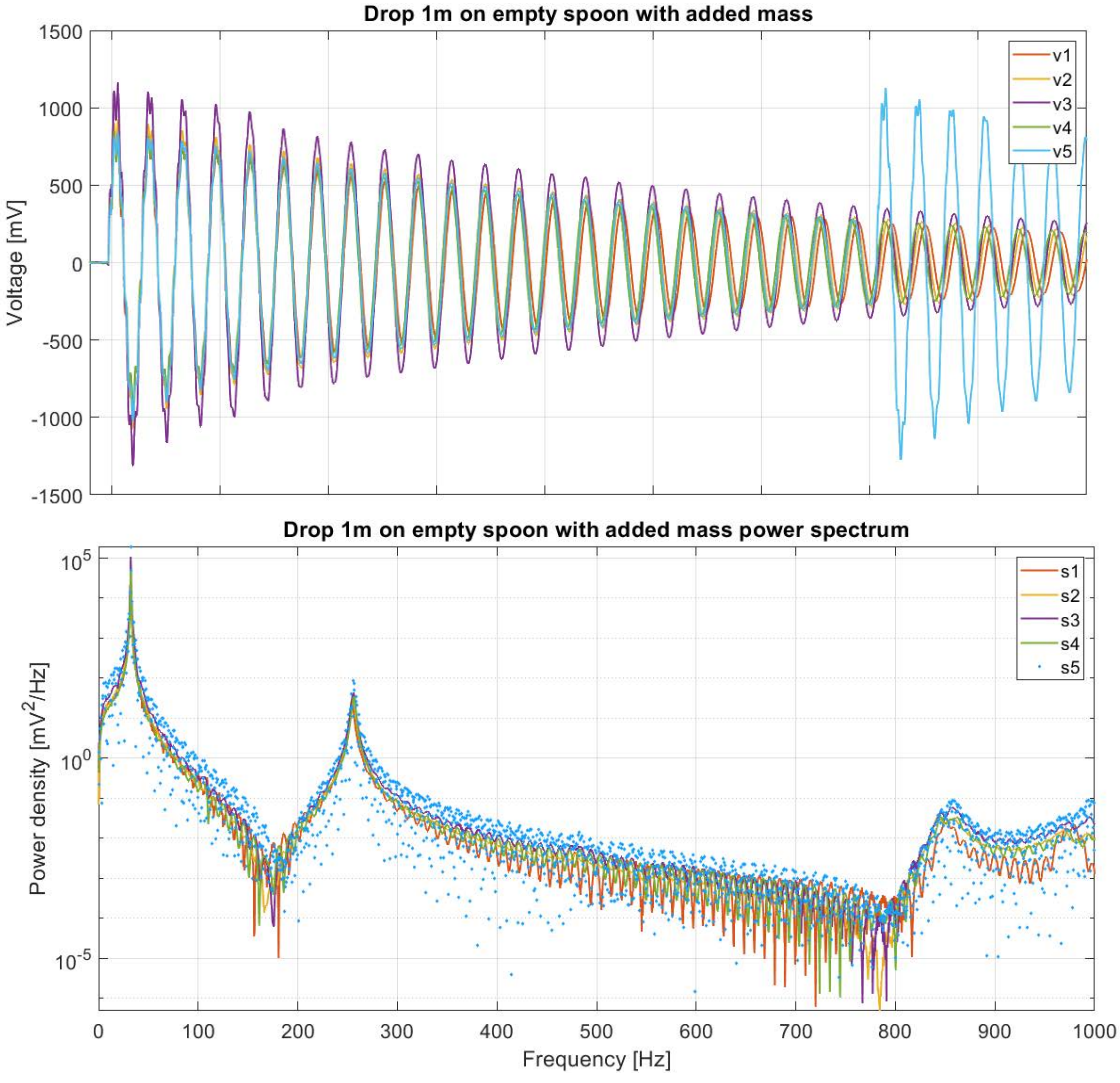

Test: drop from 1m on empty spoon with added washer (1.913g)

Test sample	Mean frequency [Hz]	$V_{MAX}\#1$ [mV]	$V_{MIN}\#1$ [mV]	V peak to peak	$V_{MAX}\#2$ [mV]	$\frac{V_{MAX}\#1}{\lvert V_{MIN}\rvert\#1}$	$\frac{V_{MAX}\#1}{V_{MAX}\#2}$	Mean ζ
#1	35.40	381	-429	810	375	0.887	1.014	0.009
#2	35.81	386	-434	819	379	0.890	1.017	0.009
#3	35.53	338	-377	716	330	0.896	1.025	0.009
#4	35.22	354	-395	749	348	0.895	1.016	0.009
#5	35.17	360	-399	760	346	0.902	1.041	0.009
Mean	35.43	364	-407	771	356	0.894	1.022	0.009
SD	0.26	20	24	43	21	0.006	0.011	0.000

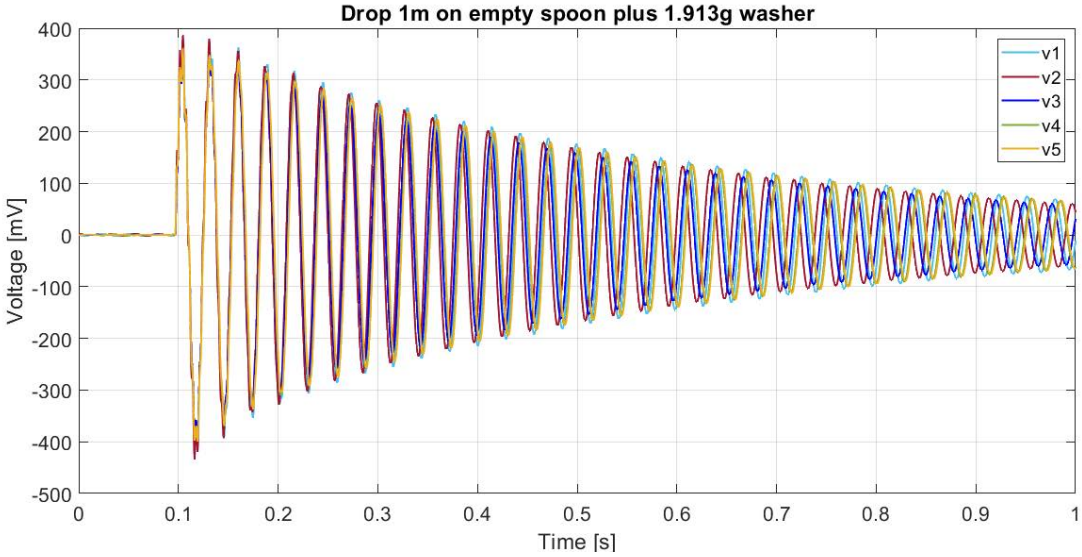

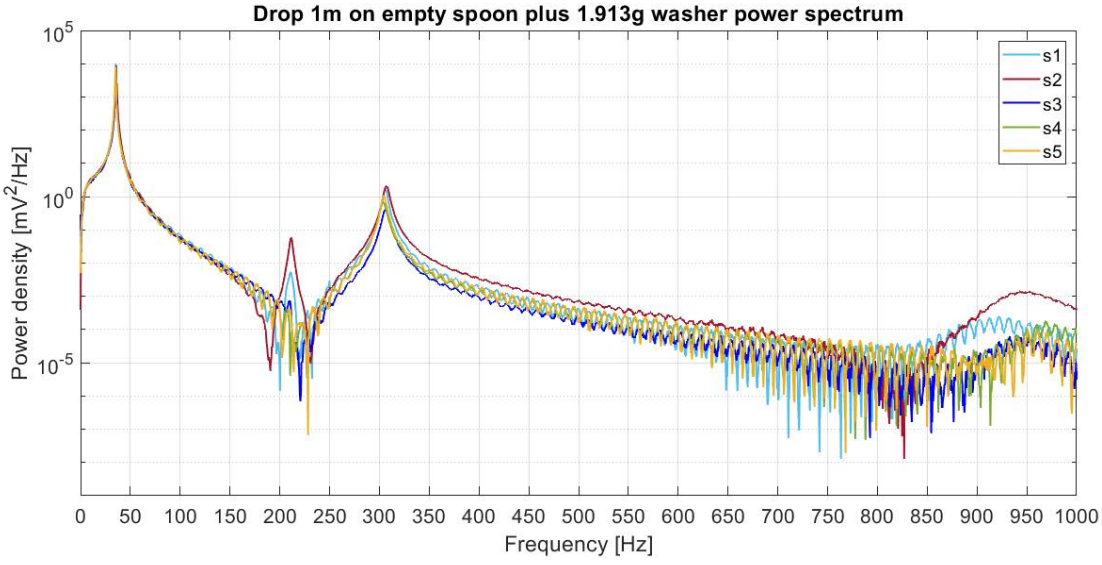

Test: drop from 1m on empty spoon with added washer (2.995 g)

Test sample	Mean frequency [Hz]	$V_{MAX}\#1$ [mV]	$V_{MIN}\#1$ [mV]	V peak to peak	$V_{MAX}\#2$ [mV]	$\frac{V_{MAX}\#1}{\lvert V_{MIN}\rvert\#1}$	$\frac{V_{MAX}\#1}{V_{MAX}\#2}$	Mean ζ
#1	31.24	347	-396	743	336	0.877	1.034	0.008
#2	30.95	220	-216	436	211	1.018	1.044	0.008
#3	31.12	242	-236	478	231	1.026	1.049	0.008
#4	31.33	364	-411	775	354	0.884	1.029	0.008
#5	31.14	329	-372	701	317	0.884	1.036	0.008
#6	31.13	345	-399	744	345	0.866	1.002	0.008
Mean	31.15	308	-338	646	299	0.926	1.032	0.008
SD	0.13	61	88	149	62	0.075	0.016	0.000

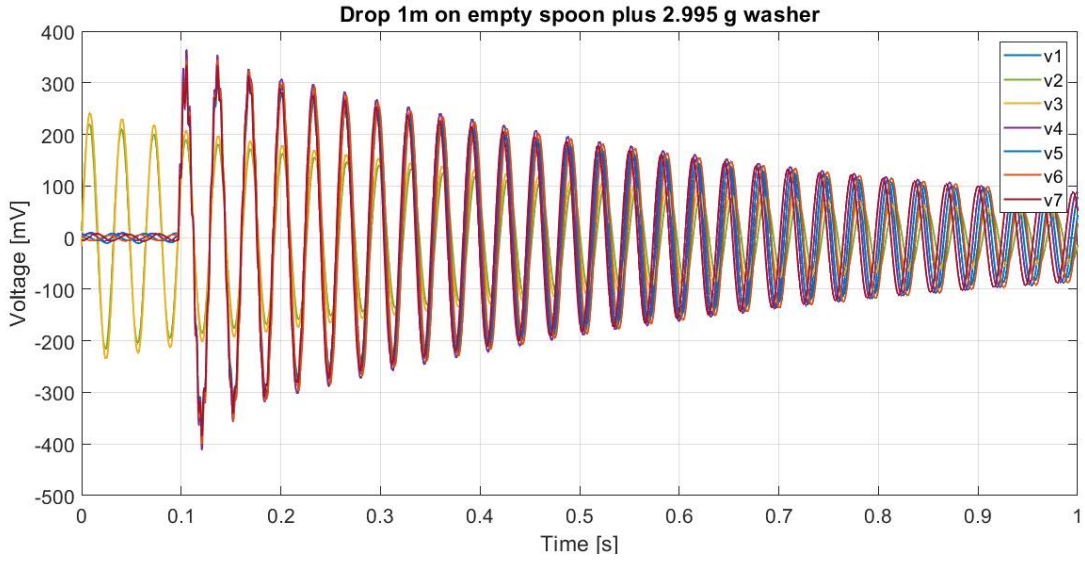

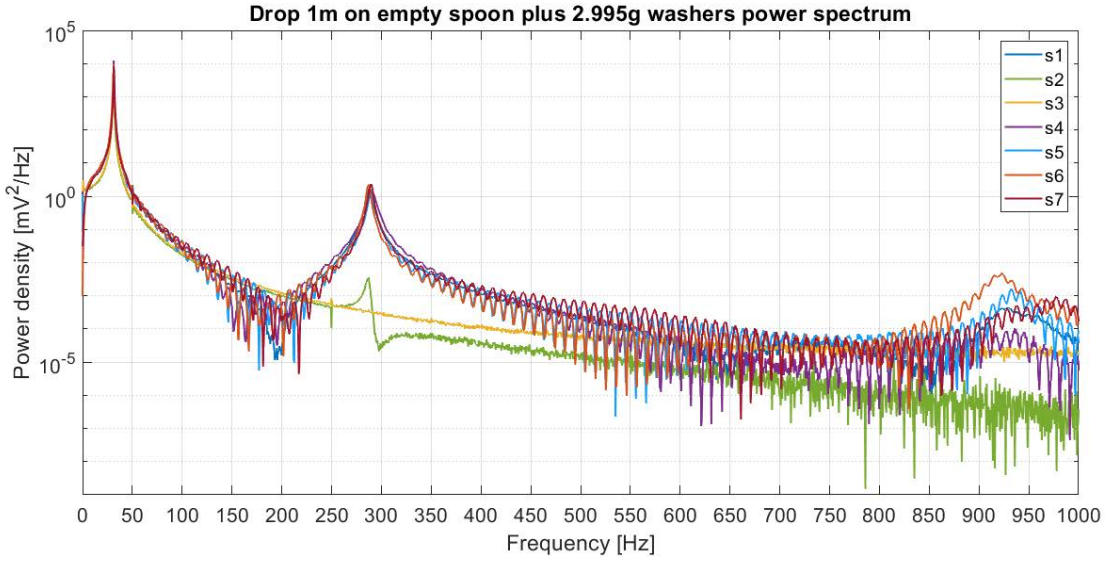

Test: drop from 1m on empty spoon with added washer (6.307 g)

Test sample	Mean frequency [Hz]	$V_{MAX}\#1$ [mV]	$V_{MIN}\#1$ [mV]	V peak to peak	$V_{MAX}\#2$ [mV]	$\frac{V_{MAX}\#1}{\lvert V_{MIN}\rvert\#1}$	$\frac{V_{MAX}\#1}{V_{MAX}\#2}$	Mean ζ
#1	23.83	71	-72	143	67	0.983	1.060	0.010
#2	23.49	51	-49	100	48	1.053	1.076	0.008
#3	23.54	236	-245	481	223	0.964	1.061	0.009
#4	23.47	238	-286	524	241	0.832	0.987	0.009
#5	23.44	224	-265	489	224	0.847	1.000	0.009
Mean	23.55	164	-183	347	161	0.936	1.037	0.009
SD	0.16	94	113	207	95	0.094	0.040	0.001

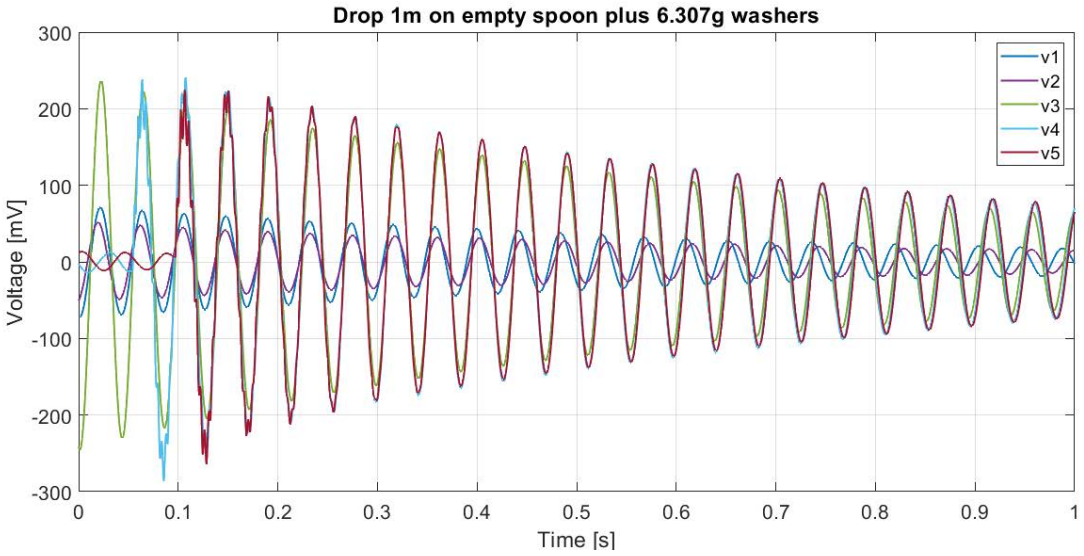

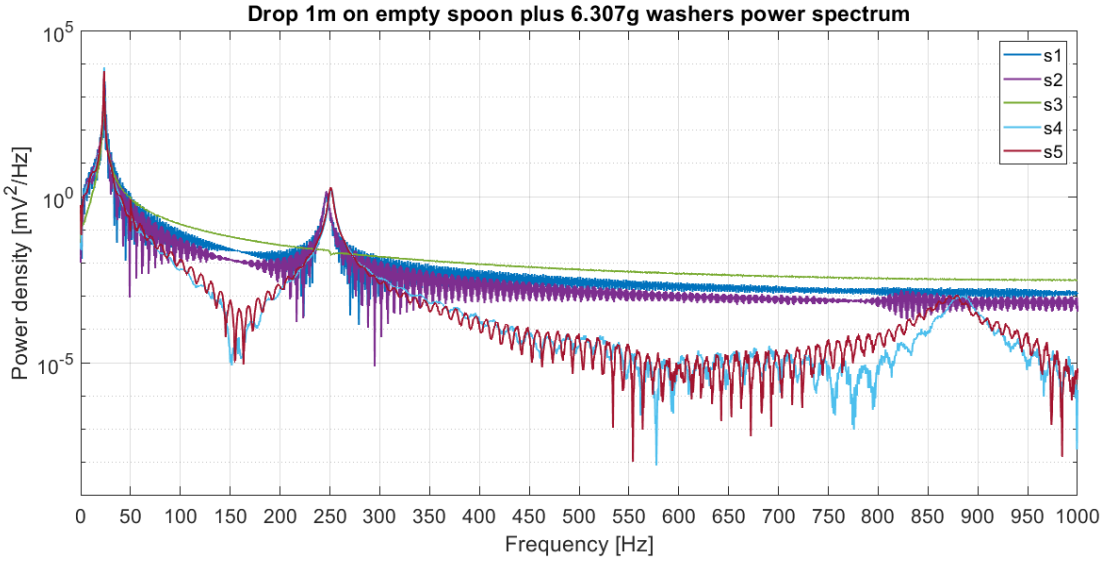

Test: drop from 1m on empty spoon with added washer (10.63g)

Test sample	Mean frequency [Hz]	$V_{MAX}\#1$ [mV]	$V_{MIN}\#1$ [mV]	V peak to peak	$V_{MAX}\#2$ [mV]	$\frac{V_{MAX}\#1}{\lvert V_{MIN}\rvert\#1}$	$\frac{V_{MAX}\#1}{V_{MAX}\#2}$	Mean ζ
#1	15.57	128	-160	288	142	0.796	0.899	0.011
#2	15.50	128	-161	289	144	0.792	0.887	0.011
#3	15.57	136	-179	315	155	0.761	0.879	0.011
#4	15.24	108	-145	254	124	0.747	0.873	0.011
#5	15.30	120	-157	277	137	0.767	0.877	0.011
Mean	15.43	124	-161	285	140	0.773	0.883	0.011
SD	0.16	10	12	22	11	0.021	0.010	0.000

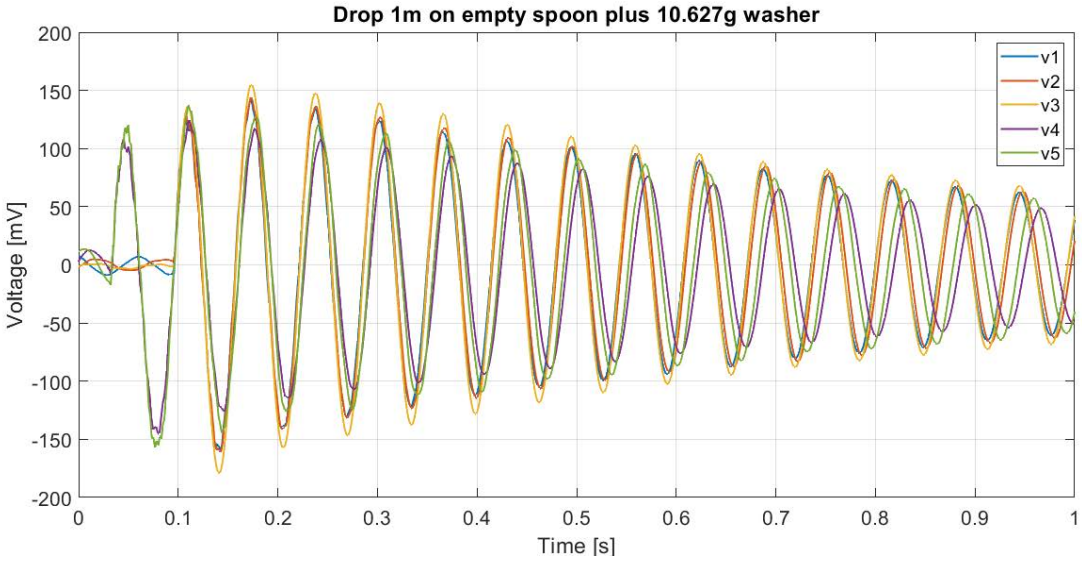

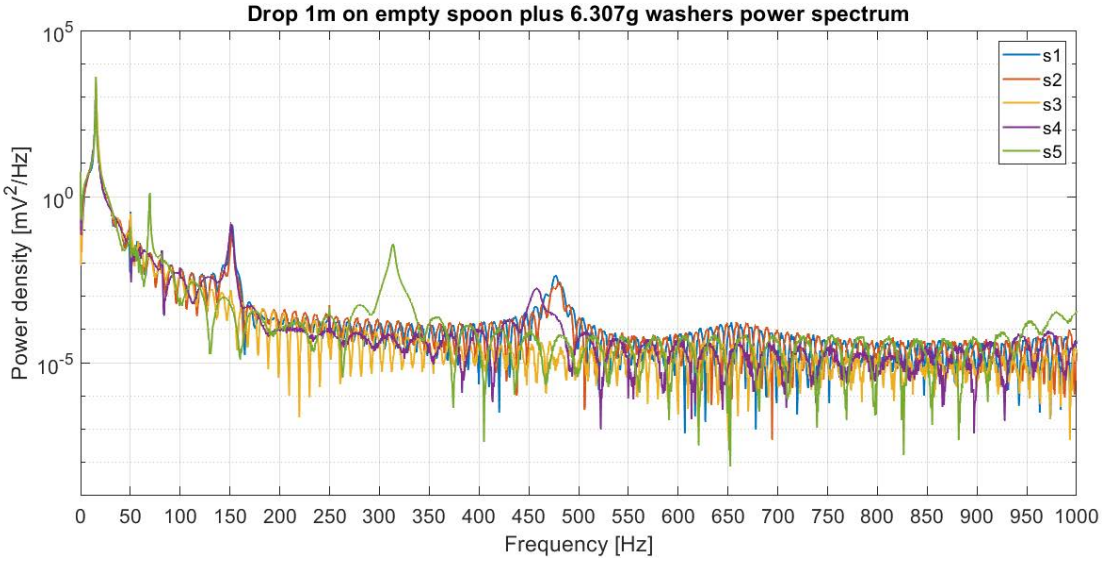

4.4.1 Summary of the results

Mean values for: empty spoon with added mass condition								
Test results	**Mean frequency [Hz]**	$V_{MAX}\#1$ **[mV]**	$V_{MIN}\#1$ **[mV]**	**Peak to peak V**	$V_{MAX}\#2$ **[mV]**	$\frac{V_{MAX\#1}}{\lvert V_{MIN\#2}\rvert}$	$\frac{V_{MAX}\#1}{V_{MAX}\#2}$	**Mean ζ**
Drop 1m + 2.4 g*	31.3	901	-1047	1948	873	0.859	1.031	0.009
Drop 1m + 1.91 g	35.43	364	-407	771	356	0.894	1.022	0.009
Drop 1m + 3.00 g	31.15	308	-338	646	299	0.926	1.032	0.008
Drop 1m + 6.30 g	23.55	164	-183	347	161	0.936	1.037	0.009
Drop 1m + 10.63 g	15.43	124	-161	285	140	0.773	0.883	0.011

**these results are not consistent with the others and might be afflicted by some errors*

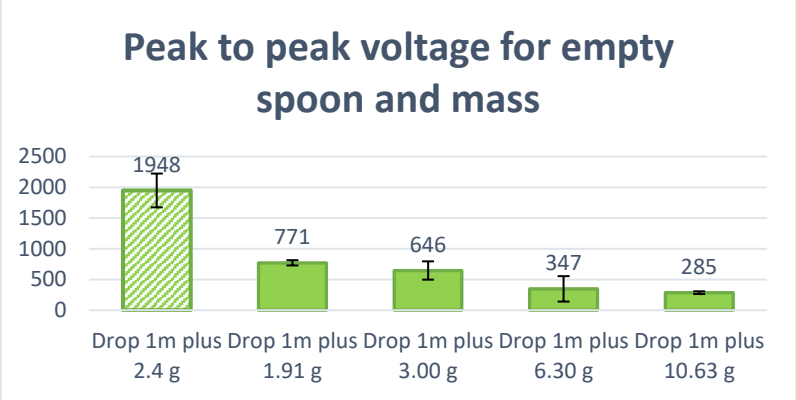

The main result of these tests is clearly that not only the added mass does not enhance the amplitude of the signal, but rather the opposite: as the added mass increases, the amplitude literally drops. For that reason, it can be said that a heavy spoon is surely harmful for the harvester.

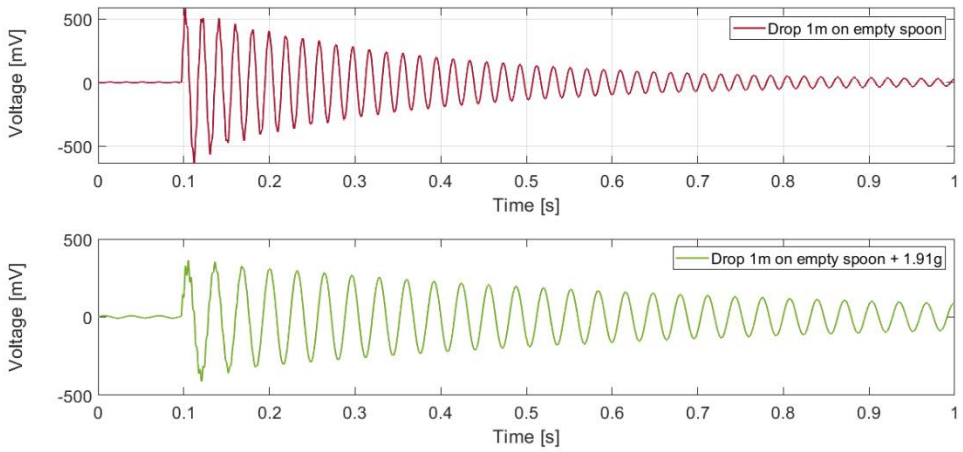

Figure 47: Comparison of signal shape between a sample from the empty spoon tests and one from the mass tests

For what concerns the signal shape, the first result is an enhanced presence of the superior modes in the beginning of the vibration. Moreover it appears also that the more the mass increases, the more the difference between the voltage of the first and second peaks diminishes, eventually becoming negative. In fact, the power spectra of the two empty cases show as well very little differences, except for a slight enhancement of the 3rd mode in the added mass case.

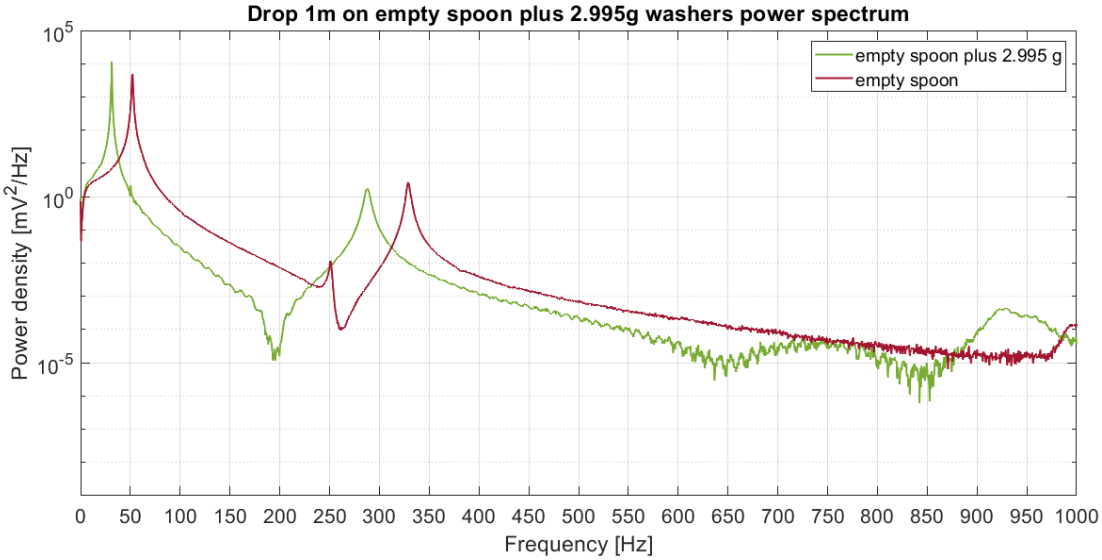

Figure 48: Comparison of signal shape between a sample from the mass tests and one of the empty spoon alone, in frequency domain

4.5 Study of impulse with the accelerometer

Test: drop impulse from 1m on full spoon (February)

Test sample	Mean frequency [Hz]	V_{MAX}#1 [mV]	V_{MIN}#1 [mV]	V peak to peak	V_{MAX} #2 [mV]	$\frac{V_{MAX}}{\lvert V_{MIN}\rvert}$	$\frac{V_{MAX}\ \#1}{V_{MAX}\ \#2}$	Mean ζ
#1	32.35	1449	-2418	3868	2424	0.599	0.598	0.116
#2	33.15	1367	-2102	3468	1803	0.650	0.758	0.084
#3	36.22	1755	-2327	4082	1972	0.754	0.890	0.119
#4	35.72	1734	-3003	4737	2867	0.577	0.605	0.095
Mean	34.36	1576	-2463	4039	2266	0.645	0.713	0.104
SD	1.90	197	384	530	478	0.079	0.139	0.017

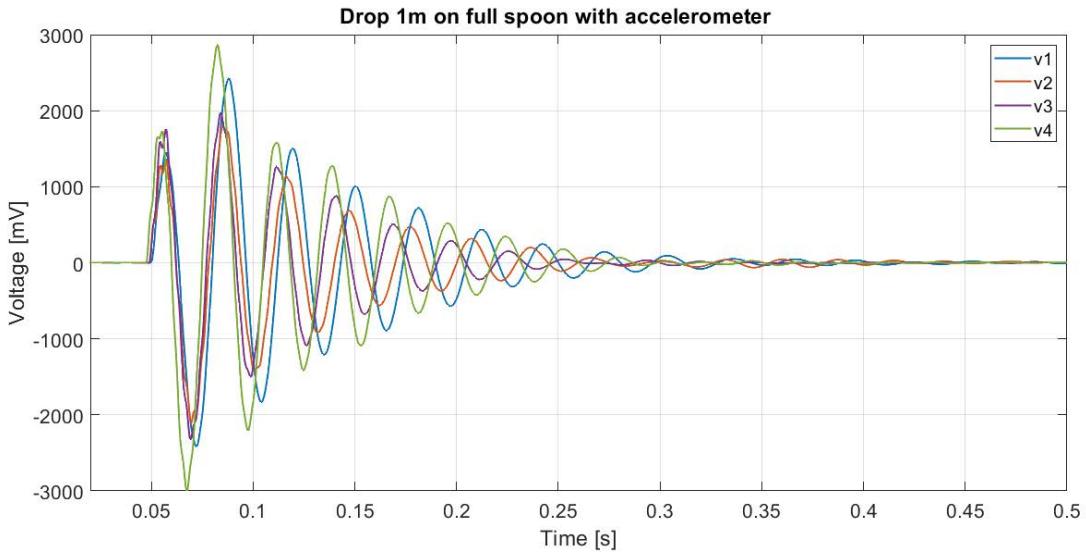

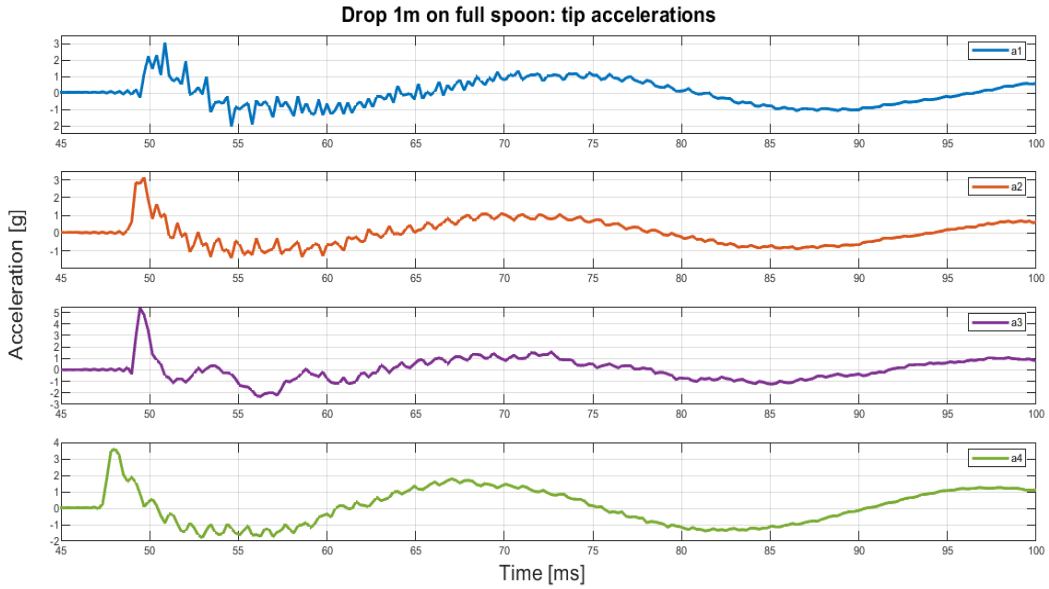

Test: drop impulse from 1m on full spoon (March)

Test sample	Mean frequency [Hz]	$V_{MAX}\#1$ [mV]	$V_{MIN}\#1$ [mV]	V peak to peak	$V_{MAX}\#2$ [mV]	$\frac{V_{MAX}}{\lvert V_{MIN}\rvert}$	$\frac{V_{MAX}\#1}{V_{MAX}\#2}$	Mean ζ
#1	31.31	882	-1648	2530	1727	0.535	0.511	0.031
#2	32.70	901	-1736	2637	1890	0.519	0.477	0.050
#3	31.31	876	-1713	2590	1937	0.511	0.452	0.048
#4	31.75	762	-1429	2191	1449	0.533	0.526	0.036
#5	31.10	901	-1763	2664	1999	0.511	0.451	0.035
#6	33.76	824	-1538	2362	1633	0.536	0.505	0.022
Mean	31.99	858	-1638	2496	1772	0.524	0.487	0.037
SD	1.04	55	130	184	209	0.012	0.032	0.010

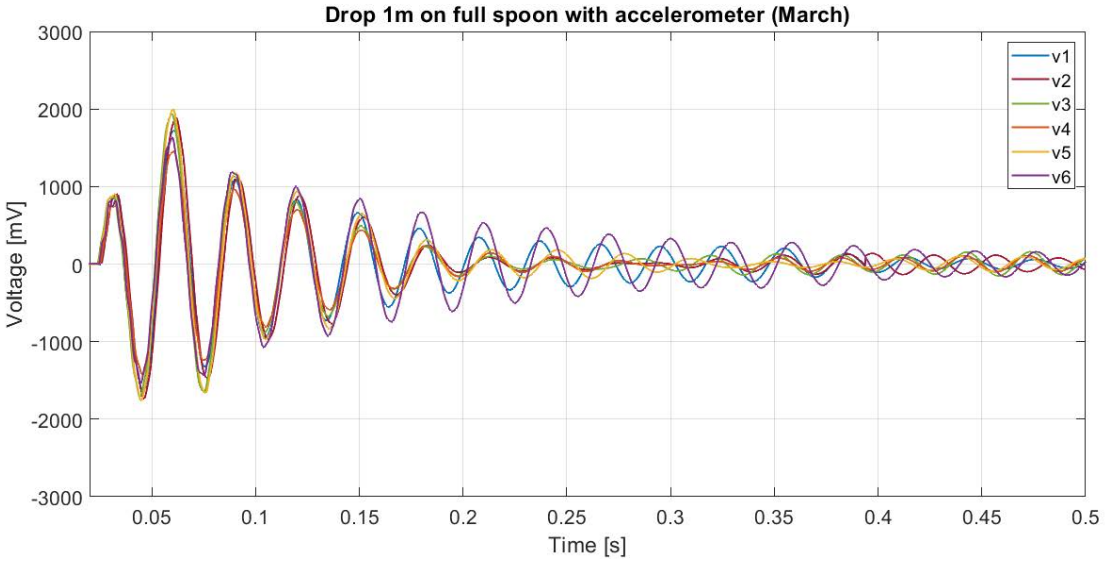

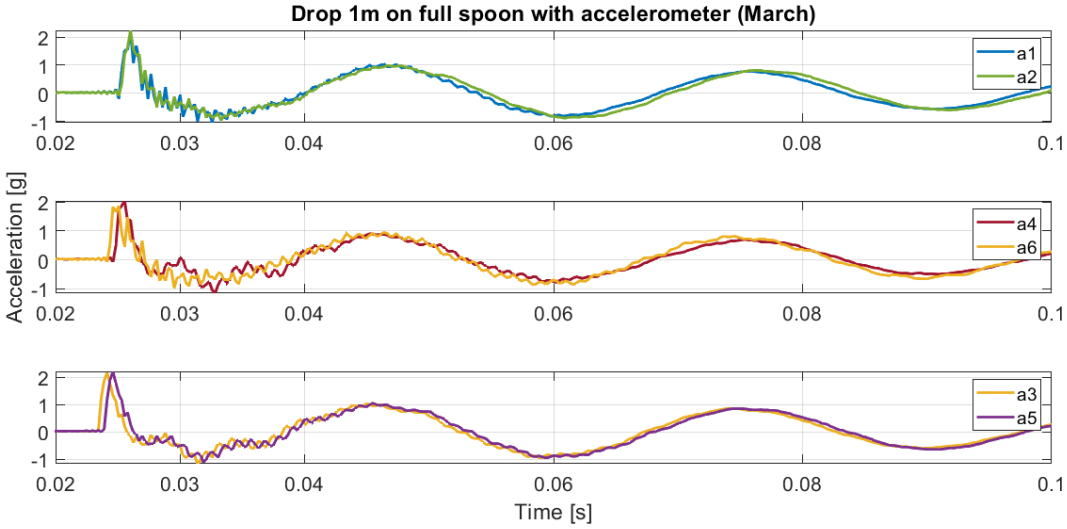

Test: drop impulse from 1m on empty spoon (February)

Test sample	Mean frequency [Hz]	V_{MAX}#1 [mV]	V_{MIN}#1 [mV]	V peak to peak	V_{MAX} #2 [mV]	$\frac{V_{MAX}}{\lvert V_{MIN}\rvert}$	$\frac{V_{MAX}\ \#1}{V_{MAX}\ \#2}$	Mean ζ
#1	52.20	670	-715	1385	471	0.938	1.423	0.014
#2	53.07	981	-1019	2000	713	0.963	1.376	0.013
#3	51.82	1059	-1056	2114	766	1.003	1.382	0.016
#4	52.65	989	-1060	2050	761	0.933	1.300	0.014
Mean	52.44	925	-962	1887	678	0.959	1.370	0.014
SD	0.54	173	166	338	140	0.032	0.051	0.001

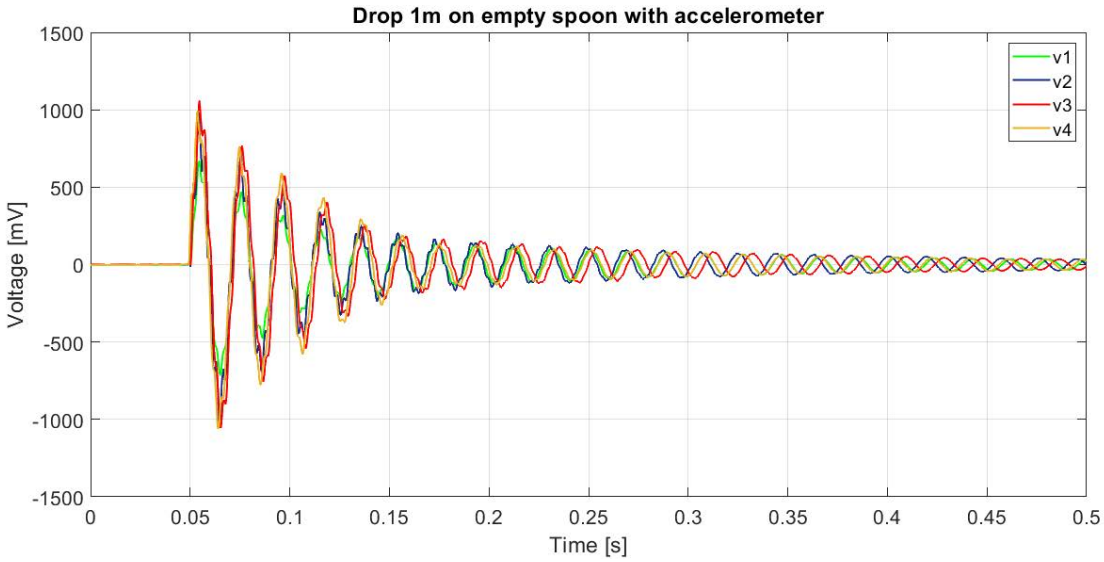

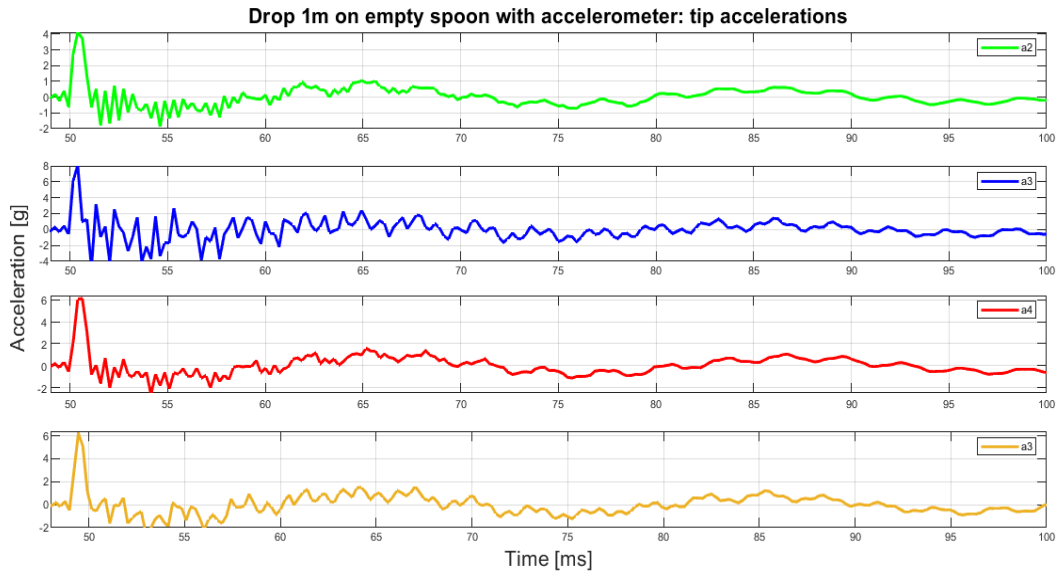

Test: drop impulse from 1m on empty spoon (March)

Test sample	Mean frequency [Hz]	V_{MAX}#1 [mV]	V_{MIN}#1 [mV]	V peak to peak	V_{MAX} #2 [mV]	$\frac{V_{MAX}}{\lvert V_{MIN}\rvert}$	$\frac{V_{MAX}\ \#1}{V_{MAX}\ \#2}$	Mean ζ
#1	46.76	213	-232	445	195	0.916	1.091	0.019
#2	48.55	536	-507	1042	379	1.058	1.415	0.021
#3	46.75	394	-385	779	290	1.023	1.358	0.024
#4	46.63	288	-286	574	215	1.008	1.341	0.009
#5	47.10	488	-480	968	358	1.016	1.361	0.013
#6	47.11	577	-574	1151	439	1.005	1.315	0.014
Mean	47.15	416	-411	827	313	1.004	1.314	0.017
SD	0.71	144	133	277	96	0.047	0.114	0.006

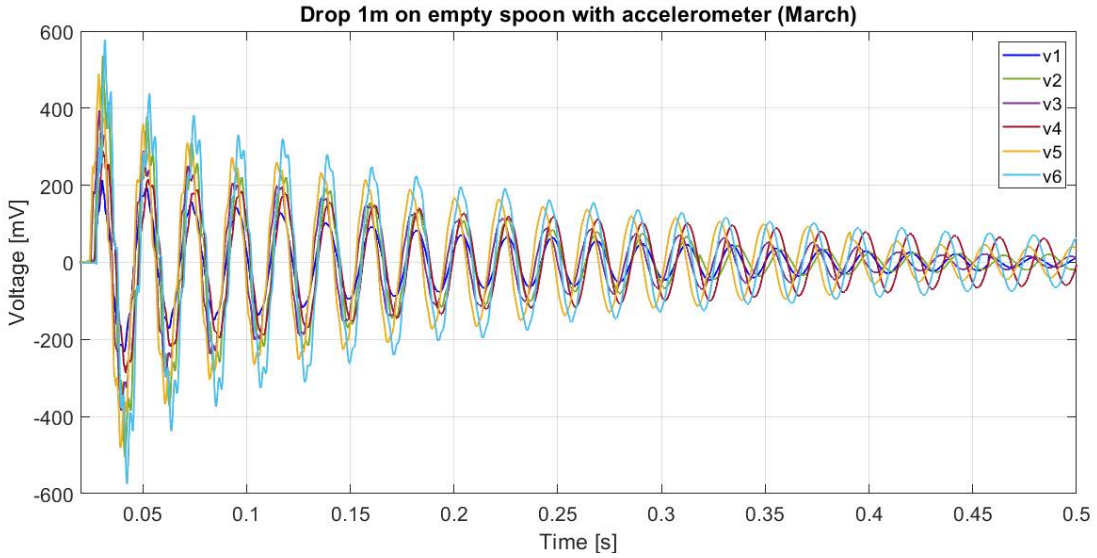

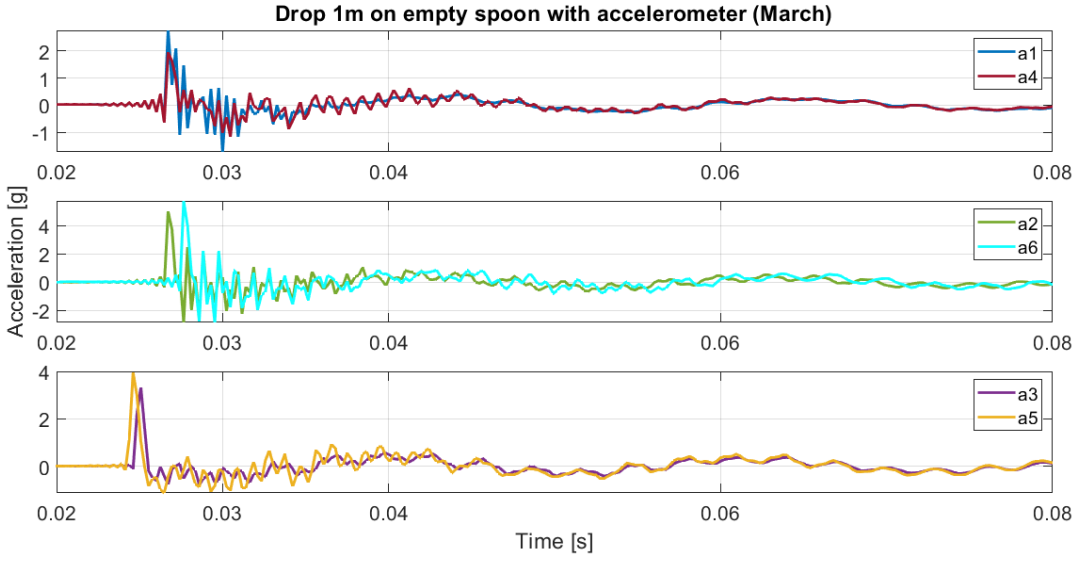

Test: drop impulse from 1m on empty spoon with added mass*

**The results obtained in this test are not consistent with the others*

Test sample	Mean frequency [Hz]	V_{MAX}#1 [mV]	V_{MIN}#1 [mV]	V peak to peak	V_{MAX} #2 [mV]	$\frac{V_{MAX}}{\lvert V_{MIN}\rvert}$	$\frac{V_{MAX}\ \#1}{V_{MAX}\ \#2}$	Mean ζ
#1	31.33	164	-156	320	96	1.054	1.714	0.017
#2	30.53	151	-68	219	181	2.231	0.836	0.020
#3	30.45	184	-68	252	58	2.705	3.144	0.014
#4	30.68	172	-157	329	106	1.095	1.622	0.015
Mean	34.36	1576	-2463	4039	2266	0.645	0.713	0.104
SD	1.90	197	384	530	478	0.079	0.139	0.017

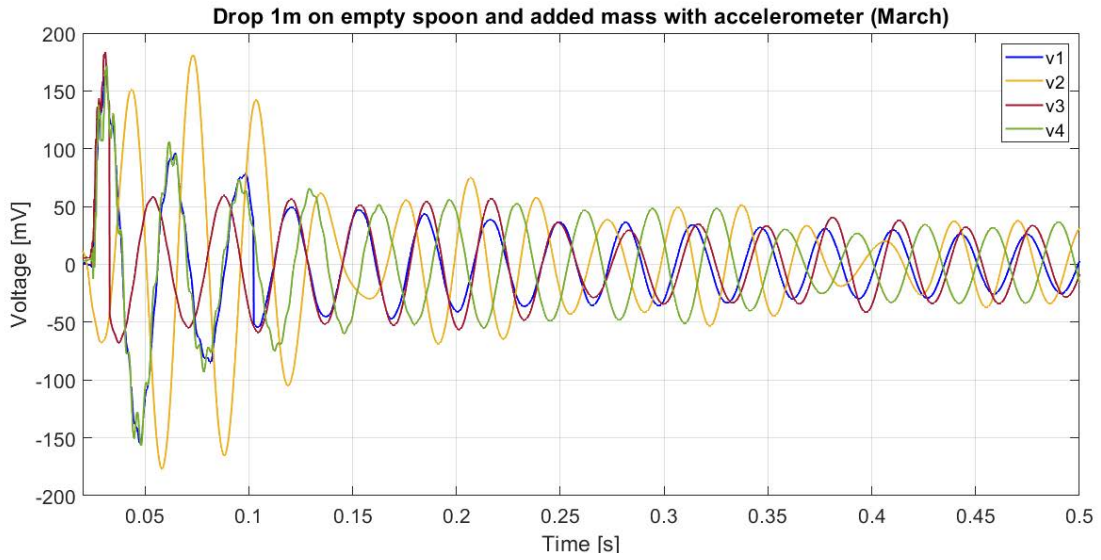

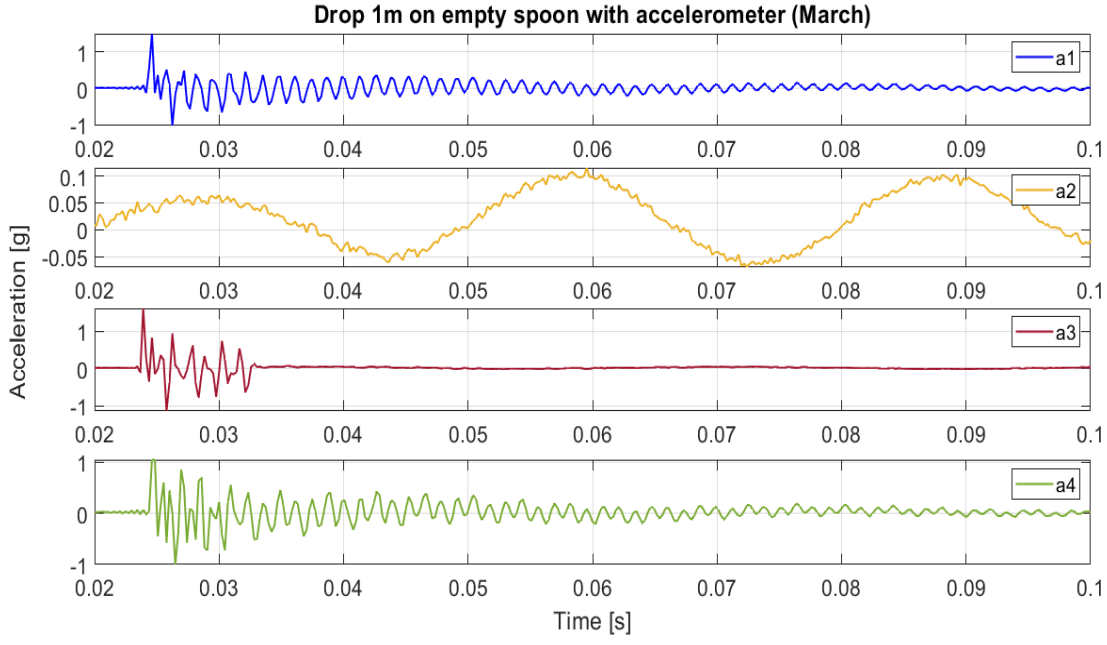

Test: frequency response function evaluation

The aim of this test was the evaluation of **FRF** between the force applied at the tip of the spoon and the electrical tension produced by it. It was performed in two different configurations: at first with the spoon full of water and then with it totally empty.

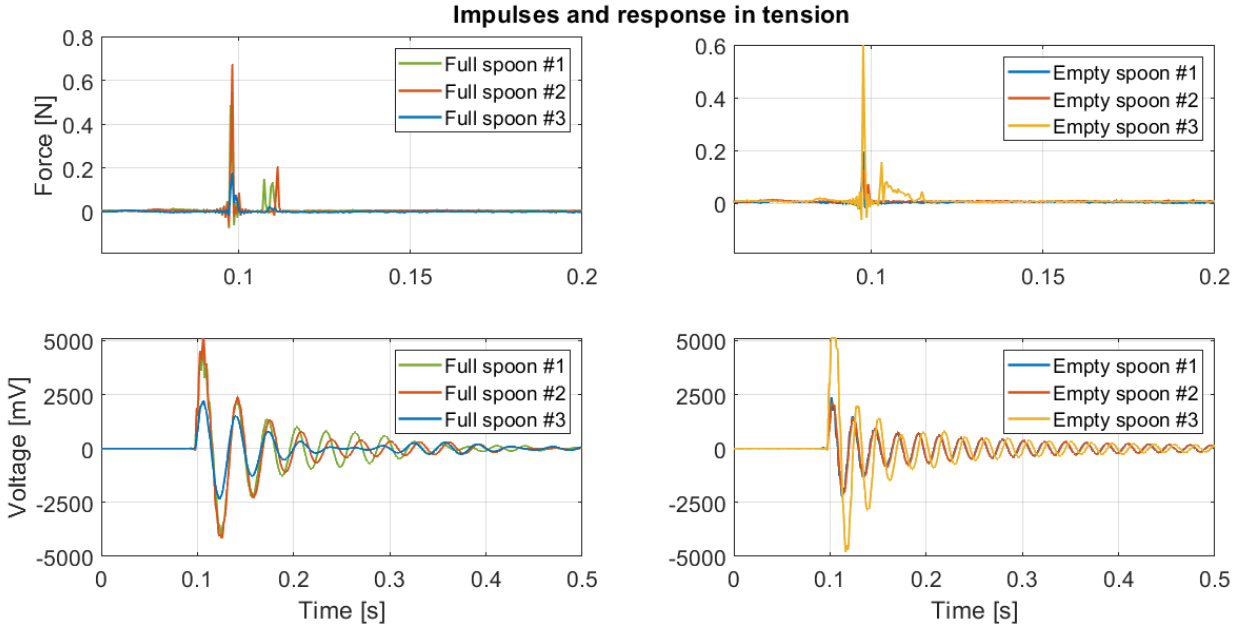

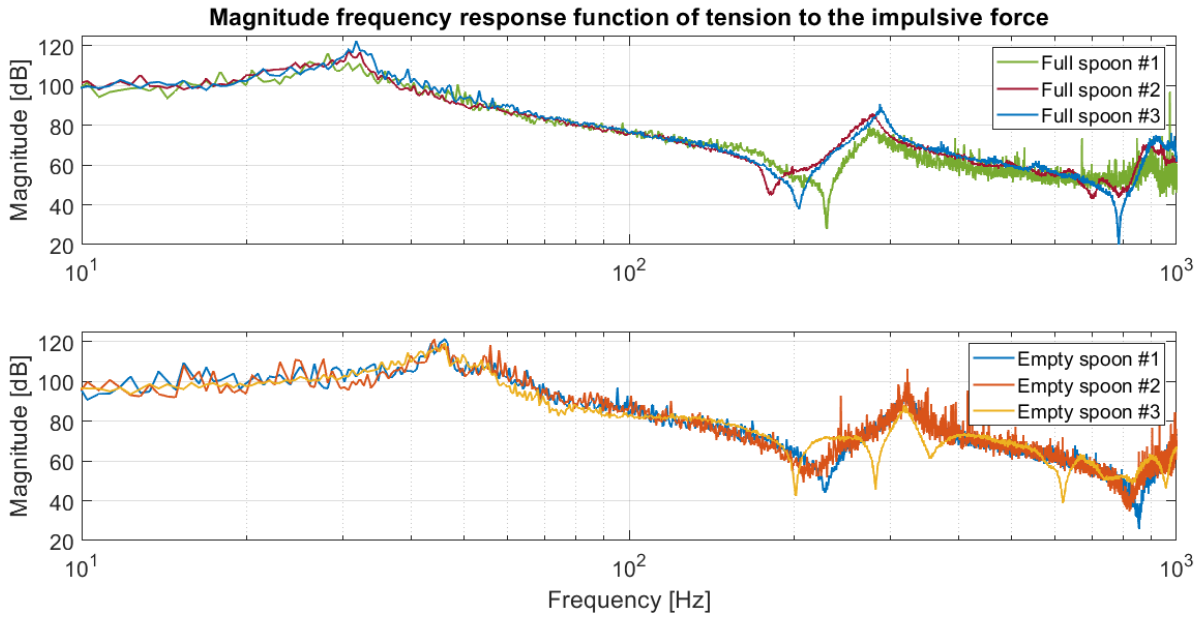

It is possible to see that the two **FRFs are extremely similar**, with the only major difference being the **position of the peaks** (which are at lower frequencies with the added mass of water).

4.5.1 Summary of the results

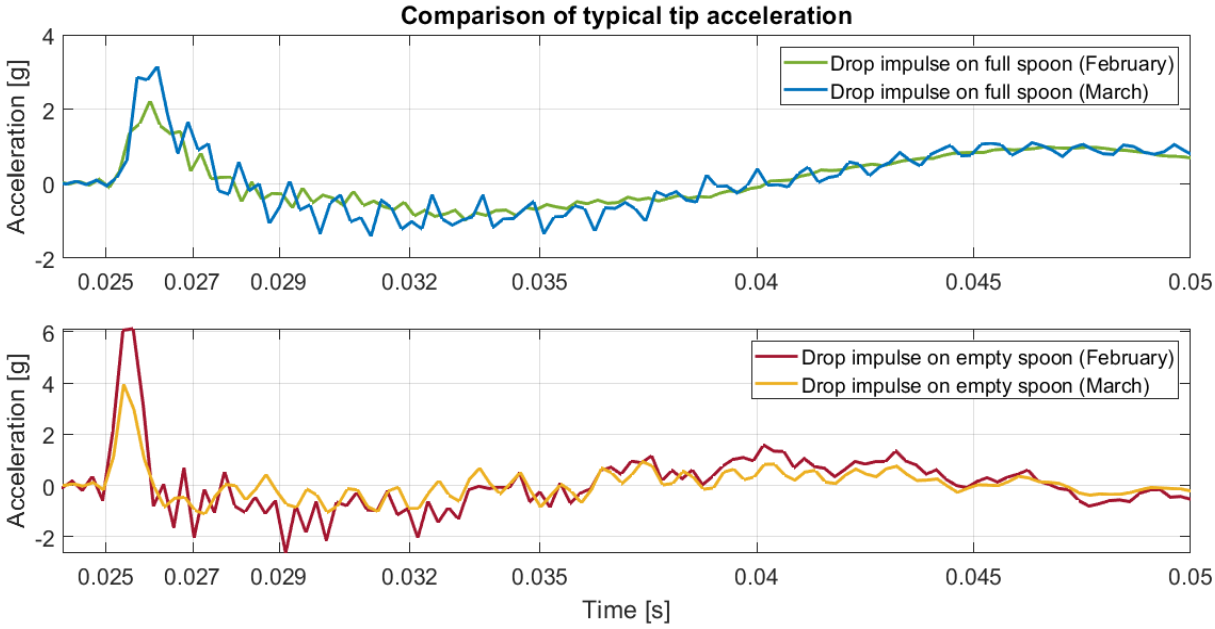

The main piece of information that can be obtained through these tests is related to the different impact mechanism: the study of the tip acceleration of the spoon offers in fact a clear hint on the different nature in the interaction of the droplet with the surface.
The differences are mainly two:

- *The maximal acceleration is somewhat higher in **absence of water***
- *The duration of the impulse appears to be much **shorter in absence of water***

In particular, it appears that the impact is circa **2.5 ms** for the **full spoon** and **1 ms** for the **empty spoon**. This could explain why the **peak to peak voltage is higher when the spoon is full of water**: the presence of water, albeit increasing the damping of the system, allows a better absorption of the kinetic energy in the impact. The tests do not show a significant difference in the results obtained February or March.
Mathematically, it would seem that the first impulse could be descripted with an exponential function (with a sharp derivate only in the first instants) and the second as a triangular impulse

4.6 Effect of resistive load: calculation of energy output and efficiency

The scope of the last tests was the evaluation of the performance of the raindrop harvester when connected to an external load. With the resulting data, it was then possible to calculate the electrical power and the efficiency of the energy conversion of the harvester

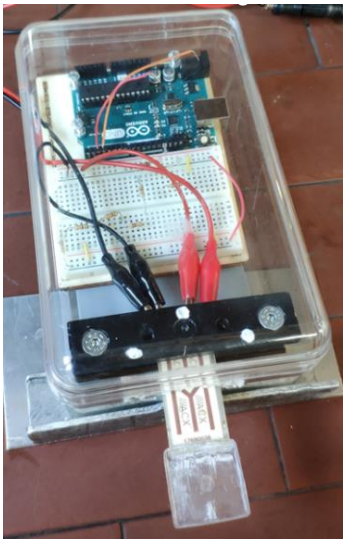

Figure 49: In this figure it is possible to see the electrical connection of the Harvester in the load tests. The electrical connectors are connected to the electrodes, just underneath the slot of the cantilever. There is a couple of connector foreach pole: one is for the load and the other for the DAQ. Both the connectors are attached in parallel to the Harvester.

The power produced by a piezoelectric harvester is not constant: it depends from the electrical load (see [12] & [7]). As shown in the figure below, there is a particular **external resistance at which the modulus of the voltage FRF is the lowest**: that means that the highest portion of energy has been lost feeding the load.

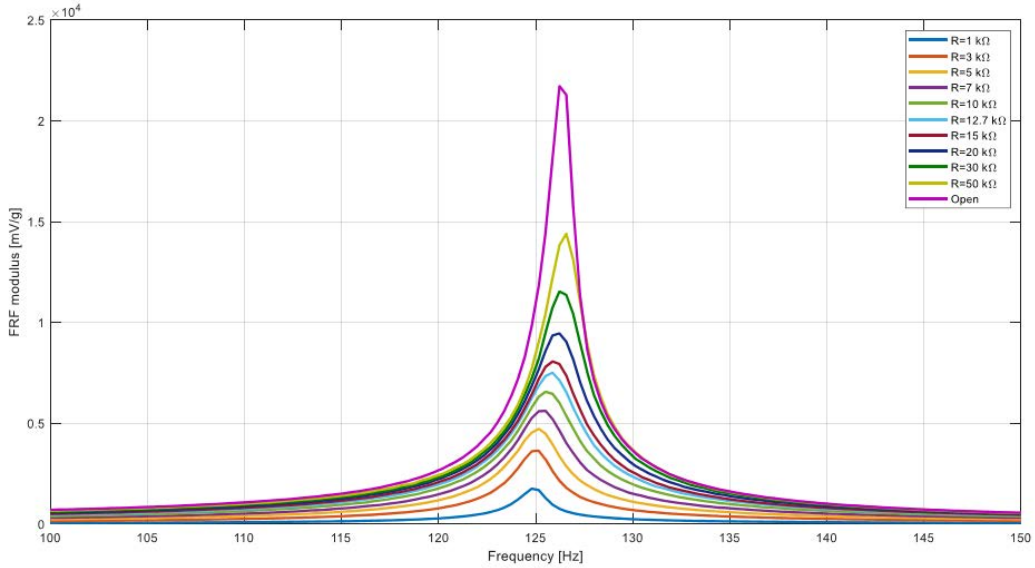

Figure 50: FRF of the harvester PPA101 as a function of resistive load, from [7]

The ideal load can be calculated with this equation (see [12]):

$$R_{opt} = 1/(\omega C_p) \tag{4.5}$$

This **optimal resistance** is not only **reduces the amplitude of the signal**: it **slightly decreases also the first mode frequency**. To obtain the highest power, the load tests where therefore performed with an overall resistance as close as possible to this ideal load. This resistance was calculated by considering as well the internal resistance of the DAQ circuit. This later was estimated, from previous works, as $\boldsymbol{R_{DAQ} = 307\ k\Omega}$. The overall resistance is thus the result of the parallel connection of the Arduino Resistance and the DAQ resistance.

$$R_{Arduino} = (\frac{1}{R_{opt}} - \frac{1}{R_{DAQ}}) \tag{4.6}$$

Test	First mode frequency [Hz]	Optimal resistance [Ω]	Arduino resistance [Ω]	DAQ resistance [Ω]
1m height fall on full spoon	*51*	*31206*	*34738*	*307000*
1m height fall on full spoon	*37*	*44209*	*51647*	*307000*

Except for the resistance, the tests were completely identical to the previous ones, which were conducted with no load. Thus, for the sake of simplicity, the height of fall for the droplet was set at 1 m (the more the height increases, the more the droplet is influenced by disturbs and can miss the spoon).

After having obtained the electric signal, the dissipated energy and the electrical power were calculated as:

$$W_{el} = \frac{1}{2R_{Arduino}} \int_0^{t_{max}} V^2\, dt \tag{4.7}$$

$$P_{el}(t) = \frac{dW_{el}(t)}{dt} \tag{4.8}$$

Test: drop from 1m on full spoon with ideal load

Test sample	Mean frequency [Hz]	V_{MAX}#1 [mV]	V_{MIN}#1 [mV]	V peak to peak	V_{MAX} #2 [mV]	$\frac{V_{MAX}}{\lvert V_{MIN}\rvert}$	$\frac{V_{MAX}\ \#1}{V_{MAX}\ \#2}$	Mean ζ
#1	36.59	729	-1301	2030	1530	0.560	0.477	0.022
#2	36.56	617	-1171	1788	1451	0.527	0.425	0.021
#3	36.53	575	-1095	1670	1314	0.525	0.438	0.021
#4	36.51	568	-1068	1636	1347	0.531	0.422	0.020
#5	36.50	619	-1172	1791	1447	0.528	0.428	0.020
#6	36.37	495	-944	1439	1151	0.525	0.430	0.021
#7	36.34	546	-1041	1587	1299	0.525	0.420	0.022
Mean	36.49	593	-1113	1706	1363	0.532	0.434	0.021
SD	0.10	73	114	187	125	0.013	0.020	0.001

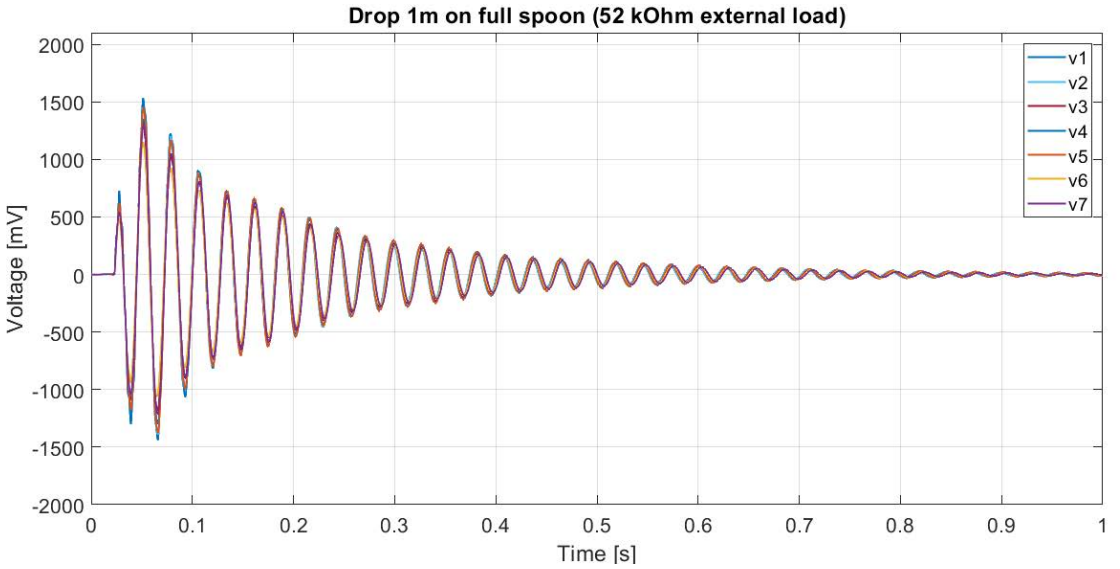

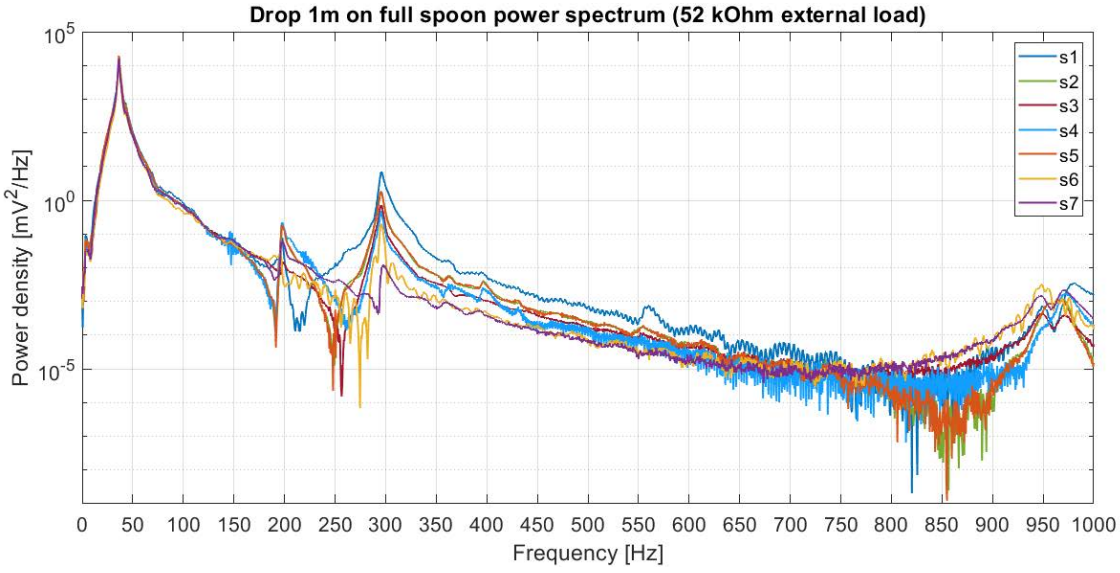

Test: drop from 1m on empty spoon with ideal load

Test sample	Mean frequency [Hz]	V_{MAX}#1 [mV]	V_{MIN}#1 [mV]	V peak to peak	V_{MAX} #2 [mV]	$\frac{V_{MAX}}{\lvert V_{MIN}\rvert}$	$\frac{V_{MAX}\ \#1}{V_{MAX}\ \#2}$	Mean ζ
#1	51.15	179	-220	399	195	0.816	0.919	0.018
#2	51.09	194	-239	434	208	0.812	0.935	0.017
#3	51.05	186	-237	423	216	0.782	0.860	0.017
#4	49.96	160	-195	356	172	0.819	0.930	0.018
#5	50.42	216	-265	481	239	0.814	0.902	0.020
#6	50.68	201	-249	450	219	0.807	0.917	0.017
Mean	50.73	189	-234	424	208	0.808	0.911	0.018
SD	0.47	19	24	43	23	0.014	0.027	0.001

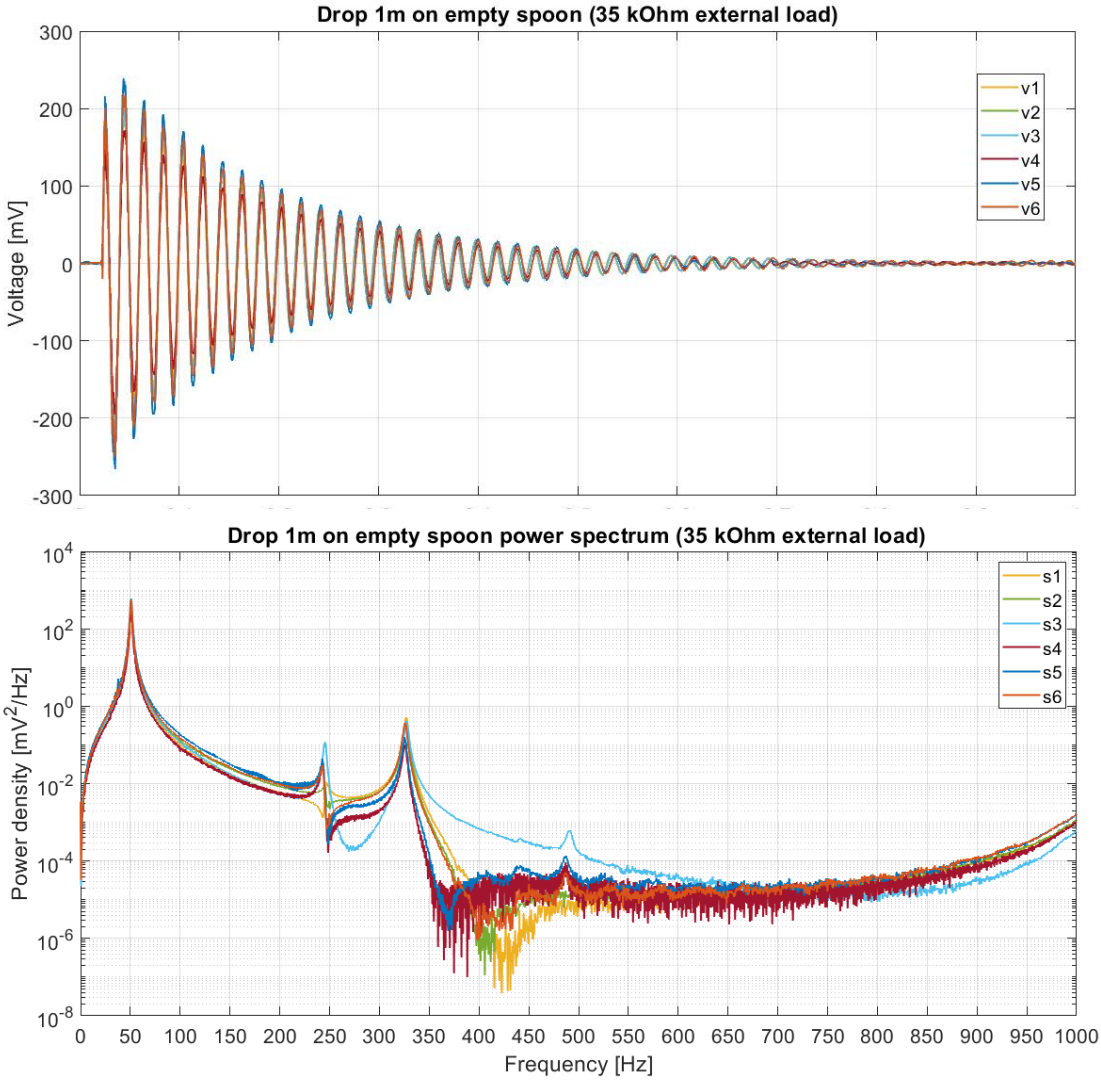

The next figures plot the result of the numerical analysis on the signal, obtained with Matlab. The upper graph plots the voltage of the output signal, the lower one the energy dissipated in the load resistance.

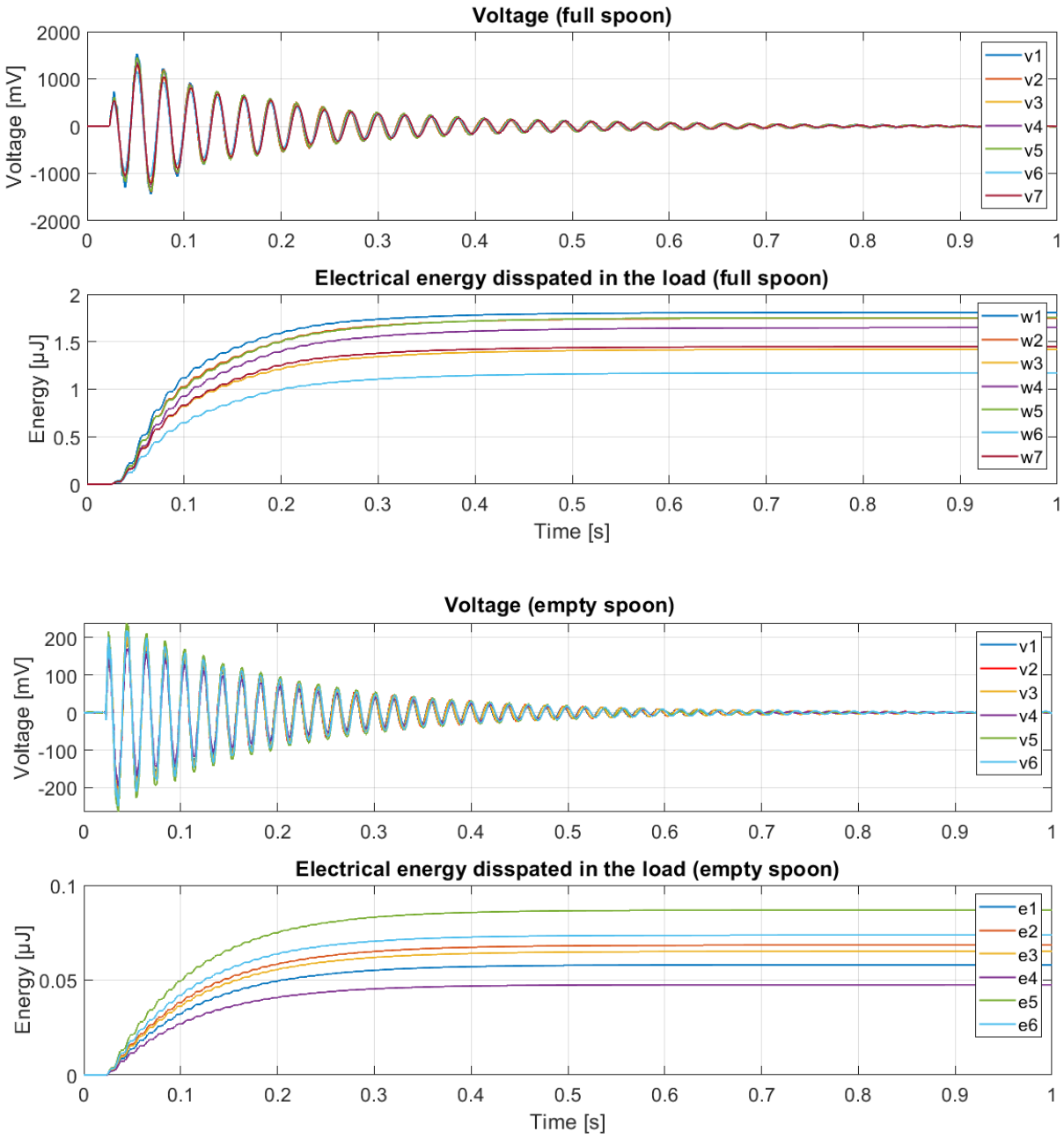

Figure 51: Result of the data elaboration: measured voltage and energy dissipated in the Arduino resistance.

The graphs in this page plot the evolution in time of electrical power:

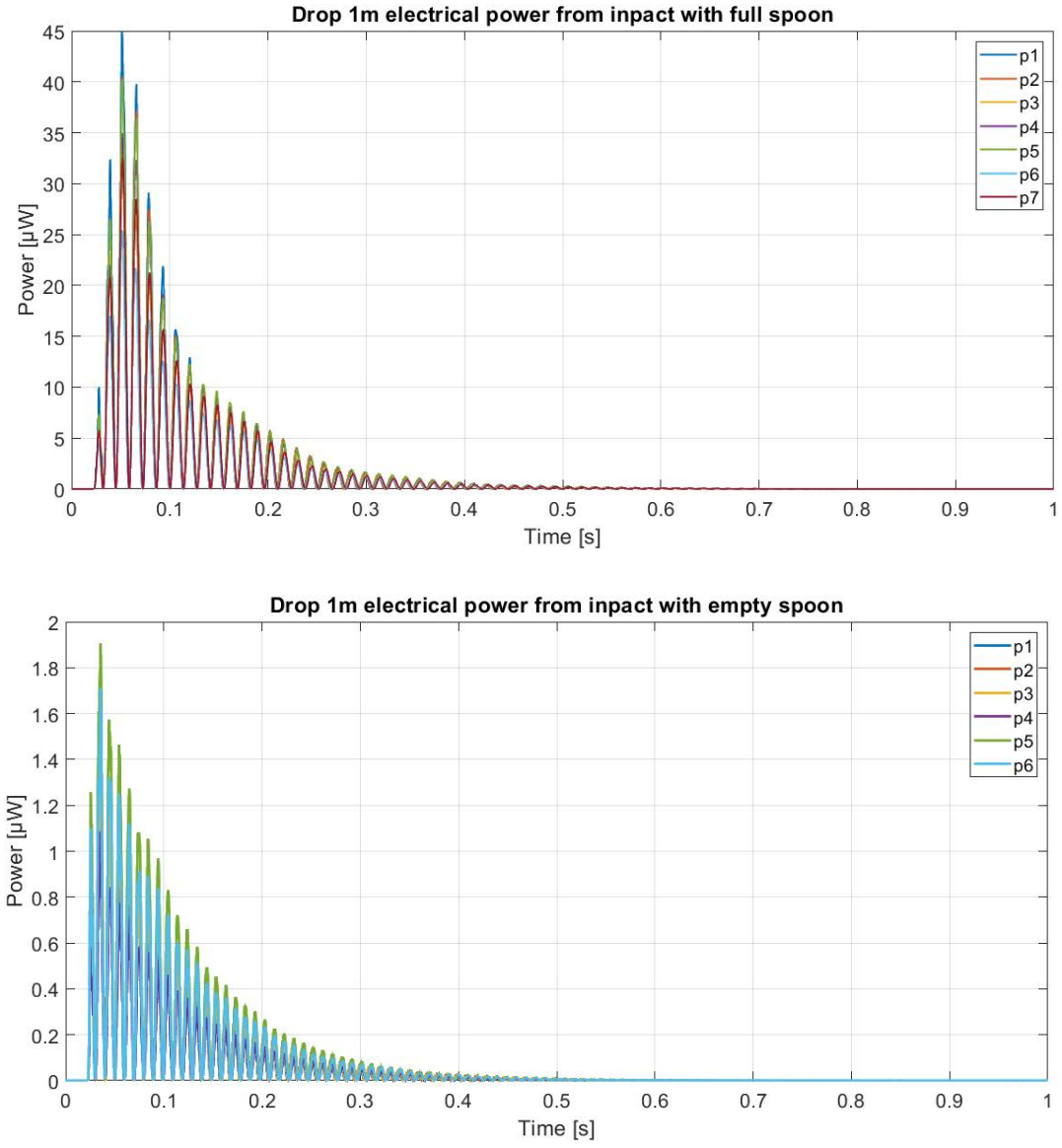

Figure 52: Electrical power that feeds the resistors in Arduino breadboard

Finally, to calculate the efficiency, it is necessary to evaluate the initial energy of a single droplet. The velocity after the fall of a droplet with a **diameter of 2 mm** is **4.0 m/s** (see 2.1, figure 23). Assuming the mass of a droplet as **0.0056 g** (3.3, tab the kinetic energy at the instant of the impact was calculated as:

$$W_{droplet} = \frac{1}{2}\, m\, v_{droplet}^2 = 448\ \mu J \tag{4.9}$$

During the impact, the droplet has already converted all its gravitational potential energy: therefore, the kinetic energy is the only component of the total mechanical energy. The efficiency can be calculated as:

$$\eta = \eta_{impact} \cdot \eta_{piezoelectric} = \frac{W_{el}}{W_{droplet}} \tag{4.10}$$

The results are summarised in the following tables:

	R =307 kΩ		**Optimal resistance**	
Full spoon	$f_{1st} = 37\ Hz$	V_{pk-pk} =2.4 V	$f_{1st} = 36.5\ Hz$	$V_{pk-pk} = 1.7\ V$
Empty spoon	$f_{1st} = 51.5\ Hz$	$V_{pk-pk} = 0.6\ V$	$f_{1st} = 50.7\ Hz$	$V_{pk-pk} = 0.4\ V$

ELECTRICAL LOAD: ARDUINO RESISTANCE				
Test typology		**Peak power [µW]**	**Energy [µJ]**	**Efficiency**
Drop 1m on full spoon	Max	44.92	1.808	0.404 %
	Min	25.44	1.172	0.262 %
	Mean	35.95	1.571	0.351 %
Drop 1m on empty spoon	Max	1.91	0.087	0.019 %
	Min	1.09	0.048	0.011 %
	Mean	1.52	0.067	0.015 %

Table 5: Influence of optimal resistance and peak power, dissipated energy and efficiency

However it should be said that ,if considering the total resistance, the result should is a little higher.

ELECTRICAL LOAD: ARDUINO RESISTANCE + DAQ RESISTANCE				
Test typology		Peak power [µW]	Energy [µJ]	Efficiency
Drop 1m on full spoon	Max	53.09	2.137	0.477 %
	Min	30.07	1.385	0.310 %
	Mean	42.49	1.857	0.415 %
Drop 1m on empty spoon	Max	2.14	0.098	0.021 %
	Min	1.22	0.054	0.012 %
	Mean	1.71	0.075	0.017 %

Table : Peak power, dissipated energy and efficiency relative to the total resistance

It is clear that these results are in accordance with those reported by Gnee et al.(see 2.2 table 3): the **maximal efficiency reported is 0.4 %.** However, it should be underlined that in our tests **there is no conversion circuit**: it is rather imaginable a drop of at least 5% when including the electrical efficiency in the computation. It appears also clear that in presence of water the efficiency is much higher than when the spoon is totally empty. This could be explained by one simple factors:

- *Very high hydrophobicity of the dry surface of the spoon*

In fact, it was possible to verify that the impact of the droplets and the surface resulted very often in the rebouncing of them. Thus in this case the efficiency of the impact is very low, resulting in an extreme low overall efficiency.

Drop from 1 m height	**Mean damping ratio (ζ_{mean})**		**Peak to Peak Voltage [mV]**	**Mean efficiency**
	Load	**Open circuit**		
Full spoon	0.015	0.021	1706	0.415%
Empty spoon	0.018	0.008	424	0.017 %

Table 7: Comparison of load tests results at 1m for full and empty configuration

Chapter 5: Conclusions

Raindrop energy harvesting is a potential application of piezoelectric energy harvesters: though atmospherical rainfall is a consequence of a huge ammount of solar energy absorbed in the hydrosphere, this energy is mostly delivered through the extreme low kinetic energy of raindrops. This is the reason why piezoelectrical harvesters, which are extremely versatile, robust and simple micro-generators, could be well suited for this application. However piezoelectric energy harvesters, especially in the form of cantilever beams, need to be adapted to the transient conditions in which they are required to work: in fact the energy transmission does not happen through a steady vibration of the base of the harvester, but rather through an impulsive force acting on the tip of the beam. The experiment conducted throughout this work were intended at first to better understand the response of a piezoelectric harvester to the raindrops; as soon as the extreme importance of the impact mechanism began to appear, it was then decided to further investigate the impact behaviour itself. These were above all the most important results:

- *The height of the fall becomes irrelevant after a certain value: this value is very low (compared to the thickness of the troposphere)*
- *A water film that totally fills the spoon on the tip of the harvester yields the best result in terms of both peak to peak voltage and energy produced*
- *Countrary to the advice in scientific literature, the dried surface of the spoon does perform very poorly, as most of the energy of the droplet appear not to be transferred to the harvester*
- *The impact duration in presence of the water film appears to be longer and smoother; on the other side, the impact with the empty surface appears to be shorter, more irregular and harsher*
- *While the efficiency of these harvesters are generally always extremely low, the sollution with the water film on the surface of the spoon is in line with the best results reported in scientific literature*

One of the most interesting sollution to improve the overall efficiency of the piezoelectric cantilever beam has been suggested in [6] and [15].

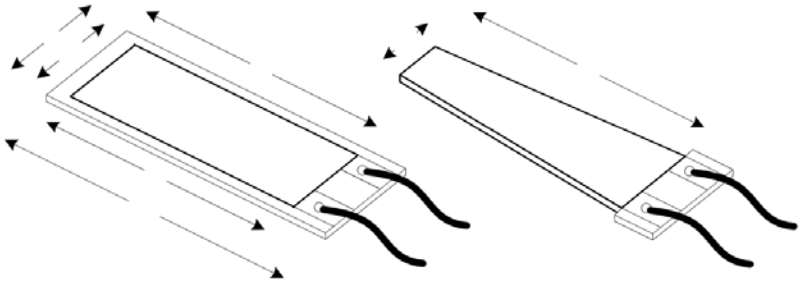

Figure 53: In the left the geometry commmonly adopted for piezoelectric cantilever beam, in the right the proposed geometry to optimize the piezoelectric energy conversion

With a smart use of the geometry it is in fact possible to improve the performance of the harvester: in a constant section cantilever, the bending moment and thus the flexion strain increases approaching the fixed constraint. The adoption of an increasing section from the extremity permits on the other hand to obtain a higher deflection along the entire beam resulting in an enhanced piezoelectric effect. The study of this geometry, as well as the study of new possible surfaces and materials for the spoon could be object of further analysis.

Appendix: Matlab script

“Data analyser”

```
x = input('dependent variable');
%npp=input('number of pseudoperiods ');
tmax = 1;
%tmax=input('interval of time to consider ');
npp = 6; %npp is the number of pseudoperiods to consider for logarithmic
decrement
ex = 4; %ex is the number of the first peak to consider
y = find(abs(t-tmax)<0.005); %Finding indices of all elements whose difference
with the value specified is 0.5.
z = t(y); %Creating a vector with the values that satisfy the above condition
[a,r]=min(abs(z-tmax));
y = y(r); %index in time vector
tmax = t(y);

clear a & r & z
close all
p1=subplot(2,1,1);
plot(t,x,'k')
hold on
grid on
clear index
clear dp & dm & i

%analysis of maximum points
xlim([0 tmax])
xi= x(1:y);
[pks,locs] = findpeaks(xi,'MinPeakDistance',30);
maxx = max(pks);
tlocs=locs*t(2); %instants of local maximum points

%pks yields the peaks of the function, whereas locs yields their indices. Two
adjacent peaks must have at least 30 elements in between them

for q=1:(length(pks)-1)
    if pks(q)> maxx*0.4/(2*tlocs(q)+q)  %elimination each peak below a threshold
       width(q) = [locs(q+1)-locs(q)];
%width of the distance between indices of consecutive peaks
    else pks(q) = 0
        width(q) = 0
    end
end

clear I & xim & max & maxx

index = find(pks); %elimination of invalid peaks (i.e pks=0)
width = find(width);
tpeaks = tlocs(index);
pks=pks(index);

plot(tpeaks,pks,':r*')
zp=0;
```

```
%logarithmic decrement for maxima
for q = 1:(length(pks)-npp-ex+1)
    dp(q) = log(pks(q+ex-1)/pks(q+npp+ex-1))/(npp)
    tdp(q) = tpeaks(q+ex-1)
end
zp = dp./sqrt(4*pi*pi+dp.*dp)
clear dp
index = 0;
index = find(zp);
zp = zp(index);
tdp = tdp(index);
clear locs & tlocs

%computation of frequency
for i = 1:length(tdp)-1
    pfreq(i) = tdp(i+1)-tdp(i);
end
pfreq = pfreq.^-1;

%analysis of minimum points
xi = -xi;
[val,locs] = findpeaks(xi,'MinPeakDistance',30);
xi = -xi;
mini = -max(val);
val = -val;
tlocs = locs*t(2);
for q = 1:length(val)-1
    if val(q) < mini*0.4/(2*tlocs(q)+q) %elimination each peak below a threshold
    else width(q) = 0
        val(q) = 0
    end
end

index = find(val); %elimination of invalid values (i.e val=0)
val = val(index);
tval = tlocs(index);
plot(tval,val,':b*')
val = -val;
clear q
tdm = 0;
%logarithmic decrement for minima
for q = 1:(length(val)-npp-ex+1)
    dm(q) = log(val(q+ex-1)/val(q+npp+ex-1))/(npp)
    tdm(q) = tval(q+ex-1)
end
zm = dm./sqrt(4*pi*pi+dm.*dm)
val = -val;
clear locs & tlocs & mini

%computation of frequency
for i=1:length(tdm)-1
    mfreq(i)=tdm(i+1)-tdm(i);
end
mfreq=mfreq.^-1;
MeanFrequency=0.5*mean(pfreq)+0.5*mean(mfreq);
```

```
clear pfreq & mfreq
clc
clear i
Ratio_FirstMax_SecondMax = (pks(1)/pks(2));
Vpp = (pks(1)-val(1));
Ratio_pp = -1*pks(1)/val(1);
zp_mean = mean(zp);
zm_mean = mean(zm);

clear index
xlabel('Time [s]')
ylabel('Voltage [mV]')
legend('signal','maxima','minima')

hold on
pz = [1,1]*mean(nonzeros(zp_mean));
tpz = [tdp(1),max(tdp)];
mz = [1,1]*mean(nonzeros(zm_mean));
tmz = [tdm(1),max(tdm)];

subplot(2,1,2)
hold on
grid on
xlim([0 tmax])
plot(tdp,zp,'r')
plot(tdm,zm,'b')
plot(tpz,pz,':r*')
plot(tmz,mz,':b*')
xlabel('Time [s]')
ylabel('Zeta')
legend('positive signal z','negative signal z','positive signal mean
z','negative signal mean z')
set(gca,'FontSize',16)
clear pz & tdp & tdm & tpz & mz & tmz

Mean_z = mean([nonzeros(zp_mean);nonzeros(zm_mean)]);
FirstMax = pks(1);
SecondMax = pks(2);
FirstMin = val(1);
T = table("Mean frequency","First Max","First Min","V peak to peak ","Second
Max","Vmax/Vmin","Ratio FirstMax/SecondMax","Mean Z");
T=
table(MeanFrequency,FirstMax,FirstMin,Vpp,SecondMax,Ratio_pp,Ratio_FirstMax_Seco
ndMax,Mean_z)

clear xi & tpeaks & freq & peaks & peaks & tval & val & dp_mean & dm_mean
clear width & Mean_z & FirstMax & SecondMax & FirstMin & MeanFrequency
clear Ratio_FirstMax_SecondMax & Ratio_pp & Ratio_FirstMax_FirstMin & Vpp
clear y & x & npp & tmax & ex & pks & val & q
```

Bibliography and sources

[1]: *Shashank Priya, Daniel J. Inman, "ENERGY HARVESTING TECHNOLOGIES", Springer 2009;*

[2]: *Mohammad Adnan Ilyas, Jonathan Swingler, "PIEZOELECTRIC ENERGY HARVESTING FROM RAINDROP IMPACTS", Energy 90 (2015);*

[3]: *Emmanuele G.G. Zampieri, "SVILUPPO DI HARVESTER PIEZOELETTRICI A BANDA LARGA", 2018;*

[4]: *Perera K, Sampath B, Dassanayake V, Hapuwatte B. Harvesting of kinetic energy of the raindrops. Int J Math Comput Phys Quantum Eng 2014;*

[5]: *Chin-Hong Wong, Zuraini Dahari,Asrulnizam abd Manaf, Muhammad Azman Miskam, "HARVESTING RAINDROP ENERGY WITH PIEZOELECTRICS: A REVIEW", Journal of electronic materials, doi: 10.1007/s11664-014-3443-4 2014 the minerals, metals & materials society*

[6]: *Kok Gnee CHUA, Yew Fong HOR and Hee C. LIM, " RAINDROP KINETIC ENERGY PIEZOELECTRIC HARVESTERS AND RELEVANT INTERFACE CIRCUITS: REVIEW, ISSUES AND OUTLOOKS", Sensors and transducer, Vol 200, Issue 5, May 2016, pp 1-15*

[7]: *Simone Giolo, "SVILUPPO DI HARVESTER PIEZOELETTRICI ADATTI A RACCOGLIERE ENERGIA DA VIBRAZIONI PERIODICHE", 2018*

[8]: *Hailing Fu, Guangzhu Chen, Nan Bai Electrode, "COVERAGE OPTIMIZATION FOR PIEZOELECTRIC ENERGY HARVESTING FROM TIP EXCITATION", Sensors 2018, 18(3), 804*

[9]: *https://www.slideshare.net/El-Rayes/vibration-energy-harvesting-between-theory-and-reality*

[10]: *https://www.newcivilengineer.com/technical-excellence/smart-infrastructure-vibration-energy/10008070.article*

[11]: *https://www.newscientist.com/gallery/dn15041-the-atlas-of-the-real-world/*

[12]: *Alberto Doria, Cristian Medè, Giulio Fanti, Daniele Desideri, Alvise Maschio and Federico Moro, "DEVELOPMENT OF PIEZOELECTRIC HARVESTERS WITH INTEGRATED TRIMMING DEVICES", Applied Sciences, 04/04/2018*

[13]: *Sean Gart, Joseph E. Mates, Constantine M. Megaridis, and Sunghwan Jung, " DROPLET IMPACTING A CANTILEVER: A LEAF-RAINDROP SYSTEM", PHYSICAL REVIEW APPLIED 3, 044019 (2015)*

[14]: *Alessandro Bertacchini, Luca Larcher, Moreno Maini, Luca Vincetti and Stefano Scorcioni, RECONFIGURABLE RF ENERGY HARVESTER WITH CUSTOMIZED DIFFERENTIAL PCB ANTENNA, J. Low Power Electron. Appl. 2015, 5(4), 257-273*

[15]: *Ciro Spataro, Fabio Viola, Pietro Romano, Rosario Miceli, "PERFORMANCES OF RAINFALL ENERGY HARVESTER", 20th IMEKO TC4 International Symposium and18th International Workshop on ADC Modelling and Testing*

[16]: *Fabio Viola, Pietro Romano, Rosario Miceli, Gianluca Acciari, Ciro Spataro, "PIEZOELECTRIC MODEL OF RAINFALL ENERGY HARVESTER", 2014 Ninth International Conference on Ecological Vehicles and Renewable Energies (EVER)*

[17]: G. Acciari, M. Caruso, M. Fricano, A. Imburgia, R. Miceli, P. Romano, G. Schettino and F. Viola, "EXPERIMENTAL INVESTIGATION ON DIFFERENT RAINFALL ENERGY HARVESTING STRUCTURES", 2018 Thirteenth International Conference on Ecological Vehicles and Renewable Energies (EVER)

[18]: Romain Guigon, Jean-Jacques Chaillout, Thomas Jager and Ghislain Despesse, "HARVESTING RAINDROP ENERGY: THEORY", SMART MATERIALS AND STRUCTURES,Smart Mater. Struct. 17 (2008) 015038 (8pp) doi:10.1088/0964-1726/17/01/015038

[19]: Romain Guigon, Jean-Jacques Chaillout, Thomas Jager and Ghislain Despesse, "HARVESTING RAINDROP ENERGY: EXPERIMENTAL STUDY", SMART MATERIALS AND STRUCTURES Smart Mater. Struct. 17 (2008) 015039 (6pp) doi:10.1088/0964-1726/17/01/015039

[20]: Gianluca Acciari, Massimo Caruso , Rosario Miceli , Member, IEEE, Luca Riggi, Pietro Romano, Giuseppe Schettino, and Fabio Viola, "PIEZOELECTRIC RAINFALL ENERGY HARVESTER PERFORMANCE BY AN ADVANCED ARDUINO-BASED MEASURING SYSTEM", IEEE TRANSACTIONS ON INDUSTRY APPLICATIONS, VOL. 54, NO. 1, JANUARY/FEBRUARY 2018

[21]: Nik Ahmad Kamil Zainal Abidin, Norkharziana Mohd Nayan , Muhammad Mokhzaini Azizan, Azuwa Ali, "ANALYSIS OF VOLTAGE MULTIPLIER CIRCUIT SIMULATION FOR RAIN ENERGY HARVESTING USING CIRCULAR PIEZOELECTRIC", Mechanical Systems and Signal Processing 101 (2018) 211–218

[22]: D Vatansever, R L Hadimani, T Shah and E Siores, "AN INVESTIGATION OF ENERGY HARVESTING FROM RENEWABLE SOURCES WITH PVDF AND PZT", SMART MATERIALS AND STRUCTURES Smart Mater. Struct. 20 (2011) 055019 (6pp) doi:10.1088/0964-1726/20/5/055019

[23]: CHIN HONG WONG, ZURAINI DAHARI, MOHAMMAD HAFIZUDDIN JUMALI, KHAIRUDIN MOHAMED, and JULIE JULIEWATTY MOHAMED, "SIMULATION AND FABRICATION OF WAGON-WHEEL-SHAPED PIEZOELECTRIC TRANSDUCER FOR RAINDROP ENERGY HARVESTING APPLICATION", Journal of ELECTRONIC MATERIALS, Vol. 46, No. 3, 2017 DOI: 10.1007/s11664-016-5201-2,©2016 The Minerals, Metals & Materials Society

[24]: Alberto Doria, Cristian Medè, Giulio Fanti, Daniele Desideri, Alvise Maschio and Federico Moro, "Development of Piezoelectric Harvesters with Integrated Trimming Devices"

[25]: A. Doria, C. Medè a, D. Desideri a, A. Maschio a, L. Codecasa b, F. Moro, "ON THE PERFORMANCE OF PIEZOELECTRIC HARVESTERS LOADED BY FINITE WIDTH IMPULSES", Mechanical Systems and Signal Processing 100 (2018) 28–42

[26]: A.L. Yarin, "DROP IMPACT DYNAMICS: SPLASHING, SPREADING, RECEDING, BOUNCING...", Annu. Rev. Fluid Mech. 2006. 38:159–92